MALLA REDDY COLLEGE OF ENGINEERING & TECHNOLOGY

MRCET CAMPUS

(AUTONOMOUS INSTITUTION – UGC, GOVT. OF INDIA)

B.Tech
Aeronautical Engineering

Department of AERONAUTICAL ENGINEERING

Aerodynamics

Prepared by:

VG Krishna Aanand
Associate Professor
Department of ANE
krishnaanand@mrcet.ac.in

AERODYNAMICS (R22A2107)

COURSE FILE

II B. Tech II Semester

(2023-2024)

Prepared By

Dr. KRISHNA ANAND V G

Associate Professor

Department of Aeronautical Engineering

MALLA REDDY COLLEGE OF ENGINEERING & TECHNOLOGY

(Autonomous Institution – UGC, Govt. of India)

MRCET VISION

- To become a model institution in the fields of Engineering, Technology and Management.
- To have a perfect synchronization of the ideologies of MRCET with challenging demands of International Pioneering Organizations.

MRCETMISSION

To establish a pedestal for the integral innovation, team spirit, originality and competence in the students, expose them to face the global challenges and become pioneers of Indian vision of modern society.

MRCET QUALITY POLICY.

- To pursue continual improvement of teaching learning process of Undergraduate and Post Graduate programs in Engineering & Management vigorously.
- To provide state of art infrastructure and expertise to impart the quality education.

PROGRAM OUTCOMES

(PO's)

Engineering Graduates will be able to:

1. **Engineering knowledge**: Apply the knowledge of mathematics, science, engineering fundamentals, and an engineering specialization to the solution of complex engineering problems.

2. **Problem analysis**: Identify, formulate, review research literature, and analyze complex engineering problems reaching substantiated conclusions using first principles of mathematics, natural sciences, and engineering sciences.

3. **Design / development of solutions**: Design solutions for complex engineering problems and design system components or processes that meet the specif ied needs with appropriate consideration for the public health and safety, and the cultural, societal, and environmental considerations.

4. **Conduct investigations of complex problems**: Use research-based knowledge and research methods including design of experiments, analysis and interpretation of data, and synthesis of the information to provide valid conclusions.

5. **Modern tool usage**: Create, select, and apply appropriate techniques, resources, and modern engineering and IT tools including prediction and modeling to complex engineering activities with an understanding of the limitations.

6. **The engineer and society**: Apply reasoning informed by the contextual knowledge to assess societal, health, safety, legal and cultural issues and the consequent responsibilities relevant to the professional engineering practice.

7. **Environment and sustainability**: Understand the impact of the professional engineering solutions in societal and environmental contexts, and demonstrate the knowledge of, and need for sustainable development.

8. **Ethics**: Apply ethical principles and commit to professional ethics and responsibilities and norms of the engineering practice.

9. **Individual and team work**: Function effectively as an individual, and as a member or leader in diverse teams, and in multidisciplinary settings.

10. **Communication**: Communicate effectively on complex engineering activities with the engineering community and with society at large, such as, being able to comprehend and write effective reports and design documentation, make effective presentations, and give and receive clear instructions.

11. **Project management and finance**: Demonstrate knowledge and understanding of the engineering and management principles and apply these to one's own work, as a member and leader in a team, to manage projects and in multi disciplinary environments.

12. **Life- long learning**: Recognize the need for, and have the preparation and ability to engage in independent and life-long learning in the broadest context of technological change.

DEPARTMENTOFAERONAUTICALENGINEERING

VISION

Department of Aeronautical Engineering aims to be indispensable source in Aeronautical Engineering which has a zeal to provide the value driven platform for the students to acquire knowledge and empower themselves to shoulder higher responsibility in building a strong nation.

MISSION

The primary mission of the department is to promote engineering education and research. To strive consistently to provide quality education, keeping in pace with time and technology. Department passions to integrate the intellectual, spiritual, ethical and social development of the students for shaping them into dynamic engineers.

QUALITY POLICY STATEMENT

Impart up-to-date knowledge to the students in Aeronautical area to make them quality engineers. Make the students experience the applications on quality equipment and tools. Provide systems, resources and training opportunities to achieve continuous improvement. Maintain global standards in education, training and services.

PROGRAMEDUCATIONALOBJECTIVES– Aeronautical Engineering

1. **PEO1 (PROFESSIONALISM & CITIZENSHIP):** To create and sustain a community of learning in which students acquire knowledge and learn to apply it professionally with due consideration for ethical, ecological and economic issues.

2. **PEO2 (TECHNICAL ACCOMPLISHMENTS):** To provide knowledge based services to satisfy the needs of society and the industry by providing hands on experience in various technologies in core field.

3. **PEO3 (INVENTION, INNOVATION AND CREATIVITY):** To make the students to design, experiment, analyze, and interpret in the core field with the help of other multi disciplinary concepts wherever applicable.

4. **PEO4 (PROFESSIONAL DEVELOPMENT):** To educate the students to disseminate research findings with good soft skills and become a successful entrepreneur.

5. **PEO5 (HUMAN RESOURCE DEVELOPMENT):** To graduate the students in building national capabilities in technology, education and research

PROGRAMSPECIFIC OUTCOMES – Aeronautical Engineering

1. To mould students to become a professional with all necessary skills, personality and sound knowledge in basic and advance technological areas.
2. To promote understanding of concepts and develop ability in design manufacture and maintenance of aircraft, aerospace vehicles and associated equipment and develop application capability of the concepts sciences to engineering design and processes.
3. Understanding the current scenario in the field of aeronautics and acquire ability to apply knowledge of engineering, science and mathematics to design and conduct experiments in the field of Aeronautical Engineering.
4. To develop leadership skills in our students necessary to shape the social, intellectual, business and technical worlds.

MALLA REDDYCOLLEGE OF ENGINEERING ANDTECHNOLOGY

II Year B.Tech. ANE- II Sem   **L/T/P/C**
3/-/-/3

(R20A2107) Aerodynamics

Objectives:

1. To introduce the concepts of mass, momentum and energy conservationrelating to aerodynamics.
2. To make the student understand the concept of vorticity, irrotationality,theory of airfoils and wing sections.
3. To introduce the basics of viscous flow.

UNIT I Basics of Aerodynamics:

Aerodynamic forces and Moments, Derivation of Lift, Drag and momentCoefficients with pressure distribution, Variation of pressure distribution with respect to angle of attack,Governing equations of flow- Continuity, momentum and Energy equations in differential form. Flow regimes based on Mach number.

UNIT - II Inviscid Incompressible Flow over Airfoil:

Governing Equation for incompressible and irrotational flow,Elementary flows and their combinations, Magnus effect, D'Alembert's Paradox, Kutta - Joukowsky theorem, kutta condition. Kelvin's circulation theorem & starting vortex, Thin airfoil theory, expressions for calculating the aerodynamic center and Center of pressure.

UNIT – III Inviscid Incompressible Flow over Wings:

Vortex filament statement of Helmholtz's vortex theorems,Biot - Savart Law, horse shoe vortex, Prandtl's Lifting line theorem - downwash and induced drag, Elliptic loading & wings of elliptic planforms, expression for induced drag.

UNIT IV Applied Aerodynamics

Lift augmentation and Drag Reduction methods - Flaps, slats, slots, winglets,Leading edge root extensions, Large Eddy Breakup device, Co- flow jet, Cuffs and vortex generators.NACA Airfoils, Circulation control, strakes. Drag augmentation methods – spoilers, Air brakes.

UNIT – V Experimental Aerodynamics

Wind tunnel and its Components, types of wind tunnels andModel testing in wind tunnels. Pressure,Temperature, Velocity measurements – Hotwire and Laser – Doppler anemometer. Force measurements– Wind tunnel balances. Flow visualization techniques- schileren and shadowgraph methods.

Text books:

1. Fundamentals of Aerodynamics, Anderson, Jr., J.D., International edition, McGraw Hill, 2001, ISBN: 0-07-118146-6.

2. Aerodynamics by L.J. Clancy

3. Compressible Aerodynamics, John D. Anderson

Reference Books:

1. Aerodynamics for Engineers, fourth edition, Bertin, J.J., Pearson Education, 2012, ISBN:81-297-0486-2.

2. Kuchemann, D., The Aerodynamic Design of Aircraft, Pergamon, 1978.

3. Shevell, R.S., Fundamentals of Flight, Indian reprint, Pearson Education, 2004, ISBN:81-297-0514-1.

4. McCormick, B.W., Aerodynamics, Aeronautics & Flight Mechanics second edition John Wiley, 1995,ISBN: 0-471-575062.

Outcomes:

1. An ability to apply thin airfoil theory to predict aerodynamic characteristics of air foil
2. Application of Elementary flows to develop real problems.
3. Development of devices to enhance aerodynamic characteristics of aircraftcomponents.

MALLA REDDDY COLLEGE OF ENGINEERING AND TECHNOLOGY

(Autonomous Institution – UGC, Govt. of India)
II BTECH II SEM - AERODYNAMICS

MODEL PAPER – I

MAXIMUM MARKS: 70

ALL QUESTIONS CARRIES EQUALMARKS

Section I

1. Derive the energy equation by applying the fundamental principle to a suitable flow model.

OR

2. Using neat sketches, explain the flow behavior past stream lined bodies placed in different mach number regimes.

Section II

3. a. Define boundary condition. Explain infinity boundary condition and wall – boundary condition.

b. Explain Rankine – oval. Derive the equation of Rankine – oval.

OR

4. A stationary circular cylinder is placed in a uniform flow stream of velocity V_∞. Obtain the equation of stream line pattern around the cylinder. Also sketch the pressure distribution over the surface of the cylinder.

Section III

5. a. Derive the fundamental equation of Prandtl's lifting line theory.

b. Obtain the expressions for coefficients of lift, induced drag, effective angleof attack for an elliptical wing plan-form. Explain the symbols used clearly.

OR

6. Define vortex filament and vortex sheet. Obtain the solution for lifting – flows over 2 – D bodies using vortex panel method. State the advantages of panel method over thin airfoil theory.

7. Using a neat sketch, explain how lift is augmented by using
a. Flap systems
b. Circulation control wing

OR

8. What is the working principleof Vortex generators? Explain in detail.

<u>**Section –V**</u>

9. Discuss briefly about types of wind tunnel and its components?

OR

10. Explain briefly about Schileren and Shadow graph methods with neat sketches.

MALLA REDDDY COLLEGE OF ENGINEERING AND TECHNOLOGY
(Autonomous Institution – UGC, Govt. of India)
II BTECH II SEM - AERODYNAMICS

MODEL PAPER – II

MAXIMUM MARKS: 70

ALL QUESTIONS CARRIES EQUALMARKS

Section I

1. a. Derive Momentum equation in integral form and differential form by applying the physical principle to a suitable flow model.

    OR

2. Derive the Navier – stokes equation.

Section II

3. A circular cylinder spinning about its own axis is placed in a uniform free – stream of velocity V_∞. Obtain the expression for the lift generated over the cylinder. State all the symbols used clearly.

    OR

4. Consider lifting flow over a circular cylinder. The lift coefficient is given by 5. Calculate the peak pressure coefficient, location of stagnation points and the points on the cylinder where the pressure equals free stream static pressure.

Section III

5. Using neat sketches, explain the effect of the presence of down wash on the local airfoil section. How the characteristics of a finite wing are different when compared to the characteristics of airfoil sections?

    OR

6. Citing necessary examples, explain the effect the aspect ratio of wings on the performance parameters.

Section IV

7. Using neat sketches explain the use of winglets in drag control.

    OR

8. Explain the function of leading edge flaps and trailing edge flaps in detail.

9. *Explain briefly about Forcemeasurements using Windtunnels?*

or

10. *Explain briefly aboutflowvisualization methods.*

Code No: R18A2107

MALLA REDDY COLLEGE OF ENGINEERING & TECHNOLOGY
(Autonomous Institution – UGC, Govt. of India)
II B.Tech II Semester Supplementary Examinations, February 2022
Aerodynamics
(AE)

Roll No										

Time: 3 hours　　　　　　　　　　　　　　　　　　　　　　**Max. Marks: 70**
Note: This question paper Consists of 5 Sections. Answer **FIVE** Questions, Choosing ONE Question from each SECTION and each Question carries 14 marks.
***

SECTION-I

1　　Obtain the expression for the aerodynamic force and moment coefficients by integrating the pressure and skin friction coefficients over the wing surface.　**[14M]**

OR

2　　Derive the Navier-Stokes equations by applying the physical principle of momentum.　**[14M]**

SECTION-II

3　　Prove that the theoretical result of lift coefficient is directly proportional to the angle of attack.　**[14M]**

OR

4　　i.　Discuss about the Kelvin circulation theorem.　**[7M]**
　　　ii.　Considering the non-lifting flow over a circular cylinder, Derive an expression for the pressure coefficient at an arbitrary point (r, θ) in this flow, and show that it reduces to $Cp = 1 - 4\sin^2\theta$ on the surface of the cylinder.　**[7M]**

SECTION-III

5　　i.　Consider a finite wing with an aspect ratio of 6. Assume an elliptical lift distribution. The lift slope for the airfoil section is 0.1/degree. Calculate and compare the lift slopes for (a) a straight wing, and (b) a swept wing, with a half-chord line sweep of 45 degrees.　**[7M]**
　　　ii.　Use the numerical 5(i), except for a lower aspect ratio of 3. From a comparison of the results from these two problems, draw some conclusions about the effect of wing sweep on the lift slope, and how the magnitude of this effect is affected by aspect ratio.　**[7M]**

OR

6　　i.　Explain how induced drag is produced by a lifting wing.　**[7M]**
　　　ii.　Based on the lifting line theory show that the downwash is constant over the span for elliptic lift distribution.　**[7M]**

SECTION-IV

7	i.	Summarize the selection criteria of vortex generators.	**[7M]**
	ii.	Outline your views on Large eddy break-up device influence on drag.	**[7M]**

OR

8	i.	Illustrate the effectives of the retractable leading-edge slat.	**[7M]**
	ii.	Appraise the aerodynamic performance of the Co-flow jet wing.	**[7M]**

SECTION-V

9	Explain the Concept of a Six-Component wind tunnel Balance with illustrations, and give the standards of force measurement.	**[14M]**

OR

10	i.	How Shadowgraph Technique work, Describe about the Working Principle of Shadowgraph Techniques.	**[7M]**
	ii.	How Schlieren Technique work, Describe about the Working Principle of Schlieren Techniques.	**[7M]**

****

Code No: **R18A2107**
MALLA REDDY COLLEGE OF ENGINEERING & TECHNOLOGY
(Autonomous Institution – UGC, Govt. of India)
II B.Tech II Semester Supplementary Examinations, June 2022
Aerodynamics
(AE)

Roll No										

Time: 3 hours   **Max. Marks: 70**

Answer Any **Five** Questions
All Questions carries equal marks.
***

1	Using neat sketches, explain the flow behaviour past streamlined bodies placed in different Mach number regimes.	**[14M]**
2	Explain the role of lift and drag coefficients in the preliminary design of an aircraft using neat sketches.	**[14M]**
3	Derive the fundamental equation of thin airfoil theory. Explain the symbols used clearly.	**[14M]**
4	Explain different types of elementary flow and Pressure distribution of non lifting flow over cylinder.	**[14M]**
5	Based on the lifting line theory show that the downwash is constant over the span for elliptic lift distribution. Explain how induced drag is produced by a lifting wing.	**[14M]**
6	Define and Derive the equation for induced drag coefficient with neat sketches.	**[14M]**

7   Explain the function of leading-edge flaps and trailing edge flaps in detail.   **[14M]**

8   Demonstrate working process of the Wind tunnel and its Components.   **[14M]**

****

LESSON PLAN

UNIT	TOPIC	No. of Classes
I **Basics of Aerodynamics**	Aerodynamic forcesand Moments	2
	Derivation of Lift, Drag and moment Coefficients with pressure distribution	2
	Variation of pressure distribution withrespect to angle of attack	2
	Governing equations of flow- Continuity	1
	momentum equationsin differentialform	1
	Energy equation in differentialform	1
	Flow regimes based on Mach NUMBER	1
2 **Inviscid Incompressible Flow over** Airfoil	Governing Equation for incompressible and irrotational flow	1
	Elementary flows and their combinations	2
	Magnus effect, D'Alembert's Paradox	1
	Kutta - Joukowsky theorem	2
	kutta condition.	1
	Kelvin's circulation theorem & startingvortex,	1
	Thin airfoil theory	1
	Expressions for aerodynamic centre	1
	Expressions for centre of pressure	1
3 **Inviscid** **Incompresible Flow over wings**	Vortex filament statement of Helmholtz's vortex theorems	1
	Biot-Savart's law	1
	horse shoe vortex	1
	Prandtl's Lifting line theorem - downwash and induced drag	1
	Elliptic loading & wings of elliptic planforms	1
	vortex induced drag.	1
	Elliptical Loading and problems	2
	expression for induced drag	1

4 **Applied** **Aerodynamics**	Drag reduction & lift augmentation - Flaps, slats, slots, winglets	2
	Leading edge root extensions, Large Eddy Breakup device,	2
	Co-flow jet, Cuffsand vortex generators. NACAAirfoils,	2
	Circulation control, strakes.	1
	Drag augmentation methods – spoilers, Air brakes.	1
5 **Experimental** **Aerodynamics**	Wind tunnel and its Components, types of wind tunnels and Model testing in wind tunnels.	2
	Pressure, Temperature, Velocity measurements	2
	Hotwire and Laser – Doppler anemometer	1
	Force measurements – Wind tunnel balances.	1
	Flow visualization techniques-schileren and shadowgraph methods.	2

UNIT – I
Basics of Aerodynamics

Introduction:

Aerodynamics is a sub-field of fluid dynamics and gas dynamics, and many aspects of aerodynamics theory are common to these fields. The term *aerodynamics* is often used synonymously with gas dynamics, the difference being that "gas dynamics" applies to the study of the motion of all gases, and is not limited to air.

Aerodynamics is primarily concerned with the forces of drag and lift, which are caused by air passing over and around solid bodies. Engineers apply the principles of aerodynamics to the designs of many different things, including buildings, bridges and even soccer balls; however, of primary concern is the aerodynamics of aircraft and automobiles.

Aerodynamics comes into play in the study of flight and the science of building and operating an aircraft, which is called **Aeronautics.** Aeronautical engineers use the fundamentals of aerodynamics to design aircraft that fly through the Earth's atmosphere.

(for detailed information: Refer **FUNDAMENTALS OF AERODYNAMICS – JOHN.D.ANDERSON)**
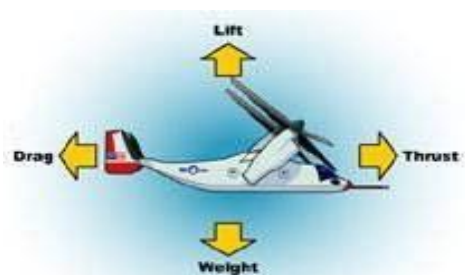
10.1   NEED FOR STUDY OF AERODYNAMICS

Aerodynamics is the way objects move through air. The rules of aerodynamics explain how an airplane is able to fly. Anything that moves through air is affected by aerodynamics, from a rocket blasting off, to a kite flying. Since they are surrounded by air, even cars are affected by aerodynamics.

Studying the motion of air around an object allows us to measure the forces of lift, which allows an aircraft to overcome gravity, and drag, which is the resistance an aircraft "feels" as it moves through the air. Everything moving through the air (including airplanes, rockets, and birds) is affected by aerodynamics.

What Are the Four Forces of Flight?

The four forces of flight are lift, weight, thrust and drag. These forces make an object move up and down, and faster or slower. The amount of each force compared to its opposing force determines how an object moves through the air.

Fig: Four Forces on an Airplane (Ref: NASA)

What Is Weight?

Gravity is a force that pulls everything down to Earth. Weight is the amount of gravity multiplied by the mass of an object. Weight is also the downward force that an aircraft must

overcome to fly. A kite has less mass and therefore less weight to overcome than a jumbo jet, but they both need the same thing in order to fly -- lift.

What Is Lift?

Lift is the push that lets something move up. It is the force that is the opposite of weight. Everything that flies must have lift. For an aircraft to move upward, it must have more lift than weight.

A hot air balloon has lift because the hot air inside is lighter than the air around it. Hot air rises and carries the balloon with it.

A helicopter's lift comes from the rotor blades. Their motion through the air moves the helicopter upward.

Lift for an airplane comes from its wings.

How Do an Airplane's Wings Provide Lift?

The shape of an airplane's wings is what makes it possible for the airplane to fly. Airplanes' wings are curved on top and flatter on the bottom. That shape makes air flow over the top faster than under the bottom. As a result, less air pressure is on top of the wing. This lower pressure makes the wing, and the airplane it's attached to, move up. Using curves to affect air pressure is a trick used on many aircraft. Helicopter rotor blades use this curved shape. Lift for kites also comes from a curved shape. Even sailboats use this curved shape. A boat's sail is like a wing. That's what makes the sailboat move.

What Is Drag?

Drag is a force that pulls back on something trying to move. Drag provides resistance, making it hard to move. For example, it is more difficult to walk or run through water than through air. Water causes more drag than air. The shape of an object also affects the amount of drag. Round surfaces usually have less drag than flat ones. Narrow surfaces usually have less drag than wide ones. The more air that hits a surface, the more the drag the air produces.

What Is Thrust?

Thrust is the force that is the opposite of drag. It is the push that moves something forward. For an aircraft to keep moving forward, it must have more thrust than drag. A small airplane might get its thrust from a propeller. A larger airplane might get its thrust from jet engines. A glider does not have thrust. It can only fly until the drag causes it to slow down and land.

10.2 INTERNAL AND EXTERNAL AERODYNAMICS

Aerodynamics is an applied science with many practical applications in engineering. No matter how elegant an aerodynamic theory may be, or how mathematically complex a numerical solution may be, or how sophisticated an aerodynamic experiment may be, all such efforts are usually aimed at one or more of the following practical objectives:

1. **External Aerodynamics: *The prediction of forces and moments on, and heat transfer to, bodies moving through a fluid (usually air).*** For example, we are concerned with the generation of lift, drag, and moments on airfoils, wings, fuselages, engine nacelles, and, most importantly, whole airplane configurations. We want to estimate the wind force on buildings, ships, and other surface vehicles. We are concerned with the hydrodynamic forces on surface ships, submarines, and torpedoes. We need to be able to calculate the aerodynamic heating of flight vehicles ranging from the supersonic transport to a planetary probe entering the atmosphere of Jupiter. These are but a few examples.

2. **Internal Aerodynamics: *Determination of flows moving internally through ducts*.** We wish to calculate and measure the flow properties inside rocket and air-breathing jet engines and to calculate the engine thrust. We need to know the flow conditions in the test section of a wind tunnel. We must know how much fluid can flow through pipes under various conditions. A recent, very interesting application of aerodynamics is high-energy chemical and gas-dynamic lasers (see Ref. 1), which are nothing more than specialized wind tunnels that can produce extremely powerful laser beams. Figure 1.5 is a photograph of an early gas-dynamiclaserdesigned in the late 1960s

10.3 AERODYNAMICS IN DIFFERENT FIELDS OF ENGINEERING

Aerodynamics is important in a number of applications other than aerospace engineering.

- It is a significant factor in any type of **vehicle design**, including automobiles.
- It is important in the prediction of forces and moments acting on **sailing vessels**.
- It is used in the **design of mechanical components** such as hard drive heads.
- **Structural engineers** also use aerodynamics, and particularly aero-elasticity, to calculate wind loads in the design of large buildings and bridges.
- **Urban aerodynamics** seeks to help town planners and designers improve comfort in outdoor spaces, create urban microclimates and reduce the effects of urban pollution.
- The field of **environmental aerodynamics** describes the ways atmospheric circulation and flight mechanics affect ecosystems.
- The aerodynamics of **internal passages** is important in heating/ventilation, gas piping, and in automotive engines where detailed flow patterns strongly affect the performance of the engine.

Airfoil Basic Geometry: The leading edge is the point at the front of the airfoil that has maximum curvature. The trailing edge is defined similarly as the point of maximum curvature at the rear of the airfoil. The chord line is a straight line connecting the leading and trailing edges of the airfoil. The chord length, or simply chord is the length of the chord line and is the characteristicdimensionof the airfoil section.
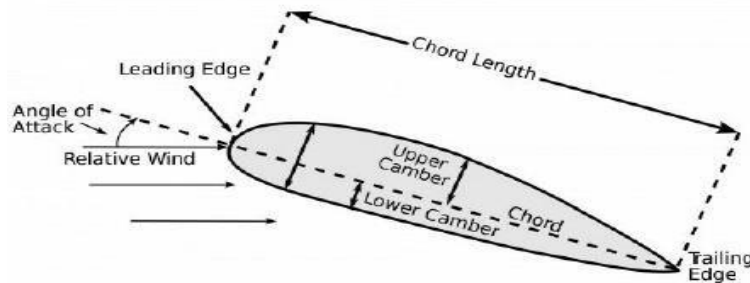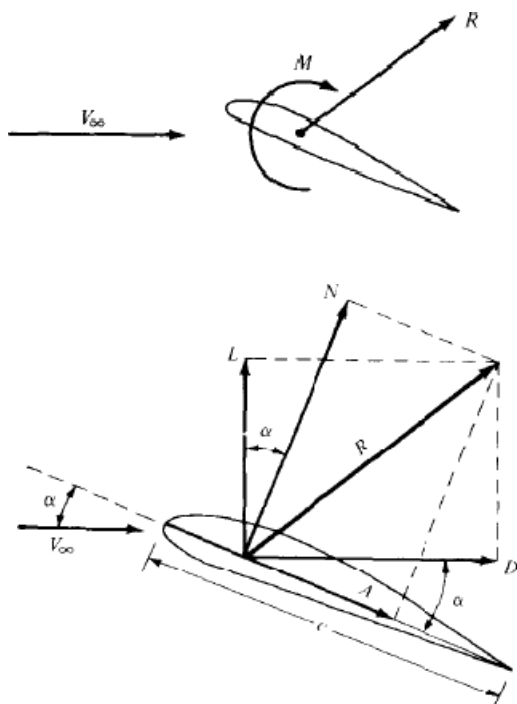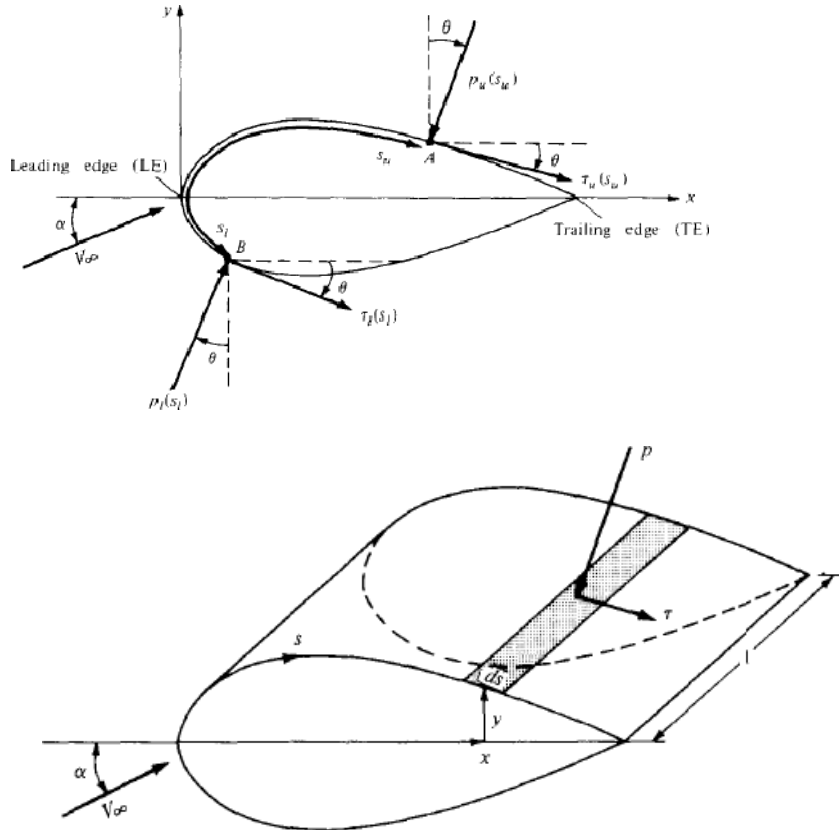

Fig: Basic Geometry of a Airfoil

3.3 Expressions for N, A, L, D (Detailed notes given in the class − derivation)

$$L = N \cos \alpha - A \sin \alpha$$

$$D = N \sin \alpha + A \cos \alpha$$ **where α − Angle of attack**
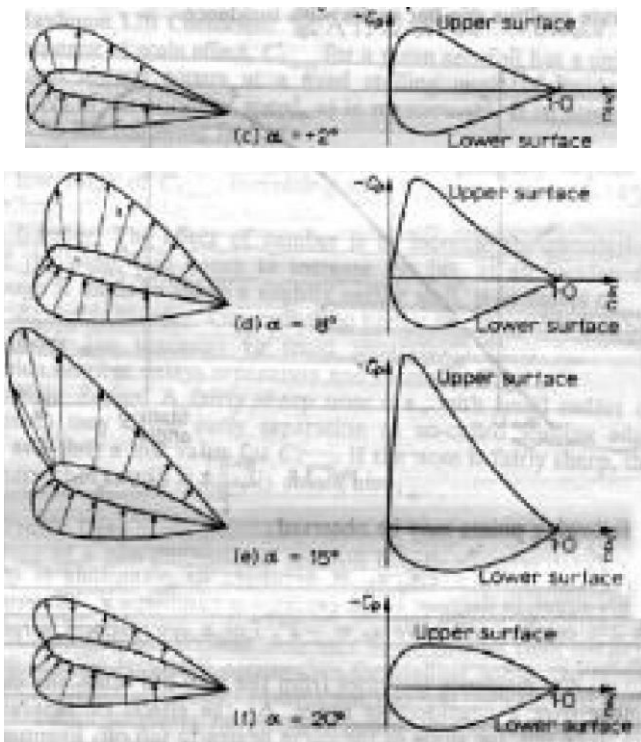
$$N' = -\int_{LE}^{TE} (p_u \cos\theta + \tau_u \sin\theta)\, ds_u + \int_{LE}^{TE} (p_l \cos\theta - \tau_l \sin\theta)\, ds_l$$

$$A' = \int_{LE}^{TE} (-p_u \sin\theta + \tau_u \cos\theta)\, ds_u + \int_{LE}^{TE} (p_l \sin\theta + \tau_l \cos\theta)\, ds_l$$

$$M'_{LE} = \int_{LE}^{TE} [(p_u \cos\theta + \tau_u \sin\theta)x - (p_u \sin\theta - \tau_u \cos\theta)y]\, ds_u$$

$$+ \int_{LE}^{TE} [(-p_l \cos\theta + \tau_l \sin\theta)x + (p_l \sin\theta + \tau_l \cos\theta)y]\, ds_l$$

3.4 Aerodynamic Coefficients (Detailed notes given in the class – Derivation)

Dynamic Pressure: q_∞: **Dynamic pressure** is the kinetic energy per unit volume of a fluid particle.

$$q_{(X)} = \frac{1}{2}\rho_{(X)} V_{(X)}^2$$
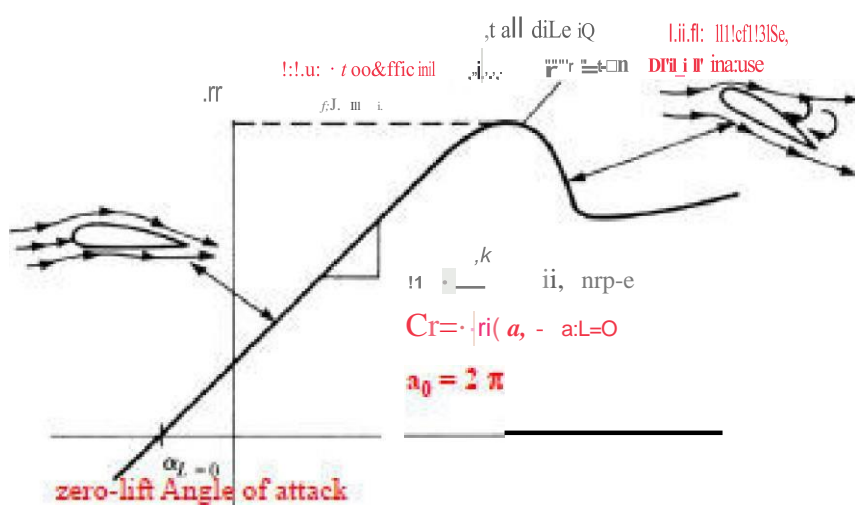
\:.\Rl..\110_- O:F PRE SS1JRE DISTRIBUI I O-   O'\'ER.
AJ AI RFOIL 'l,\iJT H .-\,N GLE OF AIT i\CK

In1. is.cid flow CrO

$$\frac{1}{c}\int_{0}^{c}(C_{p,l} - C_{p,u})\,dx$$

$$= \frac{1}{c^2}\left[\int_{0}^{c}(C_{p,u} - \dots) + \int_{1E}^{TE}(C_{p,u} - \dots)\,dy\,dy\right]$$

$$l = c_n \cos\alpha$$

$$c_d = c_n \sin\alpha + c_a \cos\alpha$$

1'HE LIFT CURVE

$$Cr = ri(a, - a:L=O$$

$$a_0 = 2\pi$$

zero-lift Angle of attack

_____

UNIT - 2
Inviscid Incompressible Flow Airfoil
2. DERIVATION OF THE GOVERNING EQUATIONS

The Conservation of Mass, Momentum and Energy within an infinitesimal small fluid element are the fundamental governing equations of all Computational Fluid Dynamics simulations. Note that one of these laws - the Conservation of Momentum – is also called as the Navier-Stokes equations. We will derive them in this Chapter. The derivation follows that of John D. Anderson's textbook on CFD (published by McGraw-Hill and listed in the Course Outline).

2.1. HISTORY AND BASIC CONCEPT OF THE GOVERNING EQUATIONS

2.1.1. History of Governing Equations of CFD
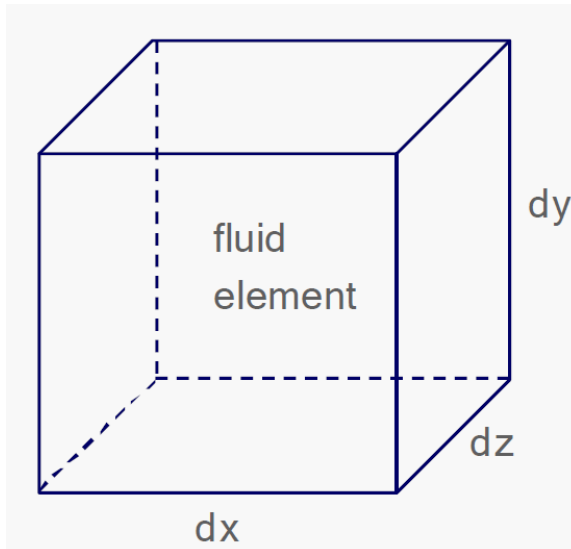
The 3 pillars of the governing equations were derived independently in history. For example, formulating the Conservation of Mass goes back to the times of ancient Greece, while formulating the Conservation of Momentum to the 18th century (formulated by Isaac Newton) and applying this to a viscous fluid to the 19th century (formulated independently by Navier and Stokes).

2.1.2. Basic concept

The basic idea behind developing the Governing Equations for CFD is to apply the 3 fundamental conservation laws, i.e.

- conservation of mass
- conservation of momentum (= Navier-Stokes equations)
- conservation of energy

to an infinitesimally small hexahedral element of dx, dy, dz dimensions (see the figure below).

2.1.3. History of Navier-Stokes equations

The Navier-Stokes equations were derived independently by French scientist Claude-Louis Navier in 1822 and Irish mathematician George Gabriel Stokes in 1845-50. They both excelled in many other fields of science, for example Navier is often viewed as the father of structural analysis (for example, he was the first to describe the equations for the neutral line in bending a beam or to define elastic modulus), while Stokes first defined kinematic viscosity, contributed to optics and spectroscopy.

From Fluid Dynamics point of view, their main contribution was that they were the first ones to apply Newton's 2nd law (conservation of momentum) to an infinitesimal small fluid element with viscosity. Stoke also made assumptions about how shear stress and viscosity relates to each other, the so-called Stokes law. We use these assumptions even nowadays.

2.1.3. "Shelving" and "undusting" the N-S equations

As we will show later, the Governing Equations, - i.e. the Navier-Stokes equations along with the Conservation of Mass and Energy written for an infinitesimal fluid element, - form a set of second order partial differential equations (PDE's), which cannot be solved manually, but which describe all natural laws governing the behaviour of a fluid element.

After their derivation, these equations were "put on a shelf" by history until the arrival of computers in the late 1960's, when they were "undusted" and their solution for some very simple problems was first successfully attempted on a computer. Nowadays, when we have very powerful multi-core computers and even supercomputers available, we can solve full 3D flows over complex configurations, such as cars, aircraft, rockets or even wind farms.

2.2. MATHEMATICAL CONCEPTS FOR DERIVING THE GOVERNING EQUATIONS

Before we show the derivation of the Governing Equations of CFD from first principles, let us review some of the necessary mathematical concepts.

2.2.1. Mathematical description of fluid state in fluid element

Consider:
- 3D Cartesian coordinate system with x, y, z coordinates
- Time denoted by "t"
- density varying with space and time, i.e. $\rho(x,y,z,t)$
- velocity varying with space and time, i.e. $V(x,y,z,t)$, with components:

$$\mathbf{V} = u\mathbf{i} + v\mathbf{j} + w\mathbf{k}$$

where
$$\left.\begin{array}{l} u(x,\ y,\ z,\ t) \\ v(x,\ y,\ z,\ t) \\ w\ (x,\ y,\ z,\ t) \end{array}\right\}$$ 3 components of velocity

---

$$
\left.\begin{matrix} \boldsymbol{i} \\ \boldsymbol{j} \\ \boldsymbol{k} \end{matrix}\right\} \quad \text{unit vectors in } x, y, z \text{ directions}
$$

2.2.2. The difference between partial $(\frac{\partial}{\partial t})$ and total $(\frac{d}{dt})$ derivatives

There are various types of derivatives in mathematics, among them the local $(\frac{\partial}{\partial t})$, and total $(\frac{d}{dt})$ derivatives. For the derivation of the Navier-Stokes equations, we will utilize these within the same equations and therefore we need to understand the difference between them.

PARTIAL DERIVATIVE $(\frac{\partial}{\partial t}, \frac{\partial}{\partial x}, \frac{\partial}{\partial y}, \frac{\partial}{\partial z})$:

Consider a quantity (or variable), which is a function of more than one parameters, e.g.

$$\rho \, (x, y, z, t)$$

Then, the partial derivatives of ρ will be the individual derivatives (i.e. rate of change) of ρ with these parameters, i.e.

partial derivative of density along x	$(\frac{\partial \rho}{\partial x})$
partial derivative of density along y	$(\frac{\partial \rho}{\partial y})$
partial derivative of density along z	$(\frac{\partial \rho}{\partial z})$
partial derivative of density with time t	$(\frac{\partial \rho}{\partial t})$

TOTAL DERIVATIVE $(\frac{d}{dt})$:

Consider again a quantity (or variable), which is a function of more than one parameters, e.g.

$$\rho \, (x, y, z, t)$$

Then, the total derivative of ρ will be $(\frac{d\rho}{dt})$ and it can be obtained by applying the chain rule from differential calculus, i.e.

$$dp = \frac{\partial \rho}{\partial x} dx + \frac{\partial \rho}{\partial y} dy + \frac{\partial \rho}{\partial z} dz + \frac{\partial \rho}{\partial t} dt$$

Dividing by dt leads to:

$$\frac{d\rho}{dt} = \frac{\partial \rho}{\partial t} + \frac{\partial \rho}{\partial x}\frac{dx}{dt} + \frac{\partial \rho}{\partial y}\frac{dy}{dt} + \frac{\partial \rho}{\partial z}\frac{dz}{dt}$$

and since

$$dx/dt = u, \ dy/dt = v, \ \text{and} \ dz/dt = w,$$

the total derivative will essentially become:

$$\frac{d\rho}{dt} = \frac{\partial \rho}{\partial t} + u\frac{\partial \rho}{\partial x} + v\frac{\partial \rho}{\partial y} + w\frac{\partial \rho}{\partial z}$$

Noting that in terms of notation $(\frac{d}{dt})$ is interchangeable with $(\frac{D}{Dt})$, we can write the general form of total derivative as:

$$(\frac{d}{dt}) = \frac{D}{Dt} \equiv \frac{\partial}{\partial t} + u\frac{\partial}{\partial x} + v\frac{\partial}{\partial y} + w\frac{\partial}{\partial z}$$

Since in Cartesian coordinates the vector operator ∇ can be expressed as:
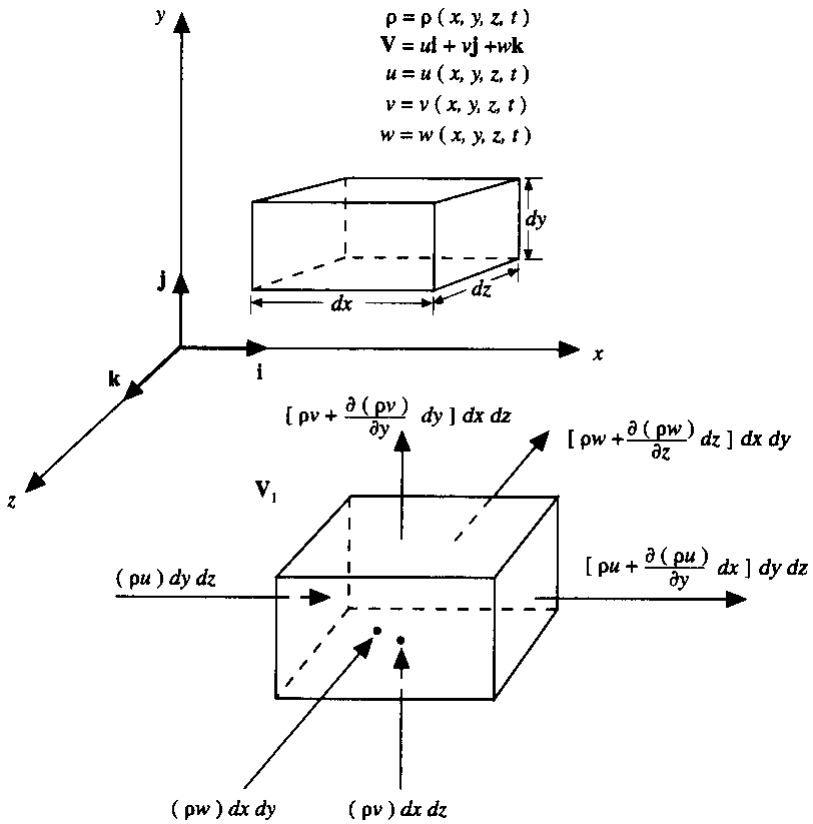
$$\nabla \equiv \mathbf{i}\frac{\partial}{\partial x} + \mathbf{j}\frac{\partial}{\partial y} + \mathbf{k}\frac{\partial}{\partial z}$$

Hence, the general expression for the total derivative is:

$$\frac{D}{Dt} \equiv \frac{\partial}{\partial t} + (\mathbf{V} \cdot \nabla)$$

2.3. CONSERVATION OF MASS FOR A FLUID ELEMENT

Consider the following fluid element, which is <u>fixed in space</u> and through which fluid flows:

$\rho = \rho\,(x, y, z, t)$
$\mathbf{V} = u\mathbf{i} + v\mathbf{j} + w\mathbf{k}$
$u = u\,(x, y, z, t)$
$v = v\,(x, y, z, t)$
$w = w\,(x, y, z, t)$

$[\,\rho v + \frac{\partial\,(\rho v)}{\partial y}\,dy\,]\,dx\,dz$

$[\,\rho w + \frac{\partial\,(\rho w)}{\partial z}\,dz\,]\,dx\,dy$

V_1

$(\rho u)\,dy\,dz$

$[\,\rho u + \frac{\partial\,(\rho u)}{\partial y}\,dx\,]\,dy\,dz$

$(\rho w)\,dx\,dy$ $(\rho v)\,dx\,dz$

Recall from Sec. 1.4.2. that the Conservation of Mass says:

mass outflow – mass inflow   =   decrease of mass in CV

net rate of mass in CV

For the fluid element above (which can be assumed to be a Control Volume – CV), let us first work out the Left Hand Side (LHS):

mass inflow in x **direction:** $(\rho u)\,dy\,dz$

mass outflow in x **direction:** $\left[\rho u + \dfrac{\partial(\rho u)}{\partial x}\,dx\right]dy\,dz$

net rate of mass in CV in x **direction:** $\left[\rho u + \dfrac{\partial(\rho u)}{\partial x}\,dx\right]dy\,dz - (\rho u)\,dy\,dz = \dfrac{\partial(\rho u)}{\partial x}\,dx\,$

_____

net rate of mass in CV in y **direction:** $\left[\rho v + \dfrac{\partial(\rho v)}{\partial y}\, dy\right] dx\ dz - (\rho v)\ dx\ dz = \dfrac{\partial(\rho v)}{\partial y}\, dx$

net rate of mass in CV in z **direction:** $\left[\rho w + \dfrac{\partial(\rho w)}{\partial z}\, dz\right] dx\ dy - (\rho w)\ dx\ dy = \dfrac{\partial(\rho w)}{\partial z}\, dx$

Therefore, the LHS of the above expression will be the sum of the terms for the 3 directions:

$$\textbf{Net mass flow} = \left[\frac{\partial(\rho u)}{\partial x} + \frac{\partial(\rho v)}{\partial y} + \frac{\partial(\rho w)}{\partial z}\right] dx\ dy\ dz$$

Now, the right hand side (RHS) of the Conservation of Mass can mathematically expressed as:

$$\textbf{Time rate of mass decrease} = -\frac{\partial}{\partial t}(\rho.\,dx.\,dy.\,dt)$$

The Conservation of Mass law can be expressed by equating the LHS and RHS expressions as:

$$\left[\frac{\partial(\rho u)}{\partial x} + \frac{\partial(\rho v)}{\partial y} + \frac{\partial(\rho w)}{\partial z}\right] dx\ dy\ dz = -\frac{\partial \rho}{\partial t}(dx\ dy\ dz)$$

$$\frac{\partial \rho}{\partial t} + \left[\frac{\partial(\rho u)}{\partial x} + \frac{\partial(\rho v)}{\partial y} + \frac{\partial(\rho w)}{\partial z}\right] = 0$$

And by recognizing that the term in the bracket is nothing else than $\quad \nabla \cdot (\rho \mathbf{V}) \quad$, one gets:

$$\boxed{\frac{\partial \rho}{\partial t} + \nabla \cdot (\rho \mathbf{V}) = 0}$$

Conservation of Mass for a <u>stationary</u> Fluid Element

Note that this is the Conservation of Mass law written for a stationary fluid element in *partial differential form.*
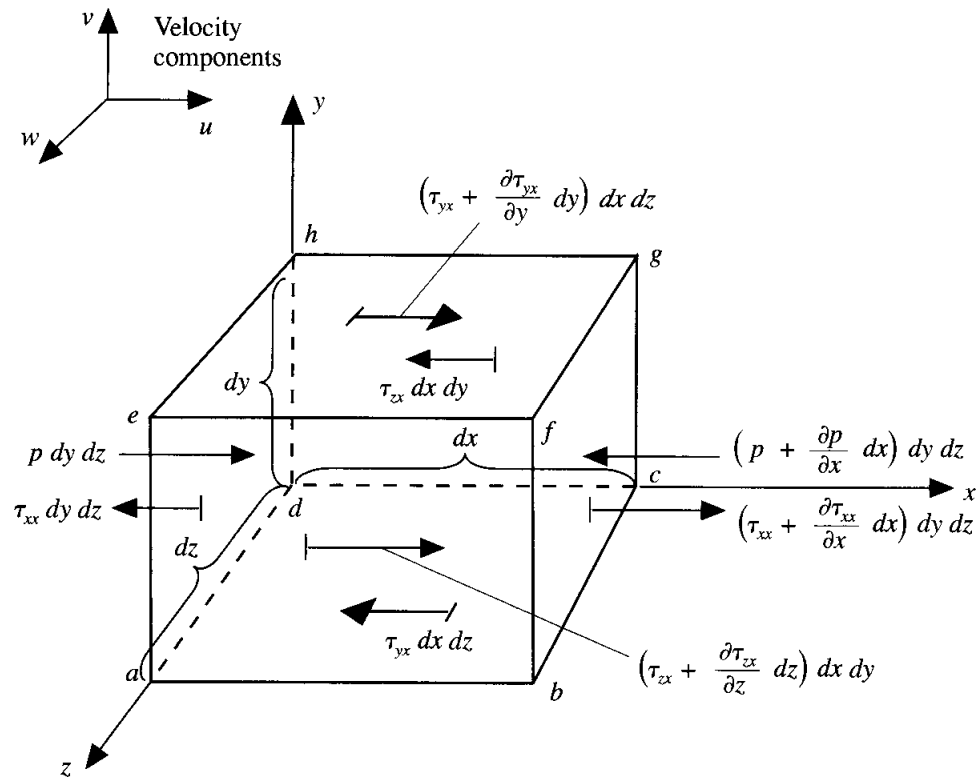
The above expression can be converted to an equivalent form for a moving fluid element (see Anderson for full details). Then the corresponding (and equivalent) form of the above expression will be:

$$\frac{D\rho}{Dt} + \rho \nabla \cdot \mathbf{V} = 0$$

Conservation of Mass for a <u>moving</u> Fluid Element

2.4. CONSERVATION OF MOMENTUM FOR AFLUID ELEMENT

Consider the following fluid element, which is <u>moving in space</u> (note that only forces in the x direction are shown):

Recall from Sec. 1.4.3. that the Conservation of Momentum says:

$$\vec{F} = m\vec{a} = m\frac{d\vec{v}}{dt}$$

_____
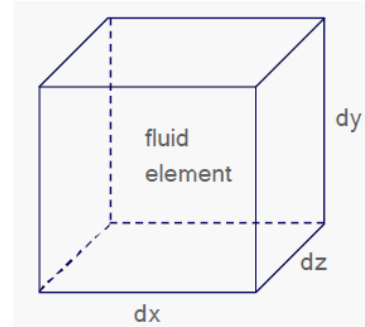
The Left Hand Side (LHS) represent the sum of forces acting on the fluid, which can be decomposed to:
- body forces (gravity)
- pressure forces
- surface forces

Body forces:
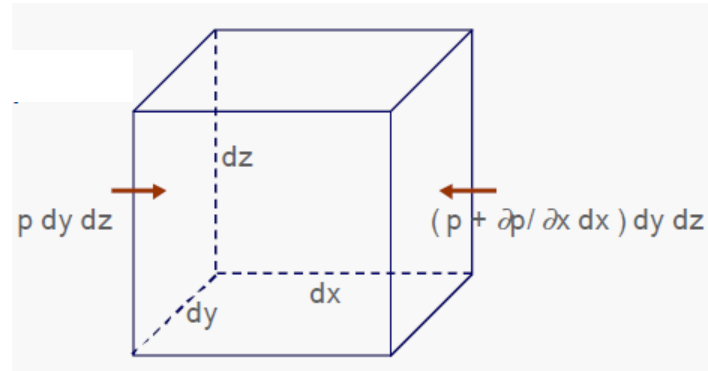
- consider a generic term called body force per unit mass: f
- for the case of gravity: $f = (dm.g/dm) = g$
- then, the generic body force on fluid element: $\rho f \, (dx \, dy \, dz)$

Pressure forces:

- consider the x component only
- pressure force acts normal to the fluid element surfaces
- net pressure force in x direction:

$$\left[p - \left(p + \frac{\partial p}{\partial x} \, dx \right) \right] dy \, dz = -\frac{\partial p}{\partial x} \, dx \, dy \, dz$$

_____

Surface forces:
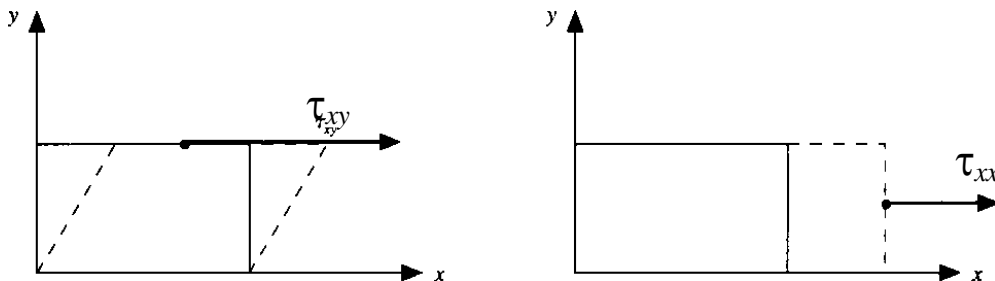
- consider again the x component only
- there are two types of stress acting on the surfaces:
    - normal stress: related to the change in the volume of fluid element
    - shear stress: related to the time rate of change of the shearing deformation

- Notation of stresses:

τ_{jk} means stress in k direction, applied to a surface perpendicular to the j axis

Example: τ_{yx} shear stress in x direction

                      τ_{xx} normal stress in x direction

- Physical meaning:
    - Normal stress: related to pressure orthogonal to surface (see Sec. 1.2.4.)
    - Shear stress: related to friction parallel to surface (see Sec. 1.2.4)

Then, for the fluid element shown earlier, - at the beginning of this section, - one can write the sum of forces acting on the fluid in the x direction as:

$$\textbf{Net force in } x \text{ direction} = \left[p - \left(p + \frac{\partial p}{\partial x} \, dx \right) \right] dy \, dz$$

$$+ \left[\left(\tau_{xx} + \frac{\partial \tau_{xx}}{\partial x} \, dx \right) - \tau_{xx} \right] dy \, dz + \left[\left(\tau_{yx} + \frac{\partial \tau_{yx}}{\partial y} \, dy \right) - \tau_{yx} \right] dx \, dz$$

$$+ \left[\left(\tau_{zx} + \frac{\partial \tau_{zx}}{\partial z} \, dz \right) - \tau_{zx} \right] dx \, dy$$

$$+ \rho f_x \, (dx. dy. dz)$$

_____

Adding and cancelling terms leads to:

$$F_x = \left[-\frac{\partial p}{\partial x} + \frac{\partial \tau_{xx}}{\partial x} + \frac{\partial \tau_{yx}}{\partial y} + \frac{\partial \tau_{zx}}{\partial z} \right] dx\ dy\ dz + \rho f_x\ dx\ dy\ dz$$

Recall, that the Conservation of Momentum is essentially Newton's 2nd law:

$$\vec{F} = m\vec{a} = m\frac{d\vec{v}}{dt}$$

in which we have just worked out the LHS for the x direction, i.e. the x component o F (F_x):

$$F_x = ma_x = m\frac{du}{dt}$$

All we need to do is to work out the terms on the Right Hand Side (RHS) of this expression, i.e. the mass of the fluid element (m):

$$m = \rho\ dV = \rho\ (dx\ dy\ dz)$$

And the acceleration in the x direction (a_x) as:

$$a_x = \frac{du}{dt} \equiv \frac{Du}{Dt}$$

Combining the above results leads to the x component of the Conservation of Momentum:

$$\rho\frac{Du}{Dt} = -\frac{\partial p}{\partial x} + \frac{\partial \tau_{xx}}{\partial x} + \frac{\partial \tau_{yx}}{\partial y} + \frac{\partial \tau_{zx}}{\partial z} + \rho f_x$$

And we could obtain similar expressions for the y and z directions too:

$$\rho\frac{Dv}{Dt} = -\frac{\partial p}{\partial y} + \frac{\partial \tau_{xy}}{\partial x} + \frac{\partial \tau_{yy}}{\partial y} + \frac{\partial \tau_{zy}}{\partial z} + \rho f_y$$

$$\rho\frac{Dw}{Dt} = -\frac{\partial p}{\partial z} + \frac{\partial \tau_{xz}}{\partial x} + \frac{\partial \tau_{yz}}{\partial y} + \frac{\partial \tau_{zz}}{\partial z} + \rho f_z$$

And this is the set of 3 equations originally derived by Navier and Stokes in 1822 and 1845, respectively, which we therefore call the **Navier-Stokes equations.**

In addition, the stress terms can be expressed by a formula, which Stokes proposed first in 1845:

$$\tau_{xx} = \lambda(\nabla \cdot \mathbf{V}) + 2\mu\frac{\partial u}{\partial x}$$

with Stoke's hypothesis:

$$\tau_{yy} = \lambda(\nabla \cdot \mathbf{V}) + 2\mu\frac{\partial v}{\partial y}$$

$$\lambda = -\frac{2}{3}\mu$$

$$\tau_{zz} = \lambda(\nabla \cdot \mathbf{V}) + 2\mu\frac{\partial w}{\partial z}$$

$$\tau_{xy} = \tau_{yx} = \mu\left[\frac{\partial v}{\partial x} + \frac{\partial u}{\partial y}\right]$$

$$\tau_{xz} = \tau_{zx} = \mu\left(\frac{\partial u}{\partial z} + \frac{\partial w}{\partial x}\right)$$

$$\tau_{yz} = \tau_{zy} = \mu\left(\frac{\partial w}{\partial y} + \frac{\partial v}{\partial z}\right)$$

Backsubstituting the above expressions into the Navier-Stokes equations leads to the full form of the Navier-Stokes equations:

$$\frac{\partial(\rho u)}{\partial t} + \frac{\partial(\rho u^2)}{\partial x} + \frac{\partial(\rho uv)}{\partial y} + \frac{\partial(\rho uw)}{\partial z} = -\frac{\partial p}{\partial x}$$

$$+ \frac{\partial}{\partial x}\left(\lambda \nabla \cdot \mathbf{V} + 2\mu \frac{\partial u}{\partial x}\right) + \frac{\partial}{\partial y}\left[\mu\left(\frac{\partial v}{\partial x} + \frac{\partial u}{\partial y}\right)\right]$$

$$+ \frac{\partial}{\partial z}\left[\mu\left(\frac{\partial u}{\partial z} + \frac{\partial w}{\partial x}\right)\right] + \rho f_x$$
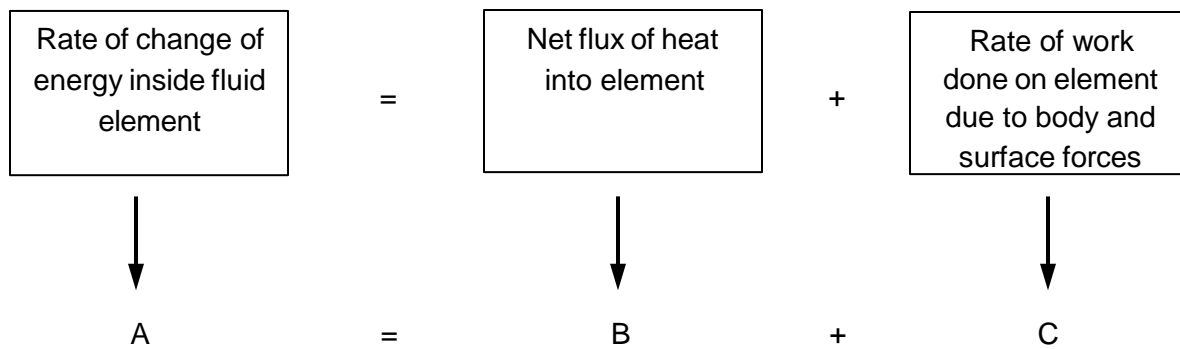
$$\frac{\partial(\rho v)}{\partial t} + \frac{\partial(\rho uv)}{\partial x} + \frac{\partial(\rho v^2)}{\partial y} + \frac{\partial(\rho vw)}{\partial z} = -\frac{\partial p}{\partial y}$$

$$+ \frac{\partial}{\partial x}\left[\mu\left(\frac{\partial v}{\partial x} + \frac{\partial u}{\partial y}\right)\right] + \frac{\partial}{\partial y}\left(\lambda \nabla \cdot \mathbf{V} + 2\mu \frac{\partial v}{\partial y}\right)$$

$$+ \frac{\partial}{\partial z}\left[\mu\left(\frac{\partial w}{\partial y} + \frac{\partial v}{\partial z}\right)\right] + \rho f_y$$

$$\frac{\partial(\rho w)}{\partial t} + \frac{\partial(\rho uw)}{\partial x} + \frac{\partial(\rho vw)}{\partial y} + \frac{\partial(\rho w^2)}{\partial z} = -\frac{\partial p}{\partial z}$$

$$+ \frac{\partial}{\partial x}\left[\mu\left(\frac{\partial u}{\partial z} + \frac{\partial w}{\partial x}\right)\right] + \frac{\partial}{\partial y}\left[\mu\left(\frac{\partial w}{\partial y} + \frac{\partial v}{\partial z}\right)\right]$$

$$+ \frac{\partial}{\partial z}\left(\lambda \nabla \cdot \mathbf{V} + 2\mu \frac{\partial w}{\partial z}\right) + \rho f_z$$

Navier-Stoke equations (Conservation Momentum fo fluid element

2.5. CONSERVATION OF ENERGY FOR AFLUID ELEMENT

Consider a fluid element, in which we will apply the Conservation of Energy principle, i.e. the 1st law of Thermodynamics:

Rate of change of energy inside fluid element	=	Net flux of heat into element	+	Rate of work done on element due to body and surface forces
A	=	B	+	C

Let us expand these terms one by one:

term A: time rate of change of energy inside fluid element

- energy consist of two components: internal energy and kinetic energy
- they are usually expressed in terms of specific energy, i.e.

$$\text{specific energy} = \frac{\text{energy}}{\text{mass}}$$

- internal energy (E):
  - represents energy due to random molecular motion
  - in form of specific internal energy it will be:

$$e = \frac{E}{M}$$

- kinetic energy (E_k):
  - energy due to the motion of fluid
  - in form of specific kinetic energy it will be:

$$e_k = \frac{E_k}{M} = \frac{\frac{1}{2}MV^2}{M} = \frac{V^2}{2}$$

- total specific energy (per unit mass of fluid):

$$e_T = e + e_k = e + \frac{V^2}{2}$$

- total energy for the volume of fluid element:

$$E_T = e_T m = (e + \frac{V^2}{2})\rho dV = (e + \frac{V^2}{2})\rho.\,dx.\,dy.\,dz$$

- time rate of change of energy inside fluid element will be the total derivative of the above, i.e.

$$\boxed{\frac{DE_T}{Dt} \equiv \frac{dE_T}{dt} = \rho\frac{\partial}{\partial t}\left(e + \frac{V^2}{2}\right)dx.\,dy.\,dz} \quad = \quad \textbf{term A}$$

---

term B: net flux of heat into fluid element

- again, consists of two sources:
  - o volumetric heating (such as absorption or radiation)
  - o heat transfer across the surface due to temperature gradients (i.e. thermal conduction)

- heat flux due to volumetric heating

  - o rate of volumetric heat addition per unit mass (for example in J/kg/s units)

  $$q^{\cdot} = \frac{Q}{M} = \frac{1}{M}\left(\frac{\partial Q}{\partial t}\right)$$

  - o Volumetric heating of fluid element

  $$Q^{\cdot} = q^{\cdot}M = q^{\cdot}(\rho.dx.dy.dz) \qquad = \textbf{term B1}$$

- heat flux from thermal conduction across fluid element

  - o heat flux in x direction, i.e. the heat transferred per unit time via thermal conduction in the x direction, i.e. across the $(dy.dz)$ face of fluid element (for example in J/m²/s units)

  $$\dot{q}_x = \frac{\partial Q_x}{\partial t} = \frac{\partial}{\partial t}\left(\frac{\partial Q}{\partial x}\right)$$

  - o heat transferred across the $(dy.dz)$ face of fluid element in unit time

  $$\dot{q}_x(dy.dz)$$

  - o net flux of heat flux in the x direction (i.e. net heat transfer in unit time):

  $$\left[\dot{q}_x - \left(\dot{q}_x + \frac{\partial \dot{q}_x}{\partial x}dx\right)\right] dy\, dz = -\frac{\partial \dot{q}_x}{\partial x}\, dx\, dy\, dz$$

  - o total heat transfer in unit time due to thermal conduction through fluid element (sum for all 3 directions x, y and z):

  $$\text{Heating of fluid element by thermal conduction} = -\left(\frac{\partial \dot{q}_x}{\partial x} + \frac{\partial \dot{q}_y}{\partial y} + \frac{\partial \dot{q}_z}{\partial z}\right) dx\, dy\, dz$$

  $$= \textbf{term B2}$$

  - o From Fourier's law, one can express the heat flux rate as:

  $$\dot{q}_x = -k\frac{\partial T}{\partial x} \qquad \dot{q}_y = -k\frac{\partial T}{\partial y} \qquad \dot{q}_z = -k\frac{\partial T}{\partial z}$$

_____
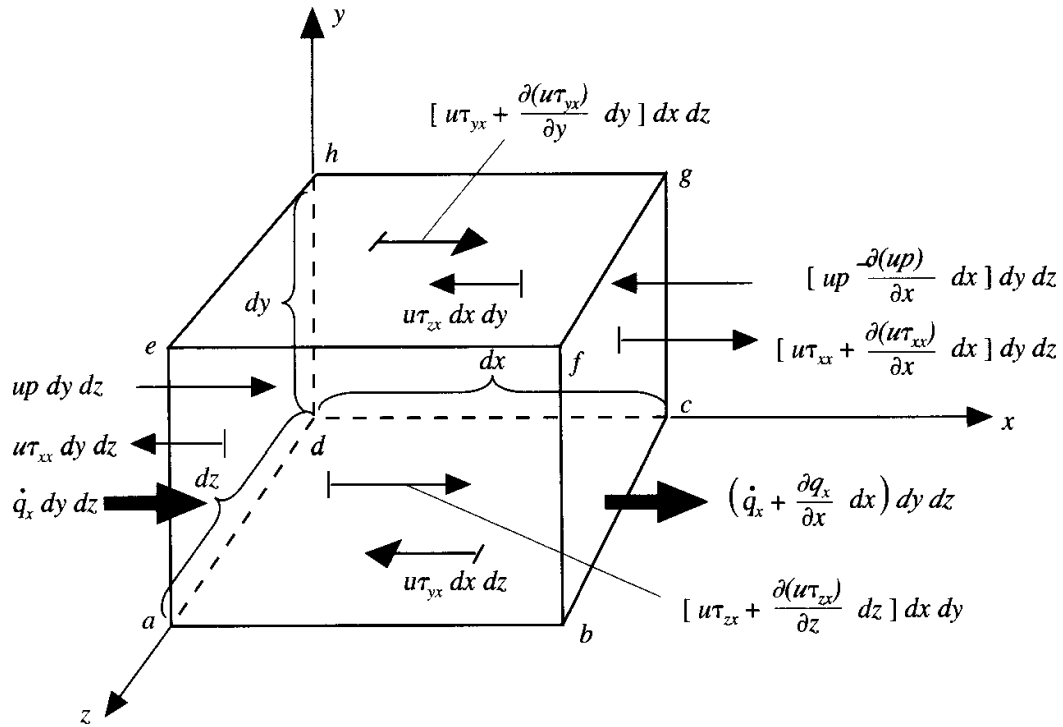
- o Finally the net flux of heat into the fluid element will be the sum of terms B1 and B2:

term B = term B1 + term B2 =

$$= \left[\rho\dot{q} - \left(\frac{\partial \dot{q}_x}{\partial x} + \frac{\partial \dot{q}_y}{\partial y} + \frac{\partial \dot{q}_z}{\partial z} \right) \right] dx \, dy \, dz$$

term B = $\left[\rho\dot{q} + \frac{\partial}{\partial x} \left(k \frac{\partial T}{\partial x} \right) + \frac{\partial}{\partial y} \left(k \frac{\partial T}{\partial y} \right) + \frac{\partial}{\partial z} \left(k \frac{\partial T}{\partial z} \right) \right] dx \, dy \, dz$

term C: rate of work done on a moving fluid element due to body and surface forces

- - rate of work = time rate of change of work = energy consumed

$$\frac{\partial W}{\partial t} = \frac{\partial (F.s)}{\partial t} = F \frac{\partial s}{\partial t} = F.v$$

- - rate of work done by the body force F_b,

$$F_b = m.f = m.g$$

where f is the generic specific body force, g in our case (see Sec. 2.4)

$$W^\cdot{}_b = F_b V = mg V = (\rho.dx.dy.dz).g.V = \rho.f.V(dx.dy.dz)$$

- rate of work done by surface forces:

  o surface forces are

    pressure forces : $(p . dx . dy)$

    shear forces : $(\tau_{yx} . dx. dz)$
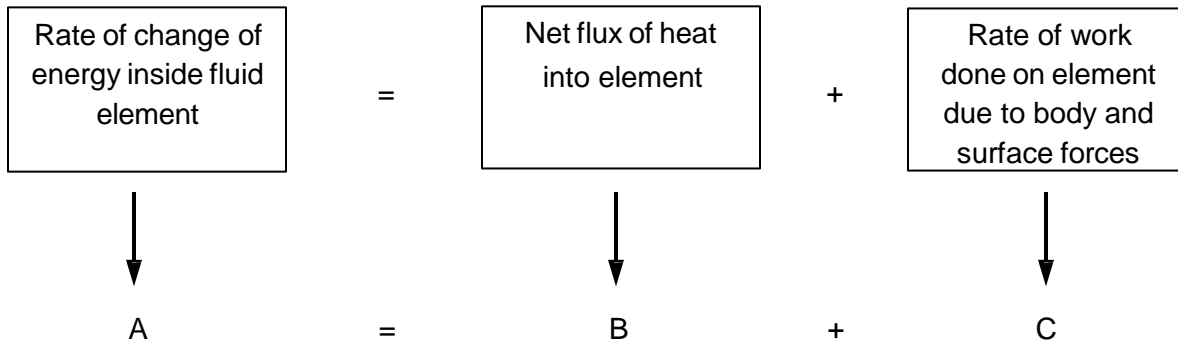
  o the rate of work done by these forces (using again $F.v$ for rate of work):

$$\left[up - \left(up + \frac{\partial(up)}{\partial x} dx \right) \right] dy\ dz = -\frac{\partial(up)}{\partial x} dx\ dy\ dz$$

$$\left[\left(u\tau_{yx} + \frac{\partial(u\tau_{yx})}{\partial y} dy \right) - u\tau_{yx} \right] dx\ dz = \frac{\partial(u\tau_{yx})}{\partial y} dx\ dy\ dz$$

$$\left[-\frac{\partial(up)}{\partial x} + \frac{\partial(u\tau_{xx})}{\partial x} + \frac{\partial(u\tau_{yx})}{\partial y} + \frac{\partial(u\tau_{zx})}{\partial z} \right] dx\ dy\ dz$$

- term C is going to be the sum of the above expressions:

$$C = -\left[\left(\frac{\partial(up)}{\partial x} + \frac{\partial(vp)}{\partial y} + \frac{\partial(wp)}{\partial z} \right) + \frac{\partial(u\tau_{xx})}{\partial x} + \frac{\partial(u\tau_{yx})}{\partial y} \right.$$
$$+ \frac{\partial(u\tau_{zx})}{\partial z} + \frac{\partial(v\tau_{xy})}{\partial x} + \frac{\partial(v\tau_{yy})}{\partial y} + \frac{\partial(u\tau_{zy})}{\partial z} + \frac{\partial(w\tau_{xz})}{\partial x}$$
$$\left. + \frac{\partial(w\tau_{yz})}{\partial y} + \frac{\partial(w\tau_{zz})}{\partial z} \right] dx\ dy\ dz + \rho f \cdot V\ dx\ dy\ dz$$

Thus, the final form of Conservation of Energy equation will be:

Rate of change of energy inside fluid element	=	Net flux of heat into element	+	Rate of work done on element due to body and surface forces

A   =   B   +   C

$$\rho \frac{D}{Dt}\left(e + \frac{V^2}{2}\right) = \rho\dot{q} + \frac{\partial}{\partial x}\left(k\frac{\partial T}{\partial x}\right) + \frac{\partial}{\partial y}\left(k\frac{\partial T}{\partial y}\right) + \frac{\partial}{\partial z}\left(k\frac{\partial T}{\partial z}\right)$$

$$- \frac{\partial(up)}{\partial x} - \frac{\partial(vp)}{\partial y} - \frac{\partial(wp)}{\partial z} + \frac{\partial(u\tau_{xx})}{\partial x} + \frac{\partial(u\tau_{yx})}{\partial y} + \frac{\partial(u\tau_{zx})}{\partial z} + \frac{\partial(v\tau_{xy})}{\partial x} + \frac{\partial(v\tau_{yy})}{\partial y}$$

$$+ \frac{\partial(v\tau_{zy})}{\partial z} + \frac{\partial(w\tau_{xz})}{\partial x} + \frac{\partial(w\tau_{yz})}{\partial y} + \frac{\partial(w\tau_{zz})}{\partial z} + \rho\mathbf{f} \cdot \mathbf{V}$$

Conservation of Energy for a <u>moving</u> fluid element

2.6. CLOSING EQUATIONS

Note that we ended up with 5 equations (1 for Conservation of Mass, 3 for Conservation of Momentum and 1 for Conservation of Energy), but with 6 unknowns:

$$\rho, \; u, \; v, \; w, \; p, \; e$$

This means that we need an additional equation to close the system of equations. For most problems involving gases (and certainly for external flows with air), we can assume that the gas behaves as a perfect gas, end hence the "perfect gas low" (or "state equation") can be used as the 6th equation to close the system:

$$p = \rho R T$$

Perfect Gas Law (1st closing equation)

R: universal gas constant (287.053 J/kg/K for air)
T: temperature (K)

_____

However, this introduces an additional, 7th variable in temperature (T), so we need yet another closing equation linking T and any of the other 6 variables.

Again, for gases we usually choose the caloric state equation for this purpose, which has the form:

$$e = c_V\,T$$

Caloric State Equation (2nd closing equation)

c_V: constant volume specific heat, i.e. the specific heat required to heat up 1 kg fluid by 1 K degree at a constant volume (units in J/kg/K)

2.7. CLOSING REMARKS

We have just derived the Governing Equations of Computational Fluid Dynamics. They are a system of 7 second order partial differential equations with 7 unknowns.

In order to solve this set of partial differential equations, a set of

- **initial conditions** (i.e. the values of ρ, u, v, w, p, e, T at the beginning of time, $t = 0$)
- **boundary conditions** (i.e. the values of ρ, u, v, w, p, e, T at the edges of the domain)

are required.

Although Navier-Stokes equations are just 3 of these 7 equations, in CFD we often call all 7 equations as the "full Navier-Stokes equations".

These equations were derived nearly 200 years ago, and they basically set 7 simple rules of nature, which each fluid element must (and indeed does) follow in a fluid flow, just like the simple rules we follow with our cars in a heavy traffic (i.e. one can leave the highway only at exits, you cannot cross through another car, you must go with the speed and direction of the neighboring cars to avoid collision etc.).

Since this set of partial differential equations (at least so far) could not be solved analytically, the arrival of the computers was needed to be able to solve them numerically (i.e. not with analytical mathematics methods, but with numerical mathematics methods).

The following sections will discuss how to reformulate these Governing Equations so that they can be solved numerically, as well as how to set up the initial and boundary conditions to obtain stable solutions.

1. Uniform flow, Sources, Sinks, Doublets

Reading: Anderson 3.9 – 3.12

Uniform Flow

Definition
A *uniform flow* consists of a velocity field where $\vec{V} = u\hat{\imath} + v\hat{\jmath}$ is a constant. In 2-D, this velocity field is specified either by the freestream velocity components u_∞, v_∞, or by the freestream speed V_∞ and flow angle α.
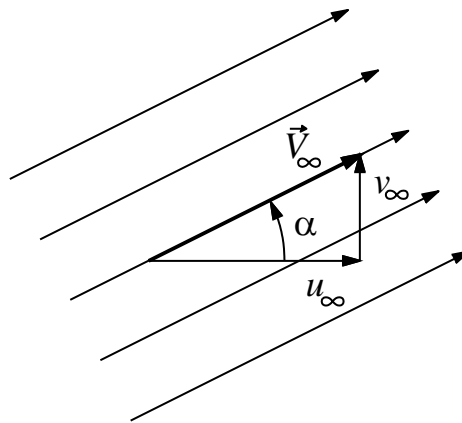
$$u = u_\infty = V_\infty \cos \alpha$$
$$v = v_\infty = V_\infty \sin \alpha$$

Note also that $V_\infty^2 = u_\infty^2 + v_\infty^2$. The corresponding potential and stream functions are

$$\varphi(x, y) = u_\infty x + v_\infty y = V_\infty (x \cos \alpha + y \sin \alpha)$$
$$\psi(x, y) = u_\infty y - v_\infty x = V_\infty (y \cos \alpha - x \sin \alpha)$$

Zero Divergence
A uniform flow is easily shown to have *zero divergence*

$$\nabla \cdot \vec{V} = \frac{\partial u_\infty}{\partial x} + \frac{\partial v_\infty}{\partial y} = 0$$

since both u_∞ and v_∞ are constants.   The equivalent statement is that $\varphi(x, y)$ satisfies Laplace's equation.

$$\nabla^2 \varphi = \frac{\partial^2 (u_\infty x + v_\infty y)}{\partial x^2} + \frac{\partial^2 (u_\infty x + v_\infty y)}{\partial y^2} = 0$$

Therefore, the uniform flow satisfies mass conservation.

Zero Curl
A uniform flow is also easily shown to be irrotational, or to have *zero vorticity*.

$$\nabla^2 \psi = \frac{\partial^2 (u_\infty y - v_\infty x)}{\partial x^2} + \frac{\partial^2 (u_\infty y - v_\infty x)}{\partial y^2} = 0$$

## Source and Sink

Definition
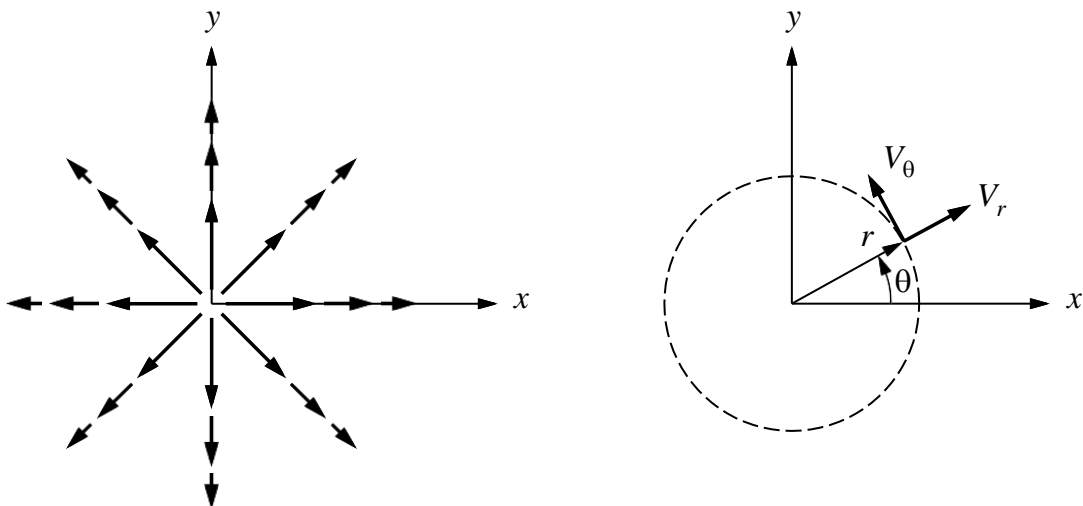
A 2-D *source* is most clearly specified in polar coordinates. The radial and tangential velocity components are defined to be

$$V_r = \frac{\Lambda}{2\pi r} \qquad , \qquad V_\theta = 0$$

where Λ is a scaling constant called the *source strength*. The volume flow rate per unit span $\dot{V}'$ across a circle of radius r is computed as follows.

$$\dot{V}' = \int_0^{2\pi} \vec{V} \cdot \hat{n} \, dA = \int_{2\pi0} V_r \, r \, d\theta = \int_{2\pi0} \frac{\Lambda}{2\pi r} r \, d\theta = \Lambda$$

Hence we see that the source strength Λ specifies the rate of volume flow issuing outward from the source. If Λ is negative, the flow is inward, and the flow is called a *sink*.

Cartesian representation

The cartesian velocity components of the source or sink are

$$u(x, y) = \frac{\Lambda}{2\pi} \frac{x}{x^2 + y^2}$$
$$v(x, y) = \frac{\Lambda}{2\pi} \frac{y}{x^2 + y^2}$$

and the corresponding potential and stream functions are as follows.

$$\varphi(x, y) = \frac{\Lambda}{2\pi} \ln \sqrt{x^2 + y^2} = \frac{\Lambda}{2\pi} \ln r$$

$\nabla^2\varphi = 0$ and $\nabla^2\psi = 0$, and hence represent physically-possible incompressible, irrotational flows.

Singularities

The origin location $(0, 0)$ is called a *singular point* of the source flow. As we approach this point, the magnitude of the radial velocity tends to infinity as

$$V_r \sim \frac{1}{r}$$
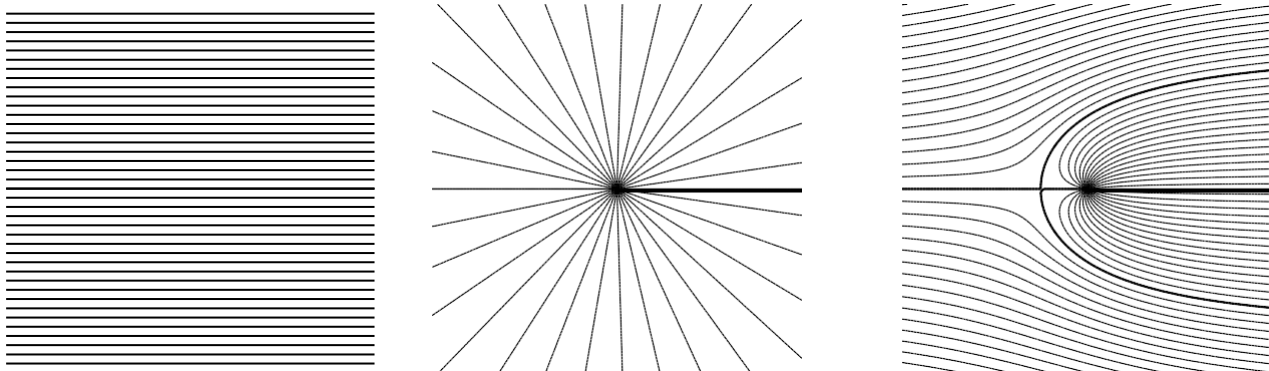
Hence the flow at the singular point is not physical, although this does not prevent us from using the source to represent actual flows. We will simply need to ensure that the singular point is located outside the flow region of interest.

Uniform Flow with Source

Two or more incompressible, irrotational flows can be combined by *superposition*, simply by adding their velocity fields or their potential or stream function fields. Superposition of a uniform flow in the x-direction and a source at the origin therefore has

$$u(x, y) = \frac{\Lambda}{2\pi}\frac{x}{x^2 + y^2} + V_\infty$$

$$v(x, y) = \frac{\Lambda}{2\pi}\frac{y}{x^2 + y^2}$$

or $\quad \varphi(x, y) = \frac{\Lambda}{2\pi}\ln\sqrt{x^2 + y^2} + V_\infty\, x = \frac{\Lambda}{2\pi}\ln r + V_\infty\, r \cos\theta$

or $\quad \psi(x, y) = \frac{\Lambda}{2\pi}\arctan(y/x) + V_\infty\, y = \frac{\Lambda}{2\pi}\theta + V_\infty\, r \sin\theta$
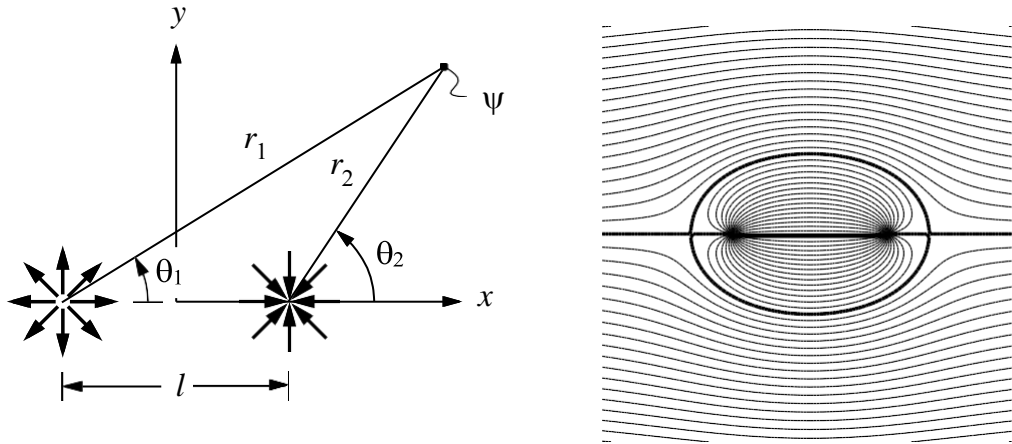
The figure shows the streamlines of the two basic flows, and also the combined flow.

The bullet-shaped heavy line on the combined flow corresponds to the *dividing streamline*, which separates the fluid coming from the freestream and the fluid coming from the source. If we replace the dividing streamline by a solid semi-infinite body of the same shape, the

We now superimpose a uniform flow in the x-direction, with a source located at $(-\ell/2, 0)$, and a sink of equal and opposite strength located at $(+\ell/2, 0)$, plus a freestream.

$$\psi = \frac{\Lambda}{2\pi}(\theta_1 - \theta_2) + V_\infty\, r \sin\theta$$
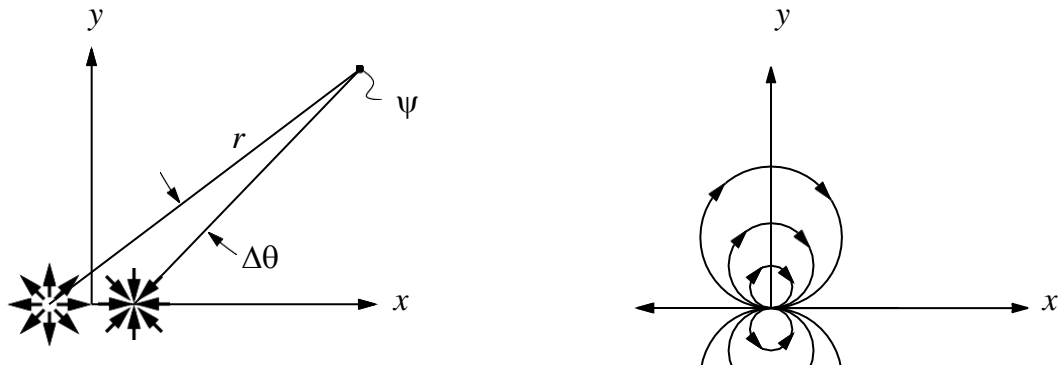
The figure on the right shows the streamlines of the combined flow. The heavy line again indicates the dividing streamline, which traces out a *Rankine oval* . All the streamlines inside the oval originate at the source on the left, and flow into the sink on the right. The net volume outflow from the oval is zero. Again, the dividing streamline could be replaced by a solid oval body of the same shape. The flow outside the oval then corresponds to the flow about this body.

Doublet

Consider a source-sink pair with strengths $\pm\Lambda$, located at $(\mp\ell/2, 0)$. Now let the separation distance ℓ approach zero, while simultaneously increasing the source and sink strengths such that the product $\kappa \equiv \ell\Lambda$ remains constant. The resulting flow is a *doublet* with strength κ.

$$\psi = \lim_{\substack{\ell \to 0 \\ \kappa=\text{const.}}} -\frac{\kappa}{2\pi\ell}\,\Delta\theta = -\frac{\kappa}{2\pi}\frac{\sin\theta}{r}$$

$$\varphi = \frac{\kappa}{2\pi} \frac{\cos\theta}{r}$$

The streamline shapes of the doublet are obtained by setting

$$\psi = -\frac{\kappa}{2\pi} \frac{\sin\theta}{r} = c = \text{constant}$$

$$r = d \sin\theta$$

where $\quad d = -\dfrac{\kappa}{2\pi c}$

In polar coordinates this is the equation for circles of diameter d, centered on $x, y = (0, \pm d/2)$.

Nonlifting Flow over Circular Cylinder
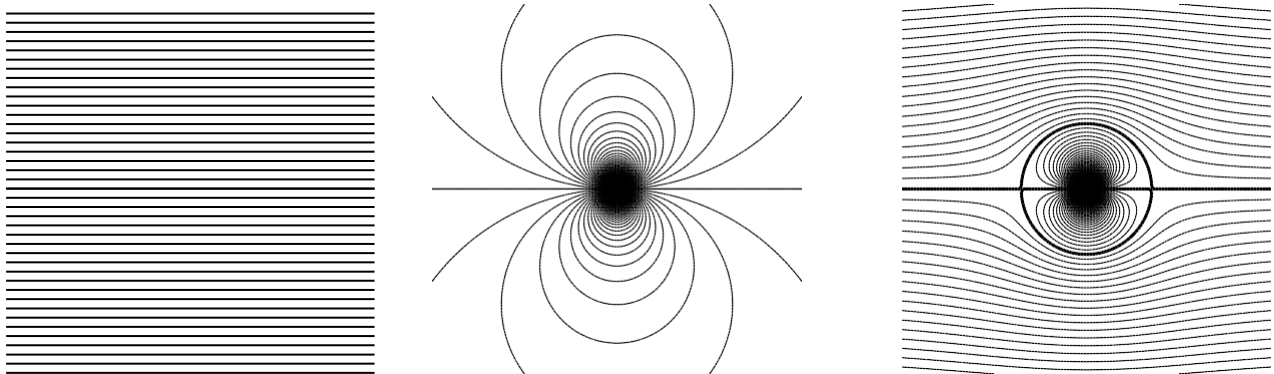
Flowfield definition

We now superimpose a uniform flow with a doublet.

$$\psi = V_\infty r \sin\theta - \frac{\kappa}{2\pi} \frac{\sin\theta}{r} = V_\infty r \sin\theta \left(1 - \frac{\kappa}{2\pi V_\infty r^2}\right)$$

or $\quad \psi = V_\infty r \sin\theta \left(1 - \dfrac{R^2}{r^2}\right)$

where $\quad R^2 \equiv \kappa/(2\pi V_\infty)$

This corresponds to the flow about a circular cylinder of radius R.

The radial and tangential velocities can be obtained by differentiating the stream function as follows.

$$V_r = \frac{1}{r}\frac{\partial\psi}{\partial\theta} = V_\infty \cos\theta \left(1 - \frac{R^2}{r^2}\right)$$

$$V_\theta = -\frac{\partial\psi}{\partial r} = -V_\infty \sin\theta \left(1 + \frac{R^2}{r^2}\right)$$

On the surface of the cylinder where $r = R$, we have

$$V_r = 0$$

$$V_\theta = -2V_\infty \sin \theta$$

The maximum surface speed of $2V_\infty$ occurs at $\theta = \pm 90°$.
The surface pressure is then obtained using the Bernoulli equation

$$p(\theta) = p_o - \frac{1}{2}\rho \left(V_r^2 + V_\theta^2 \right)$$

Substituting $V_r = 0$ and $V_\theta(\theta)$, and using the freestream value for the total pressure,

$$p_o = p_\infty + \frac{1}{2}\rho V_\infty^2$$

gives the following surface pressure distribution.

$$p(\theta) = p_\infty + \frac{1}{2}\rho V_\infty^2 \left(1 - 4 \sin^2 \theta \right)$$

The corresponding pressure coefficient is also readily obtained.

$$C_p(\theta) \equiv \frac{p(\theta) - p_\infty}{\frac{1}{2}\rho V_\infty^2} = 1 - 4 \sin^2 \theta$$

Finite Wing Theory

To date we have considered airfoil theory, or said another way, the theory of infinite wings. Real wings are, of course, finite with a defined length in the "z-direction."

Basic Wing Nomenclature

Wing Span, b – the length of the wing in the z-direction

*Wing Chord, c* – equivalent to the airfoil chord length
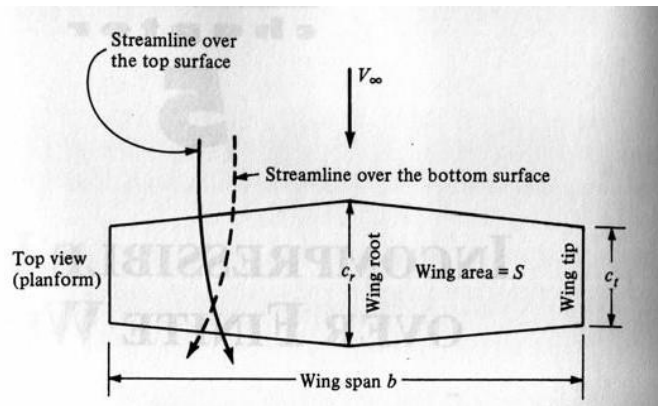
Wing Tip - the end of the wing in the span-wise direction

*Wing Root* – the center of the wing in the span-wise direction
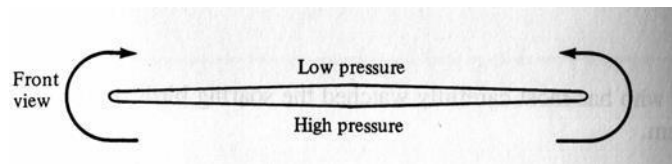
Wing Area, S

*L', D', M'* – two dimensional lift, drag and moment
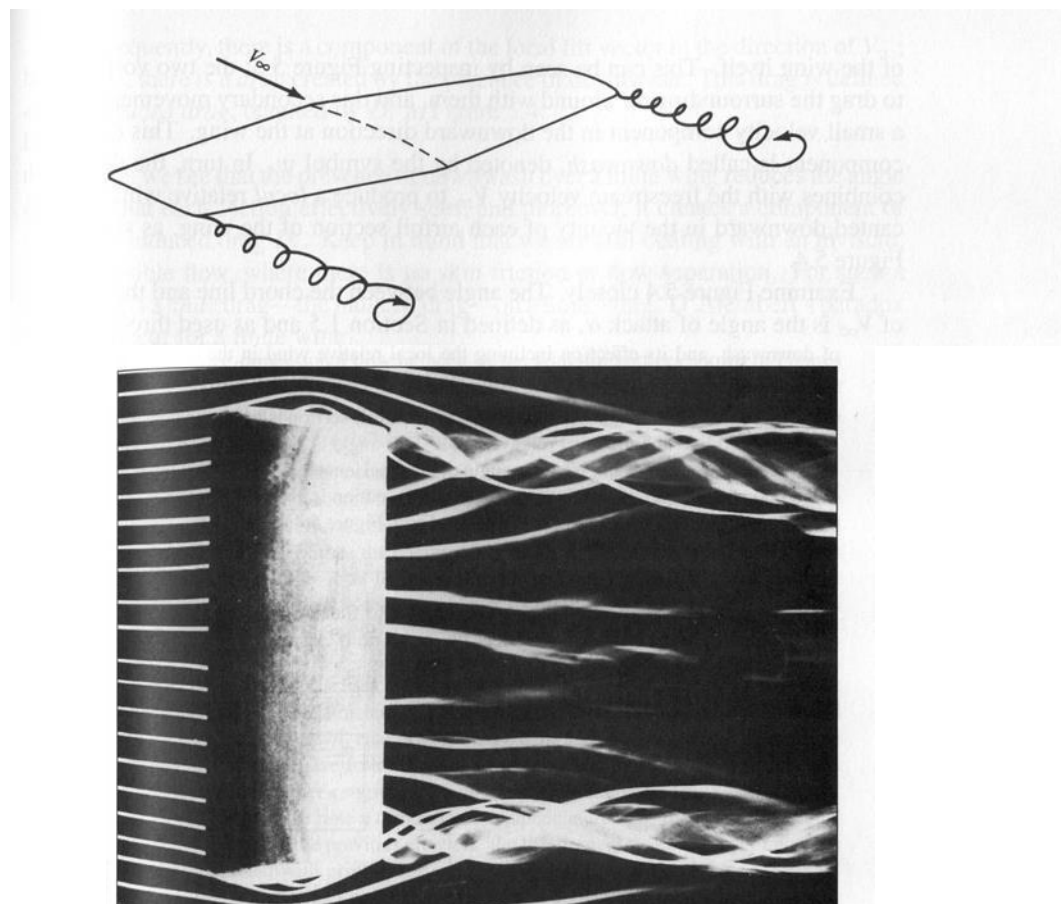
C_L, C_D, C_M - three dimensional lift drag and moment coefficients
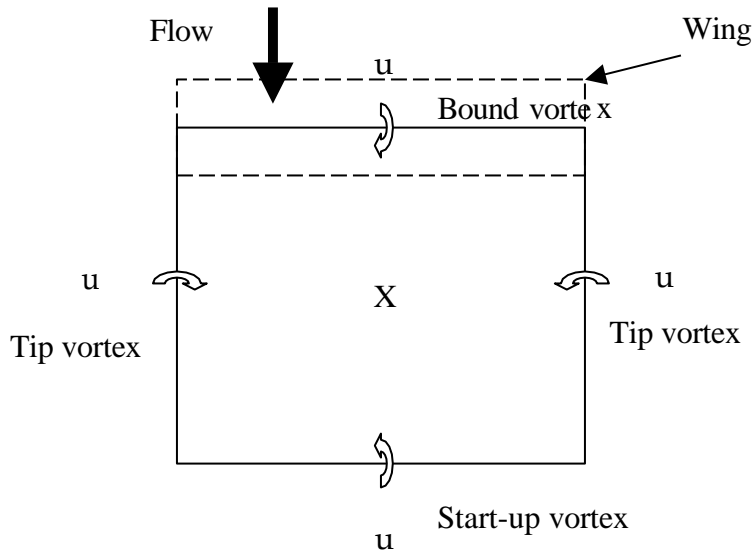
The flow over a finite wing is decidedly three dimensional, with considerable flow possible in the span-wise direction. This comes about because of the pressure difference between the top and bottom of the wing. As in two-dimensional fluid mechanics, the flow wants to move in the direction of a decreasing pressure gradient, i.e., it will usually travel from high to low pressure conditions. In effect the flow spills from the bottom to the top as shown in the figure below.

The span-wise rotation manifests itself as a wing tip vortex that continues downstream.

Interestingly the "sense" (orientation, rotation) of these wing tip vortices is consistent with taking the two-dimensional airfoil circulation, imagining that it exists off to infinity in both directions and bending it back at the wing tips. The idea is also consistent with Kelvin's theorem regarding the start-up vortex. Combining the two ideas one sees that a closed box-like vortex is formed. However, in much of the theory presented next the start-up vortex is ignored and we consider a *horseshoe vortex*.
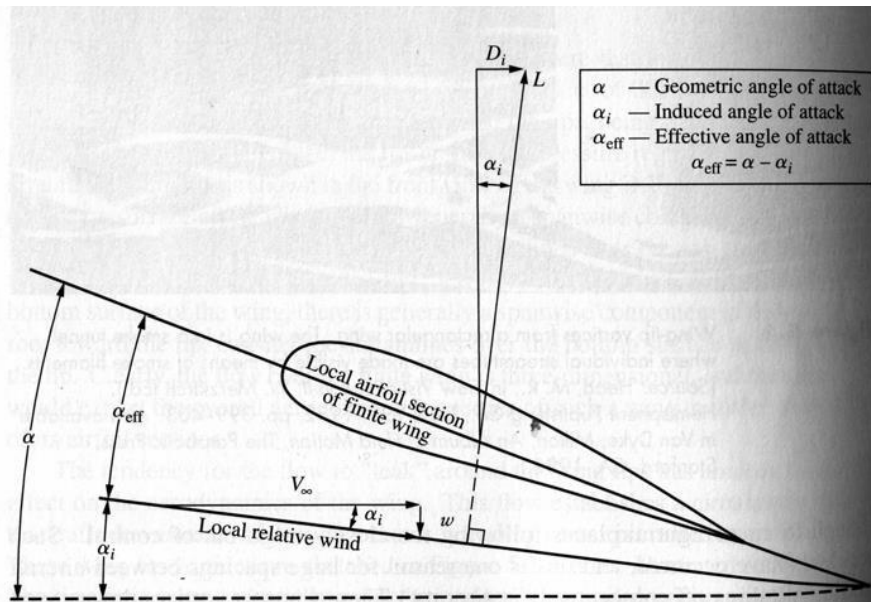
As shown in the figure, the vortices induce flow downward inside the box and upward outside the box. This flow is called the *induced velocity* or *downwash, w*. The strength of these vortices is directly related to the amount of lift generated on the wing. Aircraft inflight spacing is determined in part because of these wingtip vortices. An example is the Airbus aircraft that crashed at JFK a few days after 9/11. The spacing was too small and the Airbus's tail was buffeted by the wake vortices off a JAL 747 that was ahead of it in the flight path.

Angle of Attack

The idea that vortex motion induces downward flow changes the way we have to look at angle of attack as compared to the airfoil theory.

Geometric angle of attack, α - the angle between the airfoil chord line and the freestream velocity vector.

Induced angle of attack, α_i – the angle formed between the local relative wind and the undisturbed freestream velocity vector.

$$\tan\alpha_i = \frac{w}{V_\infty} \tag{5.1}$$

Effective angle of attack, α_{eff} – the angle formed between the airfoil chord and the local relative wind.

$$\alpha_{eff} = \alpha - \alpha_i \tag{5.2}$$

It is important to note that this also changes how we look at lift, *L,* and drag, *D.* This is because the actual lift is oriented

perpendicular to the local relative wind (since that is the wind that it sees) not the freestream velocity direction. Because of that, when we go back to our original lift and drag directions (perpendicular and parallel to the freestream) we now see a reduction in the lift as compared to what we expect from the airfoil theory and an actual drag called the *induced drag,* even though the flow is still inviscid.

What a Drag

Induced drag, D_i – drag due to lift force redirection caused by the induced flow or downwash.

Skin friction drag, D_f – drag caused by skin friction.

Pressure drag, D_p – drag due to flow separation, which causes pressure differences between front and back of the wing.

Profile drag coefficient, C_d – sum of the skin friction and pressure drag. Can be found from airfoil tests. Note the notation.
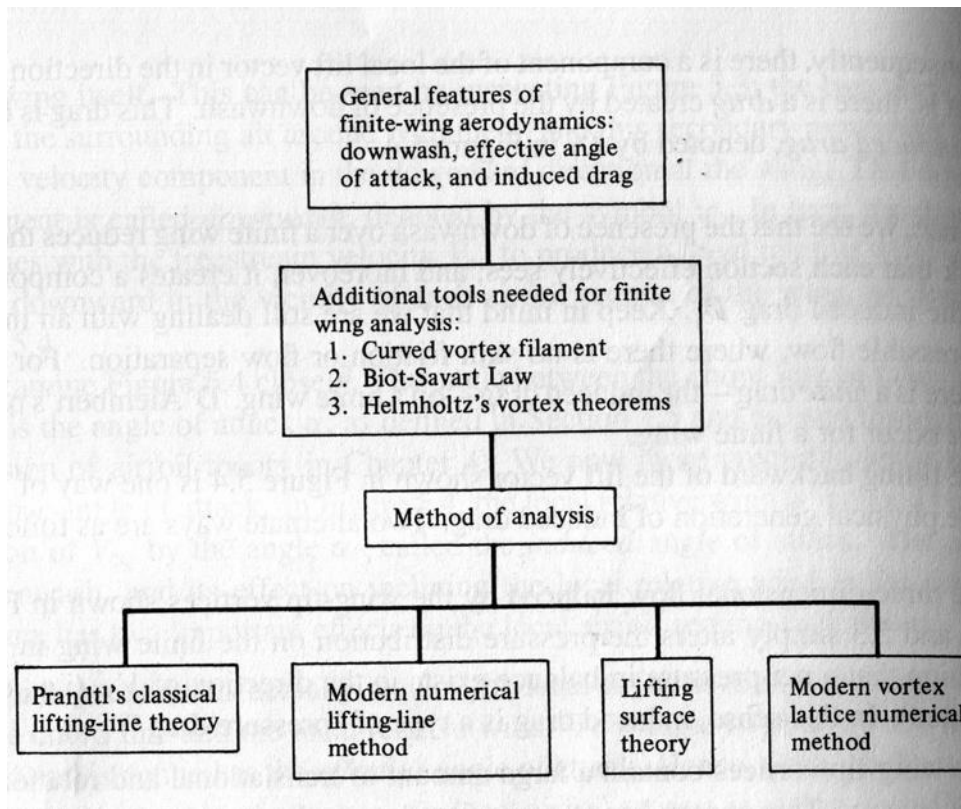
$$C_d = \frac{D_f + D_p}{q_\infty S} \tag{5.3}$$

Induced drag coefficient, C_{D_i} - nondimensional induced drag

$$C_{D_i} = \frac{D_i}{q_\infty S} \tag{5.4}$$
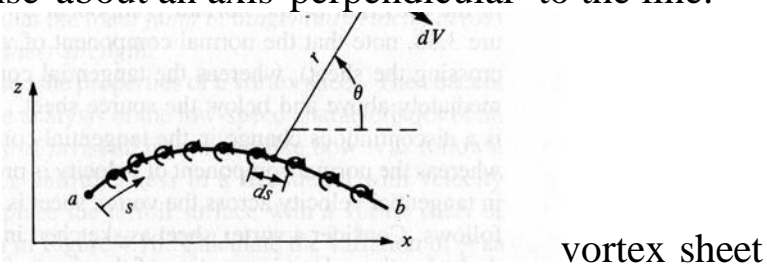
Total drag coefficient, C_D

$$C_D = C_d + C_{D_i} \tag{5.5}$$

General features of finite-wing aerodynamics: downwash, effective angle of attack, and induced drag

Additional tools needed for finite wing analysis:
1. Curved vortex filament
2. Biot-Savart Law
3. Helmholtz's vortex theorems

Method of analysis

| Prandtl's classical lifting-line theory | Modern numerical lifting-line method | Lifting surface theory | Modern vortex lattice numerical method |

Biot-Savart Law

During our discussion of panel methods we developed the idea of a vortex sheet, essentially a line along which vorticity occurs that has a rotation sense about an axis perpendicular to the line.

vortex sheet

A similar but distinctly different idea is that of *vortex filament*, which is again a line of vorticity, but this time with rotation about the line itself.
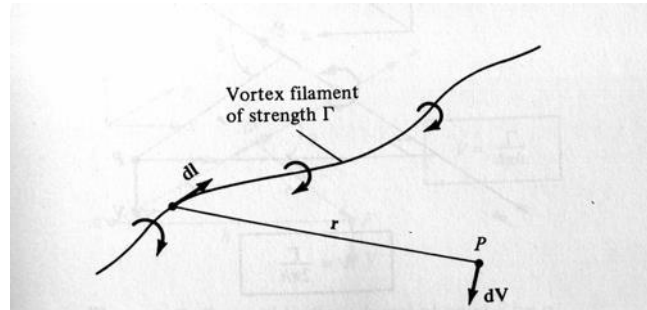
Vortex filament

The **Biot-Savart Law** defines the velocity induced by an infinitesimal length, **dl**, of the vortex filament as

$$dV = \frac{\Gamma}{4\pi} \frac{dl \times r}{|r^3|}$$

(5.6)

where

Vortex filament
of strength Γ

dl – infinitesimal length along the vortex filament
r – radius vector from **dl** to some point in space, P.
dV – infinitesimal induced velocity
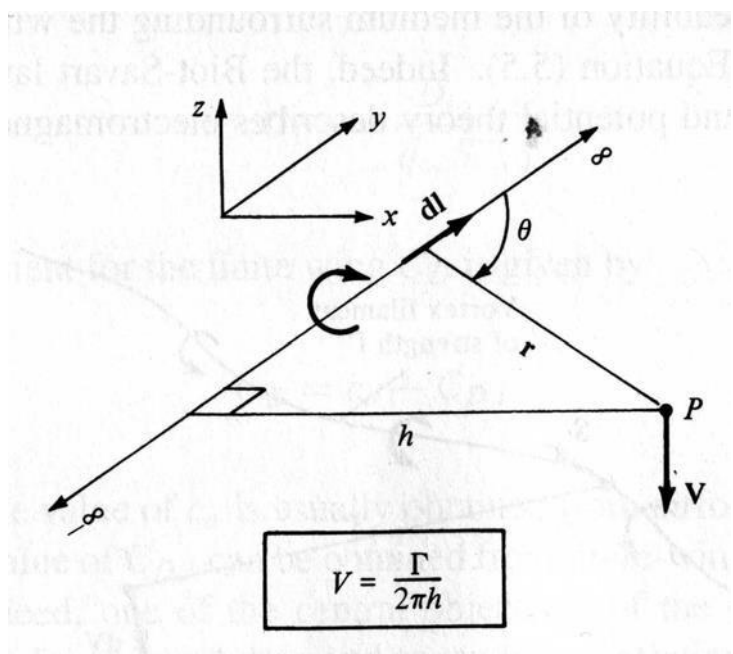
Note that this velocity is perpendicular to both **dl** and **r.**

If the vortex filament has infinite length the total induced velocity is found by integrating over its entire length

$$V = \int_{-\infty}^{\infty} \frac{\Gamma}{4\pi} \frac{dl \times r}{|r^3|}$$

(5.7)

Consider a straight vortex filament in the y-direction and a point, P, in the x-y plane. Equation (5.7) can be put into geometric functions by considering the figure below

$$V = \frac{\Gamma}{2\pi h}$$

$$V = \int_{-\infty}^{\infty} \frac{\Gamma}{4\pi} \frac{\sin\theta}{r^2} dl \qquad (5.8)$$

where θ is the angle formed by r and the filament. The geometry gives

$$r = \frac{h}{\sin\theta}, l = \frac{h}{\tan\theta}, dl = \frac{h}{\sin^2\theta} d\theta \qquad (5.9)$$

which gives

$$V = -\frac{\Gamma}{4\pi h} \int_{\pi}^{o} \sin\theta d\theta \qquad (5.10)$$

we get $l \to \pm\infty$ if we have $\theta=0$ or B.
This leads to the simple result

$$V = \frac{\Gamma}{2\pi h} \qquad (5.11)$$

same as the two dimensional theory.

If we have a "semi-infinite" filament we get

$$V = \frac{\Gamma}{4\pi} \int_0^\infty \frac{\sin\theta}{r^2} \, dl = -\frac{\Gamma}{4\pi h} \int_{\pi/2}^0 \sin\theta \, d\theta \qquad (5.12)$$

$$V = \frac{\Gamma}{4\pi h}$$

Helmholtz Theorem

1. Strength of a vortex filament remains the same along the filament.
2. A vortex filament cannot end in a fluid, i.e., it must either extend to the boundaries or form a closed path.

Additional Nomenclature

    Geometric twist – a twist of the wing about the span-wise axis that results in a change in the geometric angle of attack with span-wise position.
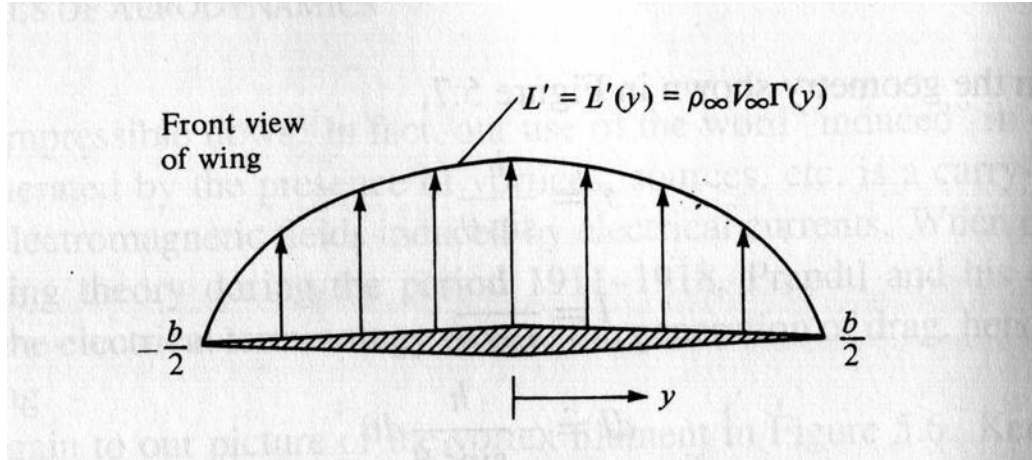
    Washout – geometric twist such that $\alpha_{tip} < \alpha_{root}$

    Washin - geometric twist such that $\alpha_{tip} > \alpha_{root}$

    Aerodynamic twist – a wing with different airfoil sections along the span, so that the zero lift angle of attack changes with span-wise position.

   Lift distribution – the local value of the lift force. This can change with span-wise position.

For example, since the pressure equalizes at the tip there is no lift there.
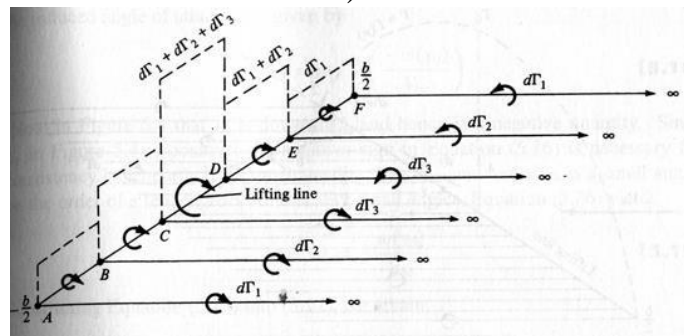
   Lift per unit span, $\boldsymbol{L'}$ - akin to pressure, i.e., force per unit area.

$$\boldsymbol{L'} = \rho_\infty V_\infty \Gamma(\boldsymbol{y}) \tag{5.13}$$

$$\boldsymbol{L} = \int\limits_{-b/2}^{b/2} \boldsymbol{L'}(\boldsymbol{y})d\boldsymbol{y} \tag{5.14}$$

If the lift changes along the span it implies that there are multiple (perhaps and infinite number of) vortex filaments.
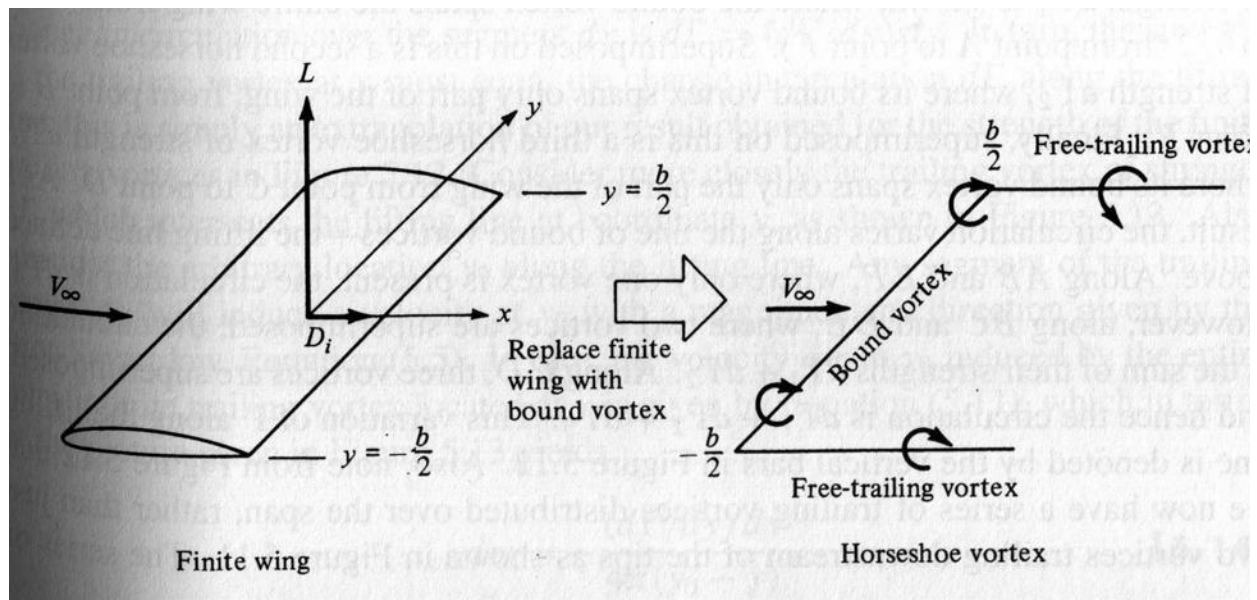
Prandtl's Lifting Line Theory

Prandtl's lifting line theory is centered about a fundamental integro-differential equation.

$$\alpha(y_o) = \frac{\Gamma(y_o)}{\pi V_\infty c(y_o)} + \alpha_{L=0}(y_o) + \frac{1}{4\pi V_\infty} \int_{-b/2}^{b/2} \frac{\left(\frac{d\Gamma}{dy}\right) dy}{y_o - y} \qquad (5.15)$$

which is used to find the circulation distribution about the wing. Equation (5.15) is useful if one knows the desired geometric angle of attack, the aerodynamic twist (i.e., "$_{L=0}$), and the wing planform (i.e., local chord length). Two approaches are presented to make use of this equation. Equation (5.15) is developed from the idea of vortex filaments.

Prandtl's lifting line theory stems from the idea of replacing a wing with a bound vortex. Helmholtz theorem then requires there to exist trailing vortices at the wing tips

Finite wing   Replace finite wing with bound vortex   Horseshoe vortex

The Biot-Savart law allows us to determine the downwash along the wing and results in:
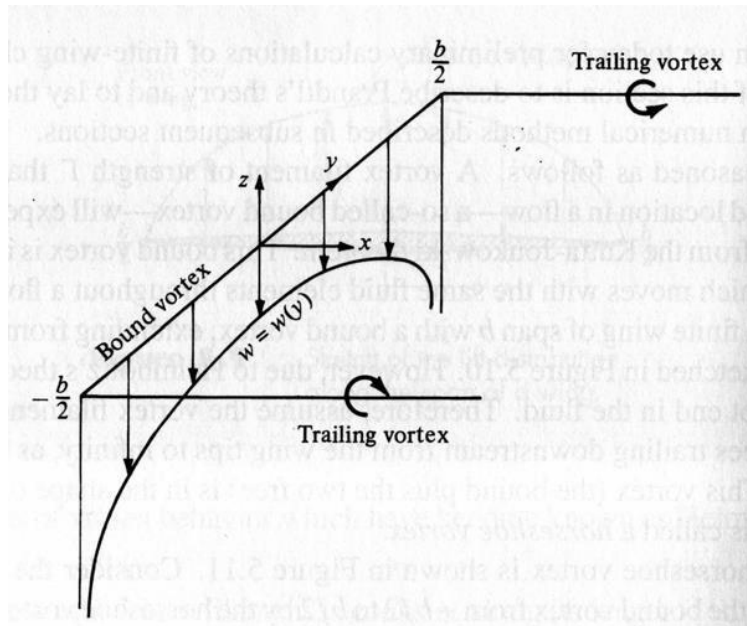
$$w(y) = - \frac{\Gamma}{4\pi \left(\frac{b}{2} + y\right)} - \frac{\Gamma}{4\pi \left(\frac{b}{2} - y\right)} \tag{5.16}$$

or
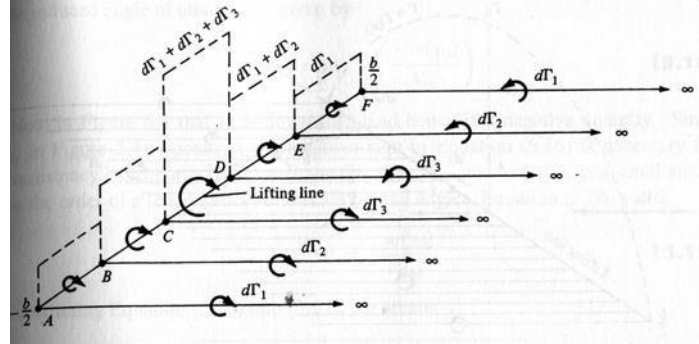
$$w(y) = -\frac{\Gamma}{4\pi} \frac{b}{\left(\frac{b}{2}\right)^2 - y^2} \tag{5.17}$$

Note that the downwash is a negative number as you would expect from the coordinate system.
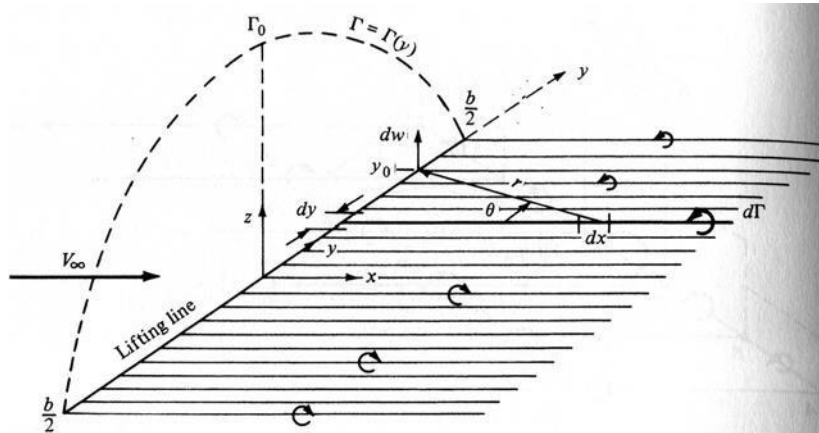
However, the single vortex filament case is not sufficient to describe the physical conditions on the wing, because of

The trouble is that the downwash at the wing tips is infinite instead of zero. Fortunately, this can be fixed if one considers a distribution of vortex filaments as shown below

It is important to note that the strength of the individual vortex filaments is equal to the jump in circulation at the point where the trailing vortex meets the bound vortex. This can be carried to the logical extreme by considering a continuous sheet of vortex filaments and their associated continuous change in circulation.

In that case the downwash induced at point y_o by the vortices at point y is given by

$$dw(y_o) = \frac{\left(\left|\frac{d\Gamma}{dy}\right|\right)|dy}{4\pi(y_o - y)} \qquad (5.18)$$

So that if one integrates from wingtip to wingtip

$$w(y_o) = -\frac{1}{4\pi} \int_{-b/2}^{b/2} \frac{\left(\frac{d\Gamma}{dy}\right) dy}{(y_o - y)}$$ (5.19)

Relationship between ' distribution and downwash at y_o

Using Equation (5.1), but recognizing that w is a negative number

$$\alpha_i(y_o) = \tan^{-1}\left(\frac{-w(y_o)}{V_\infty}\right)$$ (5.1b)

for small angles Eq. (5.1b) gives

$$\alpha_i(y_o) = \frac{1}{4\pi V_\infty} \int_{-b/2}^{b/2} \frac{\left(\frac{d\Gamma}{dy}\right) dy}{(y_o - y)}$$ (5.20)

Recall the two dimensional lift coefficient for an airfoil

$$C_l \left[=a_o \, \alpha_{eff} - \alpha_{L=0}\right] = 2\pi \left[\alpha_{eff}\right] - \alpha_{L=0}$$ (5.21)

where

$$\alpha_{eff} = \alpha_{eff}(y_o) \text{ because of downwash}$$

$$\alpha_{L=0} = \alpha_{L=0\,f}(y_o) \text{ because of aerodynamic twist}$$

but

$$L' = \frac{1}{2}\rho_\infty V_\infty^2 c(y_o) C_l = \rho_\infty V_\infty \Gamma(y_o)$$ (5.22)

then

$$C_l = \frac{2\Gamma(y_o)}{V_\infty c(y_o)} \qquad (5.23)$$

Combining Eqs. (5.21) & (5.23) gives

$$\alpha_{eff} = \frac{\Gamma(y_o)}{\pi V_\infty c(y_o)} + \alpha_{L=0} \qquad (5.24)$$

which is clearly a function of y_o.

Recall notes Eq. (5.2)

$$\alpha_{eff} = \alpha - \alpha_i \qquad (5.2)$$

and combine Eq. (5.2) with (5.24) & (5.20) to get

$$\alpha(y_o) = \frac{\Gamma(y_o)}{\pi V_\infty c(y_o)} + \alpha_{L=0}(y_o) + \frac{1}{4\pi V_\infty} \int_{-b/2}^{b/2} \frac{\left(\frac{d\Gamma}{dy}\right)dy}{y_o - y} \qquad (5.15)$$

Fundamental Equation of Prandtl's Lifting Line Theory

Once $\Gamma(y_o)$ is known L, C_L, D_i, C_{D_i} follow directly.

$$L'(y_o) = \rho_\infty V_\infty \Gamma(y_o) \qquad (5.13)$$

$$L = \int_{-b/2}^{b/2} L'(y)dy \qquad (5.14)$$

$$C_L = \frac{2}{V_\infty S} \int_{-b/2}^{b/2} \Gamma(y)\,dy \tag{5.25}$$

$$D_i = \int_{-b/2}^{b/2} L_i' \alpha_i\,dy \tag{5.26}$$

$$C_{D_i} = \frac{2}{V_\infty S} \int_{-b/2}^{b/2} \Gamma(y)\alpha_i(y)\,dy \tag{5.27}$$
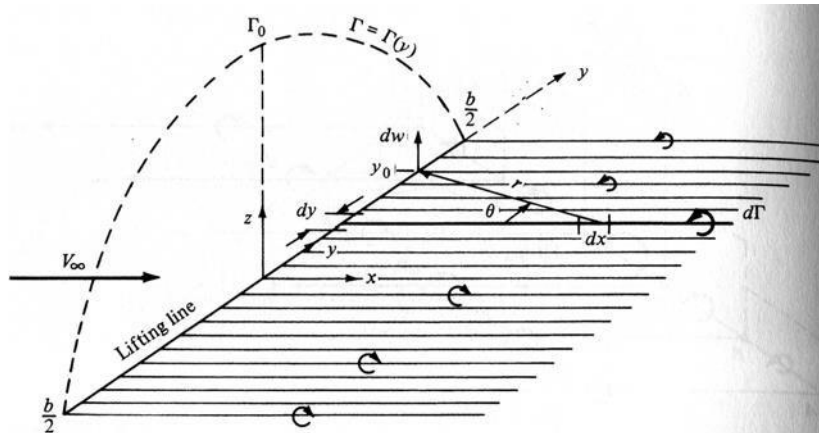
Two approaches can be taken from this point

1. *Direct* – A wing planform is given with a distribution of aerodynamic twist, Eq. (5.15) is solved and lift and drag information extracted.
2. *Inverse* – A lift distribution is proposed and the corresponding planform distribution developed.

Inverse Approach – Elliptic Lift Distribution

Prandtl's lifting line theory can be used in an inverse approach by assuming the form of the lift distribution and using Eq. (5.15) to determine the wing planform. The most famous example of this is the *elliptic lift distribution* which is found directly from an *elliptic circulation distribution*.

$$\Gamma(y) = \Gamma_o \sqrt{1 - \left(\frac{2y}{b}\right)^2} \qquad (5.28)$$

where we can use $L'(y) = \rho_\infty V_\infty \Gamma(y)$ to show

$$L'(y) = \rho_\infty V_\infty \Gamma_o \sqrt{1 - \left(\frac{2y}{b}\right)^2} \qquad (5.29)$$

Recall that Eq. (5.19) requires $\dfrac{d\Gamma}{dy}$, so

$$\frac{d\Gamma}{dy} = -\frac{4\Gamma_o}{b^2} \frac{y}{\sqrt{1 - \dfrac{4y^2}{b^2}}} \qquad (5.30)$$

so that the downwash becomes

$$w(y_o) = \frac{\Gamma_o}{\pi b^2} \int_{-b/2}^{b/2} \frac{y}{\sqrt{1 - \dfrac{4y^2}{b^2}}\,(y_o - y)}\,dy \tag{5.31}$$

we can again invoke geometry and use

$$y = \frac{b}{2}\cos\theta, \qquad dy = -\frac{b}{2}\sin\theta\, d\theta \tag{5.32}$$

where $\theta : \pi \to 0$ as $y : -\dfrac{b}{2} \to \dfrac{b}{2}$

So Eq. (5.31) becomes

$$w(\theta_o) = -\frac{\Gamma_o}{2\pi b}\int_{\pi}^{0} \frac{\cos\theta}{\cos\theta_o - \cos\theta}\, d\theta \tag{5.33}$$

or

$$w(\theta_o) = -\frac{\Gamma_o}{2\pi b}\int_{0}^{\pi} \frac{\cos\theta}{\cos\theta - \cos\theta_o}\, d\theta \tag{5.34}$$

which is a standard integral form

$$w(\theta_o) = -\frac{\Gamma_o}{2\pi b}\frac{\pi \sin n\theta_o}{\sin\theta_o} \qquad \text{with } n{=}1 \tag{5.35}$$

$$w(\theta_o) = -\frac{\Gamma_o}{2b} \tag{5.36}$$

Downwash is constant for an Elliptical Lift Distribution

However, this also implies:

$$\alpha_i = -\frac{w}{V_\infty} = \frac{\Gamma_o}{2bV_\infty} \tag{5.37}$$

Induced a.o.a. is constant for an Elliptical Lift Distribution

In the end we want to determine the lift and drag coefficient for the elliptic lift distribution and also the shape of this wing. To do this we go back to Eqs. (5.14) and (5.29)

$$L = \int_{-b/2}^{b/2} L'(y)\,dy = \rho_\infty V_\infty \Gamma_o \int_{-b/2}^{b/2}\sqrt{1-\left(\frac{2y}{b}\right)^2}\,dy$$

$$= \rho_\infty V_\infty \Gamma_o \int_0 \sqrt{1-\cos^2\theta}\left(-\frac{b}{2}\right)\sin\theta\,d\theta$$

$$= \rho_\infty V_\infty \Gamma_o \frac{b}{2}\pi \int_0^\pi \sqrt{\sin^2\theta}\,\sin\,d\theta = \rho_\infty V_\infty \Gamma_o \frac{b}{2}\pi \int_0^\pi \sin^2\theta\,d\theta \tag{5.38}$$

$$= \rho_\infty V_\infty \Gamma_o \frac{b}{2}\left[\frac{\theta}{2} - \frac{\sin 2\theta}{4}\right]_0^\pi = \rho_\infty V_\infty \Gamma_o \frac{b}{2}\,\frac{\pi}{2}$$

$$L = \rho_\infty V_\infty \Gamma_o \frac{b\pi}{4}$$

$$\tag{5.39}$$

We can next use the definition of C_L and Eq. (5.39) to give

$$L = \frac{1}{2}\rho_\infty V_\infty^2 SC_L = \rho_\infty V_\infty \Gamma_o \frac{b}{4}\pi \qquad (5.40)$$

or

$$\Gamma_o = \frac{2V_\infty SC_L}{b\pi} \qquad (5.41)$$

Then going back to Eq. (5.37) we find

$$\alpha_i = \frac{\Gamma_o}{2bV_\infty} = \frac{SC_L}{b^2\pi} \qquad (5.42)$$

Nomenclature

Aspect Ratio, $AR = \dfrac{b^2}{S}$ \qquad (5.43)

So that

$$\alpha_i = \frac{C_L}{\pi AR} \qquad (5.44)$$

We can then get induced drag from Eq. (5.27)

$$C_{D_i} = \frac{2}{V_\infty S} \int_{-b/2}^{b/2} \Gamma(y)\alpha_i(y)dy \qquad (5.27)$$

$$C_{D_i} = \frac{2\alpha_i}{V_\infty S} \int_{-b/2}^{b/2} \Gamma_o \sqrt{1 - \left(\frac{2y}{b}\right)^2}\, dy$$

$$= \frac{2\alpha_i \Gamma_o}{V_\infty S} \int_\pi^0 \sqrt{1 - \cos^2\theta} \left(-\frac{b}{2}\right) \sin\theta\, d\theta \qquad \boxed{\text{geometry}}$$

$$= \frac{\alpha_i \Gamma_o b}{V_\infty S} \int_0^\pi \sin^2\theta\, d\theta = \frac{\alpha_i \Gamma_o b}{V_\infty S} \left[\frac{1}{2}\theta - \frac{1}{4}\sin 2\theta\right]_0^\pi$$

$$C_{D_i} = \frac{\alpha_i \Gamma_o b}{V_\infty S} \frac{\pi}{2} \qquad\qquad (5.45)$$

Which can be rewritten by substituting Eqs. (5.41) and (5.44) into (5.45)

$$C_{D_i} = \frac{C_L}{\pi AR} \frac{2V_\infty S C_L}{b\pi} \frac{b}{V_\infty S} \frac{\pi}{2}$$

$$\boxed{\begin{array}{l} C_{D_i} = \dfrac{C_L^2}{\pi AR} \qquad\qquad (5.46) \\[2em] C_{D_i} \propto C_L^2 \text{ - a typical drag result} \\[2em] C_{D_i} \propto \dfrac{1}{AR} \text{ - use high AR wing (long and thin)} \end{array}}$$

But what's the geometry?!!!

The geometry can be found by going back to the lift coefficient and Eqs. (5.23), (5.21) and (5.2)

$$C_l = \frac{2\Gamma(y_o)}{V_\infty c(y_o)} \qquad\qquad (5.23)$$

$$C_l = 2\pi\left[\alpha_{eff}\right] - \alpha_{L=0} \qquad\qquad (5.21)$$

$$\alpha_{eff} = \alpha - \alpha_i \qquad\qquad (5.2)$$

Then using the idea that the induced a.o.a. is constant and if there is no aerodynamic twist we see from Eqs. (5.21) and (5.2) that

$$C_l = const. \qquad\qquad (5.47)$$
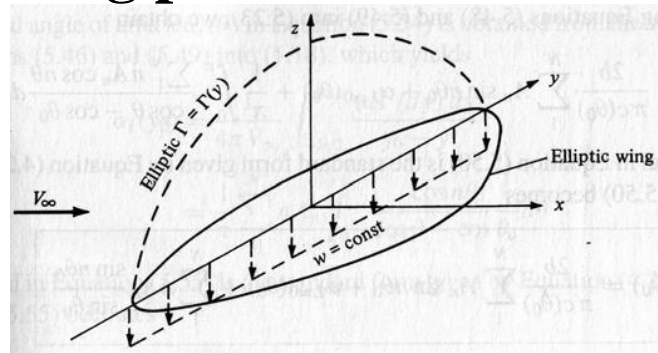
Elliptic Lift Distribution
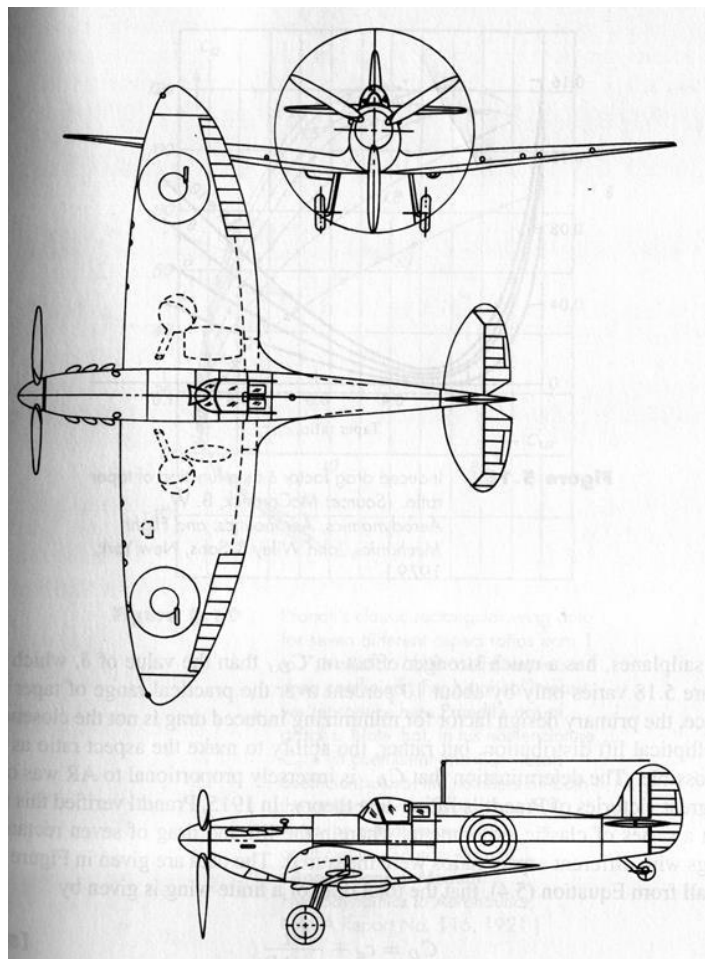
Combining Eqs. (5.47) and (5.23) gives

$$const. = \frac{2\Gamma(y_o)}{V_\infty c(y_o)} \Rightarrow c(y_o) = const._2\ \Gamma(y_o) \qquad\qquad (5.48)$$

With the end result:

An elliptic lift distribution is found from an elliptic wing planform.

Application of Prandtl's Lifting Line Theory for an Elliptic Wing

The previous section demonstrated that an elliptic wing planform develops an elliptic lift distribution but did not answer the question of how one can find the aerodynamic properties of an elliptic wing. Consider an elliptic wing

$$c(y) = c_r \sqrt{1 - \left(\frac{2y}{b}\right)^2} \tag{5.49}$$

It is clear from Eq. (5.23) that C_l can be written in terms of Γ_o but Eqs. (5.21) & (5.2) also show that C_l depends on α_i, which in turn depends on C_L, which then depends on an integrated value of C_l. What's needed is a way to close the loop. To do this consider again Eqs. (5.23), (5.21) and (5.2)

$$C_l = \frac{2\Gamma_o}{V_\infty c_r} = 2\pi\left[\alpha_{eff} - \alpha_{L=0}\right]$$

$$= \frac{2\Gamma_o}{V_\infty c_r} = 2\pi\left[\alpha - \alpha_i - \alpha_{L=0}\right]$$

$$= 2\pi\left[\alpha - \frac{\Gamma_o}{2bV_\infty} - \alpha_{L=0}\right]$$

from which we see

$$\Gamma_o\left[\frac{\pi}{V_\infty c_r} + \frac{\pi}{V_\infty b}\right] = 2\pi\left[\alpha - \alpha_{L=0}\right]$$

$$\Gamma_o = \frac{2\pi V_\infty\left[\alpha - \alpha_{L=0}\right]}{\left[\frac{2}{c_r} + \frac{\pi}{b}\right]} \tag{5.50}$$

Therefore, given the root chord, span and airfoil shape Γ_o can be found. Upon rearranging Eq. (5.41)
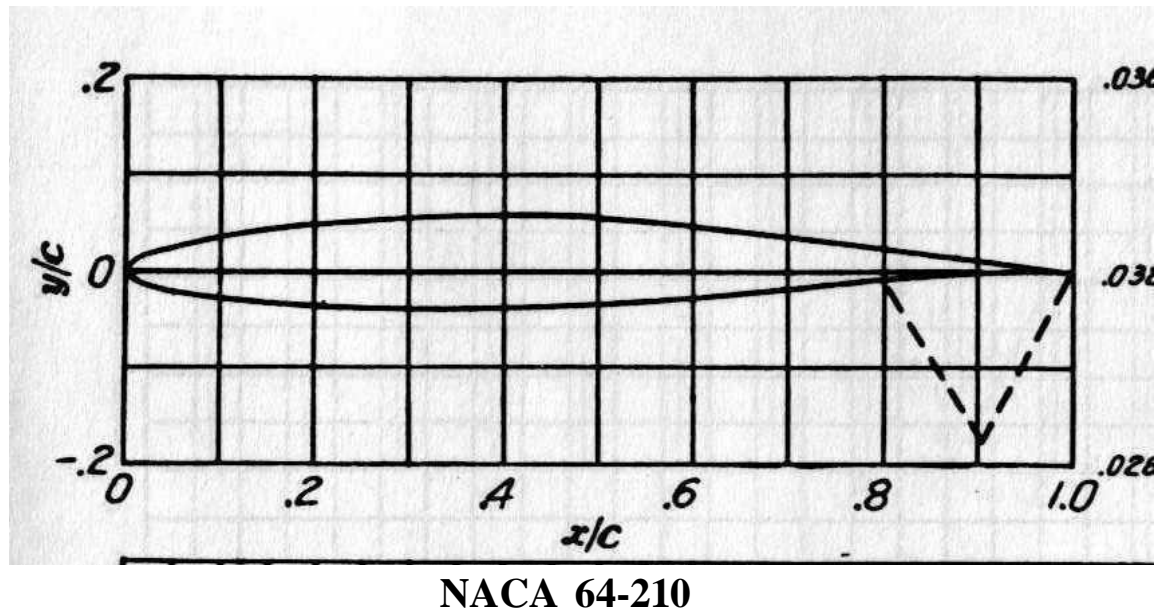
$$C_L = \frac{b\pi\Gamma_o}{2V_\infty S} \qquad\qquad (5.41b)$$
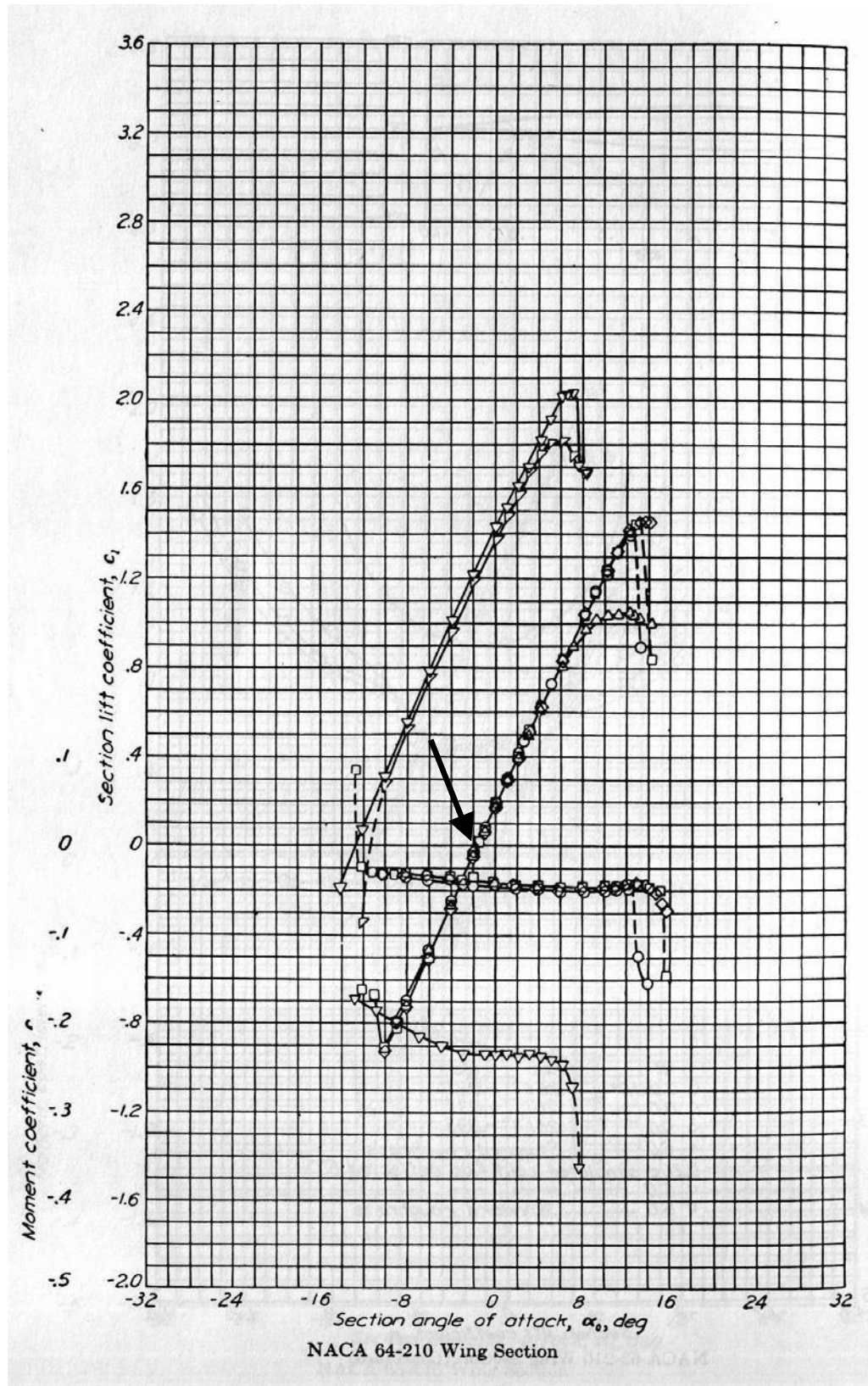
and from Eq. (5.46)

$$C_{D_i} = \frac{C_L^2}{\pi AR} \qquad\qquad (5.46)$$

Example Problem: Consider an elliptic wing with 10m span and 2.5m root chord. If the wing is made up of NACA 64-210 wing sections and is flying 50m/s at a geometric angle of attack of 8 degrees, compute

1. C_L and C_{D_i}
2. L and D_i
3. The acceleration of this wing if it has a mass of 1 Mg at sea level.

NACA 64-210

NACA 64-210 Wing Section

The chart shows that $\alpha_{L=0} \approx -1.8^o$, so that

$$\Gamma_o = \frac{2\pi \left(50m\ /s\right)\left[8^o - \left(-1.8^o\right)\right]}{\left[\dfrac{2}{2.5m} + \dfrac{\pi}{10m}\right]} = 48.23 \frac{m^2 \cdot rad}{\sec}$$

$$S = \pi \frac{b}{2} \frac{c_r}{2} = \frac{\pi \left(10m\right)\left(2.5m\right)}{4} = 19.63m^2$$

$$AR = b^2 \Big/ S = \left(10m\right)^2 \Big/ 19.63m^2 = 5.09$$

$$C_L = \frac{b\pi\Gamma_o}{2V_\infty S} = \frac{\pi \left(10m\right)\left(48.23\dfrac{m^2 \cdot rad}{\sec}\right)}{2 \left(50m/s\right) \left(19.63m^2\right)}$$

$$\boxed{\begin{aligned} C_L &= 0.77 \\[1em] C_{D_i} &= \frac{C_L^2}{\pi AR} = \frac{\left(0.77\right)^2}{\pi \left(5.09\right)} = 0.037 \end{aligned}}$$

Lift and Drag calculations

$$L = \frac{1}{2}\rho_\infty V_\infty^2 S C_L$$

$$L = \frac{1}{2}\left(1.225kg\ /m^3\right)\left(50m/s\right)^2 \left(19.63m^2\right)(0.77) = 23.1kN$$

$$D_i = \frac{1}{2}\rho_\infty V_\infty^2 S C_{D_i}$$

$$D_i = \frac{1}{2}\left(1.225kg\ /m^3\right)\left(50m/s\right)^2 \left(19.63m^2\right)(0.037) = 1.1kN$$

So it can lift 2.38Mg

UNIT-IV

APPLIED AERODYNAMICS

LIFT AUGMENTATION METHODS

Flaps are a kind of high-lift device used to reduce the stalling speed of an aircraft wing at a given weight. Flaps are usually mounted on the wing trailing edges of a fixed-wing aircraft. Flaps are used to reduce the take-off distance and the landing distance. Flaps also cause an increase in drag so they are retracted when not needed.

Extending the wing flaps increases the camber or curvature of the wing, raising the maximum lift coefficient or the upper limit to the lift a wing can generate. This allows the aircraft to generate the required lift at a lower speed, reducing the stalling speed of the aircraft, and therefore also the minimum speed at which the aircraft will safely maintain flight. The increase in camber also increases the wing drag, which can be beneficial during approach and landing, because it slows the aircraft. In some aircraft configurations, a useful side effect of flap deployment is a decrease in aircraft pitch angle, which lowers the nose thereby improving the pilot's view of the runway over the nose of the aircraft during landing. In other configurations, however, depending on the type of flap and the location of the wing, flaps can cause the nose to rise (pitch-up), obscuring the pilot's view of the runway.

There are many different designs of flaps, with the specific choice depending on the size, speed and complexity of the aircraft on which they are to be used, as well as the era in which the aircraft was designed. Plain flaps, slotted flaps, and Fowler flaps are the most common. Krueger flaps are positioned on the leading edge of the wings and are used on many jet airliners.

The Fowler, Fairey-Youngman and Gouge types of flap increase the wing area in addition to changing the camber. The larger lifting surface reduces wing loading, hence further reducing the stalling speed.

Some flaps are fitted elsewhere. Leading-edge flaps form the wing leading edge and when deployed they rotate down to increase the wing camber. The de Havilland DH.88 Comet racer had flaps running beneath the fuselage and forward of the wing trailing edge. Many of the Waco Custom Cabin series biplanes have the flaps at mid-chord on the underside of the top wing.

Principles of operation

The general airplane lift equation demonstrates these relationships:

$$L = \frac{1}{2} \rho v^2 S C_L$$
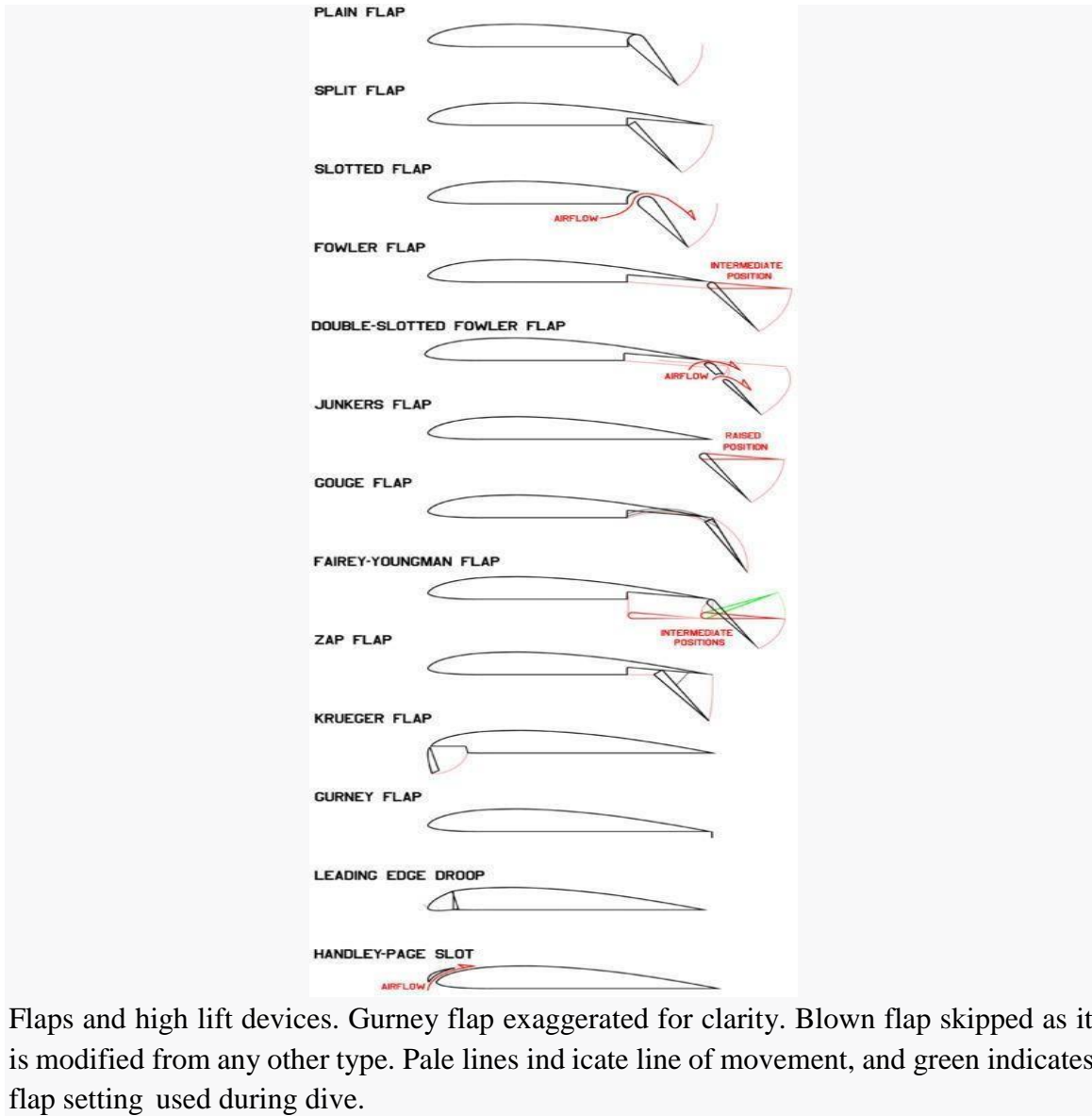
where:

- *L* is the amount of *Lift* produced,
- ρ is the air density,
- *V* is the true airspeed of the airplane or the *Velocity* of the airplane, relative to the air
- **S** is the area of the wing
- **C$_L$** is the *lift coefficient*, which is determined by the shape of the airfoil used and the angle at which the wing meets the air (or angle of attack).

Here, it can be seen that increasing the area (S) and lift coefficient (**C$_L$**) allow a similar amount of lift to be generated at a lower airspeed (V).

Extending the flaps also increases the drag coefficient of the aircraft. Therefore, for any given weight and airspeed, flaps increase the drag force. Flaps increase the drag coefficient of an aircraft due to higher induced drag caused by the distorted spanwise lift distribution on the wing with flaps extended. Some flaps increase the wing area and, for any given speed, this also increases the parasitic drag component of total drag.

Types of flap

Flaps and high lift devices. Gurney flap exaggerated for clarity. Blown flap skipped as it is modified from any other type. Pale lines ind icate line of movement, and green indicates flap setting used during dive.

Plain flap

The rear portion of airfoil rotates downwards on a simple hinge mounted at the front of the flap increasing the camber of airfoil. This increase in camber ensures lift augmentation compared to normal airfoil without flap. Owing to the greater efficiency of other flap types, the plain flap is normally only used where simplicity is required.

Split flap

"Split flap" redirects here. For the display type, see Split-flap display.

The rear portion of the lower surface of the a irfoil hinges downwards from the leading edge of the flap, while the upper surface stays immobile. This can cause large changes in longitudinal trim, pitching the nose either down or up. At full deflection, a split flaps acts much like a spoiler, adding significantly to drag coefficient. It also adds a little to lift

coefficient. It was invented by Orville Wright and James M. H. Jacobs in 1920, but only became common in the 1930s and was then quickly superseded. The Douglas DC-1 (progenitor to the DC-3 and C-47) was one of the first of many aircraft types to use split flaps.

Slotted flap

A gap between the flap and the wing forces high pressure air from below the wing over the flap helping the airflow remain attached to the flap, increasing lift compared to a split flap. Additionally, lift across the entire chord of the primary airfoil is greatly increased as the velocity of air leaving its trailing edge is raised, from the typical non- flap 80% of freestream, to that of the higher-speed, lower-pressure air flowing around the leading edge of the slotted flap. Any flap that allows air to pass between the wing and the flap is considered a slotted flap. The slotted flap was a result of research at Handley-Page, a variant of the slot that dates from the 1920s, but was not widely used until much later. Some flaps use multiple slots to further boost the effect.

Fowler flap

A split flap that slides backwards, before hinging downward, thereby increasing first chord, then camber. The flap may form part of the upper surface of the wing, like a plain flap, or it may not, like a split flap, but it must slide rearward before lowering. As a defining feature – distinguishing it from the Gouge Flap – it always provides a slot effect. Invented by Harlan D. Fowler in 1924, and tested by Fred Weick at NACA in 1932. They were first used on the Martin 146 prototype in 1935, and in production on the 1937 Lockheed Super Electra, and are still in widespread use on modern aircraft, often with multiple slots.

Junkers flap

A slotted plain flap fixed below the trailing edge of the wing, and rotating about its forward edge. When not in use, it has more drag than other types, but is more effective at creating additional lift than a plain or split flap, while retaining their mechanical simplicity. Invented by Otto Mader at Junkers in the late 1920s, they were most often seen on the Junkers Ju 52 and the Junkers Ju 87 *Stuka*, though the same basic design can also be found on many modern ultralights, like the Denney Kitfox.

Gouge flap: A type of split flap that slides backward along curved tracks that force the trailing edge downward, increasing chord and camber without affecting trim or requiring any additional mechanisms.[17] It was invented by Arthur Gouge for Short Brothers in 1936 and used on the Short Empire and Sunderland flying boats, which used the very thick Shorts A.D.5 airfoil. Short Brothers may have been the only company to use this type.

Fairey-Youngman flap

Drops down (becoming a Junkers Flap) before sliding aft and then rotating up or down. Fairey was one of the few exponents of this design, which was used on the Fairey Firefly and Fairey Barracuda. When in the extended position, it could be angled up (to a negative angle of incidence) so that the aircraft could be dived vertically without needing excessive trim changes.

Zap flap

Commonly, but incorrectly, called the Zapp flap, it was invented by Edward F. Zaparka while he was with Berliner/Joyce and tested on a General Aircraft Corporation Aristocrat in 1932 and on other types periodically thereafter, but it saw little use on production aircraft other than on the Northrop P-61 Black Widow. The leading edge of the flap is mounted on a track, while a point at mid chord on the flap is connected via an arm to a pivot just above the track. When the flap's leading edge moves aft along the track, the triangle formed by the track, the shaft and the surface of the flap (fixed at the pivot) gets narrower and deeper, forcing the flap down.[18]

Krueger flap

A hinged flap which folds out from under the wing's leading edge while not forming a part of the leading edge of the wing when retracted. This increases the camber and thickness of the wing, which in turn increases lift and drag. This is not the same as a leading edge droop flap, as that is formed from the entire leading edge. Invented by Werner Krüger in 1943 and evaluated in Goettingen, Krueger flaps are found on many modern swept wing airliners.

Gurney flap

A small fixed perpendicular tab of between 1 and 2% of the wing chord, mounted on the high pressure side of the trailing edge of an airfoil. It was named for racing car driver Dan Gurney who rediscovered it in 1971, and has since been used on some helicopters such as the Sikorsky S-76B to correct control problems without having to resort to a major redesign. It boosts the efficiency of even basic theoretical airfoils (made up of a triangle and a circle overlapped) to the equivalent of a conventional airfoil. The principle was discovered in the 1930s, but was rarely used and was then forgotten. Late marks of the Supermarine Spitfire used a bead on the trailing edge of the elevators, which functioned in a similar manner.

Leading edge flap

The entire leading edge of the wing rotates downward, effectively increasing camber and also slightly reducing chord. Most commonly found on fighters with very thin wings unsuited to other leading edge high lift devices.

Blown flap

A type of Boundary Layer Control System, blown flaps pass engine-generated air or exhaust

original (internally blown flap) which blows compressed air from the engine over the top of the flap, the externally blown flap, which blows engine exhaust over the upper and lower surfaces of the flap, and upper surface blowing which blows engine exhaust over the top of the wing and flap. While testing was done in Britain and Germany before the Second World War,[24] and flight trials started, the first production aircraft with blown flaps wasn't until the 1957 Lockheed T2V SeaStar. Upper Surface Blowing was used on the Boeing YC-14 in 1976.

Flaps during takeoff

Depending on the aircraft type, flaps may be partially extended for takeoff. When used during takeoff, flaps trade runway distance for climb rate: using flaps reduces ground roll but also reduces the climb rate. The amount of flap used on takeoff is specific to each type of aircraft, and the manufacturer will suggest limits and may indicate the reduction in climb rate to be expected. The *Cessna 172S Pilot Operating Handbook* generally recommends 10° of flaps on takeoff, especially when the ground is rough or soft.

Flaps during landing

Flaps may be fully extended for landing to give the aircraft a lower stall speed so the approach to landing can be flown more slowly, which also allows the aircraft to land in a shorter distance. The higher lift and drag associated with fully extended flaps allows a steeper and slower approach to the landing site, but imposes handling difficulties in aircraft with very low wing loading (i.e. having little weight and a large wing area). Winds across the line of flight, known as *crosswinds*, cause the windward side of the aircraft to generate more lift and drag, causing the aircraft to roll, yaw and pitch off its intended flight path, and as a result many light aircraft land with reduced flap settings in crosswinds. Furthermore, once the aircraft is on the ground, the flaps may decrease the effectiveness of the brakes since the wing is still generating lift and preventing the entire weight of the aircraft from resting on the tires, thus increasing stopping distance, particularly in wet or icy conditions. Usually, the pilot will raise the flaps as soon as possible to prevent this from occurring.[2]

Maneuvering flaps

Some gliders not only use flaps when landing, but also in flight to optimize the camber of the wing for the chosen speed. While thermalling, flaps may be partially extended to reduce the stall speed so that the glider can be flown more slowly and thereby reduce the rate of sink, which lets the glider use the rising air of the thermal more efficiently, and to turn in a smaller circle to make best use of the core of the thermal. At higher speeds a negative flap setting is used to reduce the nose-down pitching moment. This reduces the balancing load required on the horizontal stabilizer, which in turn reduces the trim drag associated with keeping the glider in longitudinal trim Negative flap may also be used during the initial stage of an

aerotow launch and at the end of the landing run in order to maintain better control by the ailerons.

Like gliders, some fighters such as the Nakajima Ki-43 also use special flaps to improve maneuverability during air combat, allowing the fighter to create more lift at a given speed, allowing for much tighter turns. The flaps used for this must be designed specifically to handle the greater stresses and most flaps have a maximum speed at which they can be deployed. Control line model aircraft built for precision aerobatics competition usually have a type of maneuvering flap system that moves them in an opposing direction to the elevators, to assist in tightening the radius of a maneuver.

Flap tracks

Extending flaps often run on guide tracks. Where these run outside the wing structure they may be faired in to streamline them and protect them from damage. Some track fairings are designed to act as anti-shock bodies, which reduce drag caused by local sonic shock waves where the airflow becomes transonic at high speeds.

Thrust gates

Thrust gates, or gaps, in the trailing edge flaps may be required to minimize interference between the engine flow and deployed flaps. In the absence of an inboard aileron, which provides a gap in many flap installations, a modified flap section may be needed. The thrust gate on the Boeing 757 was provided by a single-slotted flap in between the inboard and outboard double-slotted flaps. The A320, A330, A340 and A380 have no inboard aileron. No thrust gate is required in the continuous, single-slotted flap. Interference in the go-around case while the flaps are still fully deployed can cause increased drag which must not compromise the climb gradient.

Wingtip devices are intended to improve the efficiency of fixed-wing aircraft by reducing drag.[1] Although there are several types of wing tip devices which function in different manners, their intended effect is always to reduce an aircraft's drag by partial recovery of the tip vortex energy. Wingtip devices can also improve aircraft handling characteristics and enhance safety for following aircraft. Such devices increase the effective aspect ratio of a wing without greatly increasing the wingspan. Extending the span would lower lift-induced drag, but would increase parasitic drag and would require boosting the strength and weight of the wing. At some point, there is no net benefit from further increased span. There may also be operational considerations that limit the allowable wingspan (e.g., available width at airport gates).

Wingtip devices increase the lift generated at the wingtip (by smoothing the airflow across the upper wing near the tip) and reduce the lift-induced drag caused by wingtip vortices, improving lift-to-drag ratio. This increases fuel efficiency in powered aircraft and increases cross-country speed in gliders, in both cases increasing range.

Winglet

The term "winglet" was previously used to describe an additional lifting surface on an a ircraft, like a short section between wheels on fixed undercarriage. Richard Whitcomb's research in the 1970s at NASA first used winglet with its modern meaning referring to near-vertical extension of the wing tips. The upward angle (or *cant*) of the winglet, its inward or outward angle (or *toe*), as well as its size and shape are critical for correct performance and are unique in each application. The wingtip vortex, which rotates around from below the wing, strikes the cambered surface of the winglet, generating a force that angles inward and slightly forward, analogous to a sailboat sailing close hauled. The winglet converts some of the otherwise-wasted energy in the wingtip vortex to an apparent thrust. This small contribution can be worthwhile over the aircraft's lifetime, provided the benefit offsets the cost of installing and maintaining the winglets.

Another potential benefit of winglets is that they reduce the intensity of wake vortices. Those trail behind the plane and pose a hazard to other aircraft.[12] Minimum spacing requirements between aircraft operations at airports are largely dictated by these factors. Aircraft are classified by weight (e.g. "Light," "Heavy," etc.) because the vortex strength grows with the aircraft lift coefficient, and thus, the associated turbulence is greatest at low speed a nd high weight, which produced a high angle of attack.

Winglets and wingtip fences also increase efficiency by reducing vortex interference with laminar airflow near the tips of the wing,[13] by ' moving' the confluence of low-pressure (over wing) and high-pressure (under wing) air away from the surface of the wing. Wingtip vortices create turbulence, originating at the leading edge of the wingtip and propagating backwards and inboard. This turbulence 'delaminates' the airflow over a small triangular section of the outboard wing, which destroys lift in that area. The fence/winglet drives the area where the vortex forms upward away from the wing surface, since the center of the resulting vortex is now at the tip of the winglet.

Aircraft such as the Airbus A340 and the Boeing 747-400 use winglets while other designs such as later versions of the Boeing 777 and the Boeing 747-8 have raked wingtips. The fuel economy improvement from winglets increases with the mission length.[14] Blended winglets allow a steeper angle of attack reducing takeoff distance.

Wingtip fence

A wingtip fence refers to the winglets including surfaces extending both above and below the wingtip, as described in Whitcomb's early research. Both surfaces are shorter than or equivalent to a winglet possessing similar aerodynamic benefits. The Airbus A310-300 was the first airliner with wingtip fences in 1985. It was followed by the A300-600, the A320, and the A380. The A320 Enhanced, A320neo, A350 and A330neo have blended winglets rather than wingtip fences. The An-148 uses wingtip fences.

Canted winglets

Boeing announced a new version of the 747 in October 1985, the 747-400 introduced in 1989, with an extended range and capacity, using a combination of winglets and increased span to carry the additional load. The winglets increased the 747-400's range by 3.5% over the 747-300, which is otherwise aerodynamically identical but has no winglets. Winglets are preferred for Boeing derivative designs based on existing platforms, because they allow maximum re-use of existing components. Newer designs are favoring increased span, other wingtip devices or a combination of both, whenever possible.

The Ilyushin Il-96 was the first Russian and modern jet to feature winglets in 1988. The Bombardier CRJ-100/200 was the first regional airliner to feature winglets in 1992. The A340/A330 followed with canted winglets in 1993/1994. The Tupolev Tu-204 was the first narrowbody aircraft to feature winglets in 1994. The Airbus A220 (née CSeries), from 2016, has canted winglets.

Blended winglets

A blended winglet is attached to the wing with a smooth curve instead of a sharp angle and is intended to reduce interference drag at the wing/winglet junction. A sharp interior angle in this region can interact with the boundary layer flow causing a drag inducing vortex, negating some of the benefit of the winglet. Seattle-based Aviation Partners develops blended winglets as retrofits for the Gulfstream II, Hawker 800 and the Falcon 2000.

On 18 February 2000, blended winglets were announced as an option for the Boeing 737-800; the first shipset was installed on 14 February 2001 and entered revenue service with Hapag-Lloyd Flug on 8 May 2001.[19] The Aviation Partners/Boeing 8 ft (2.4 m) extensions decrease fuel consumption by 4% for long-range flights and increase range by 130 or 200 nmi (240 or 370 km) for the 737-800 or the derivative Boeing Business Jet as standard.[1] Also offered for the 737 Classic, many operators have retrofitted their fleets with these for the fuel savings. Aviation Partners Boeing also offers blended winglets for the 757 and 767. In 2006 Airbus tested two candidate blended winglets, designed by Winglet Technology and Airbus for the Airbus A320 family.[21] In 2009 Airbus launched its "Sharklet" blended winglet, designed to enhance the payload-range of its A320 family and reduce fuel burn by up to 4% over longer sectors. This corresponds to an annual CO_2 reduction of 700 tonnes per aircraft.[23] The A320s fitted with Sharklets were to be delivered from 2012. They are used on the A320neo, the A330neo and the A350. They are also offered as a retrofit option.

Raked wingtip

Raked wingtips, where the tip has a greater wing sweep than the rest of the wing, are featured on some Boeing Commercial Airplanes to improve fuel efficiency, takeoff and climb performance. Like winglets, they increase the effective wing aspect ratio and diminish wingtip vortices, decreasing lift-induced drag. In testing by Boeing and NASA, they reduce drag by as much as 5.5%, compared to 3.5% to 4.5% for conventional winglets.[1] While an increase in span would be more effective than a same-length winglet, its bending moment is greater. A 3 ft (91 cm) winglet gives the performance gain of a 2 ft (61 cm) span increase but has the bending force of a 1 ft (30 cm) span increase.[25]

The short-range Boeing 787-3 would have had a 170 ft (51.7 m) wingspan to fit in ICAO Aerodrome Reference Code D. Its wingspan was decreased by using blended winglets instead of raked wingtips.

Raked wingtips are installed on the Boeing 767-400ER (first flight on October 9, 1999), the Boeing 777-200LR/300ER/Freighter (February 24, 2003), the 737-derived Boeing P-8 Poseidon (25 April 2009), the Boeing 787-8/9/10 (December 15, 2009), the Boeing 747-8 Intercontinental and Freighter (February 8, 2010) and will be on the Boeing 777X planned for 2019. The Embraer E-jet E2 wing has a raked wingtip.
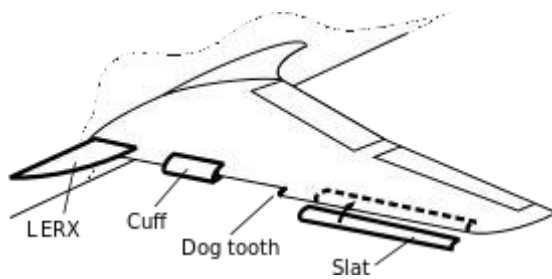
Split-tip

The McDonnell Douglas MD-11 was the first aircraft with split scimitar winglets in 1990.

The Boeing 737 MAX uses a new type of wingtip device. Resembling a three-way hybrid between a winglet, wingtip fence, and raked wingtip, Boeing claims that this new design should deliver an additional 1.5% improvement in fuel economy over the 10-12% improvement already expected from the 737 MAX.

For the 737 Next Generation, Aviation Partners Boeing has introduced a similar design to the 737 MAX wingtip device known as the Split Scimitar Winglet, with United Airlines as the launch customer

A **leading-edge extension** (**LEX**) is a small extension to an aircraft wing surface, forward of the leading edge. The primary reason for adding an extension is to improve the airflow at high angles of attack and low airspeeds, to improve handling and delay the stall. A dog tooth can also improve airflow and reduce drag at higher speeds.

Leading–edge slat

A leading-edge slat is an aerodynamic surface running spanwise just ahead of the wing leading edge. It creates a leading edge slot between the slat and wing which directs air over the wing surface, helping to maintain smooth airflow at low speeds and high angles of attack. This delays the stall, allowing the aircraft to fly at a higher angle of attack. Slats may be made fixed, or retractable in normal flight to minimize drag.

Dogtooth extension

A **dogtooth** is a small, sharp zig-zag break in the leading edge of a wing. It is usually used on a swept wing, to generate a vortex flow field to prevent separated flow from progressing outboard at high angle of attack. The effect is the same as a wing fence. It can also be used on straight wings in a drooped leading edge arrangement.

Where the dogtooth is added as an afterthought, as for example on the Hawker Hunter and some variants of the Quest Kodiak, the dogtooth is created by adding an extension to the outer section of the leading edge.

Leading-edge cuff

A leading edge cuff (or wing cuff) is a fixed aerodynamic device employed on fixed-wing aircraft to introduce a sharp discontinuity in the leading edge of the wing in the same way as a dogtooth. It also typically has a slightly drooped leading edge to improve low-speed characteristics.

A leading-edge cuff is a wing leading-edge modification, usually a lightly drooped outboard leading-edge extension. In most cases of outboard leading-edge modification, the wing cuff starts about 50–70% half-span and spans the outer leading edge of the wing.

The main goal is to produce a more gradual and gentler stall onset, without any spin departure tendency, particularly where the original wing has a sharp/asymmetric stall behaviour with a passive, non- moving, low-cost device that would have a minimal impact on performance. A further benefit is to lowering stall speed, with lower approach speeds and shorter landing distances. They may also, depending on cuff location, improve aileron control at low speed.

Leading-edge root extension

A leading-edge root extension (LERX) is a small fillet, typically roughly triangular in shape, running forward from the leading edge of the wing root to a point along the fuselage. These are often called simply leading-edge extensions (LEX), although they are not the only kind. To avoid ambiguity, this article uses the term LERX.

On a modern fighter aircraft LERXes induce controlled airflow over the wing at high angles of attack, so delaying the stall and consequent loss of lift. In cruising flight the effect of the LERX is minimal. However at high angles of attack, as often encountered in a dog fight or during takeoff and landing, the LERX generates a high-speed vortex that attaches to the top of the wing. The vortex action maintains a smooth airflow over the wing surface well past the normal stall point at which the airflow would otherwise break up, thus sustaining lift at very high angles.

LERX were first used on the Northrop F-5 "Freedom fighter" which flew in 1959, and have since become commonplace on many combat aircraft. The F/A-18 Hornet has especially large examples, as does the Sukhoi Su-27 and the CAC/PAC JF-17 Thunder. The Su-27 LERX help make some advanced maneuvers possible, such as the Pugachev's Cobra, the Cobra Turn and the Kulbit.

A long, narrow sideways extension to the fuselage, attached in this position, is an example of a chine.

Leading-edge vortex controller

Leading-edge vortex controller (LEVCON) systems are a continuation of leading-edge root extension (LERX) technology, but with actuation that allows the leading edge vortices to be modified without adjusting the aircraft's attitude [4]. Otherwise they operate on the same principles as the LERX system to create lift augmenting leading edge vortices during high angle of attack flight.

This system has been incorporated in the Russian Sukhoi Su-57 and Indian HAL LCA Navy.
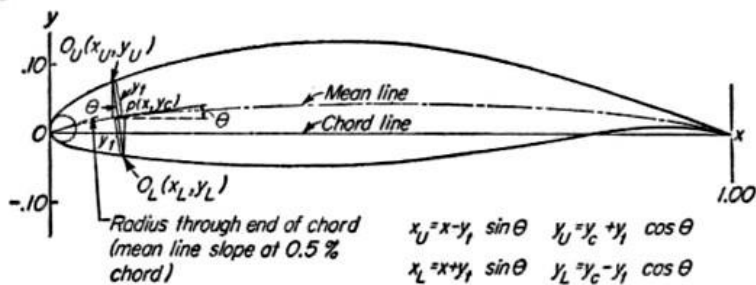
The LEVCONs actuation ability also improves its performance over the LERX system in other areas. When combined with the thrust vectoring controller (TVC), the aircraft controllability at extreme angles of attack is further increased, which assists in stunts which require supermaneuverability such as Pugachev's Cobra. Additionally, on the Sukhoi Su-57 the LEVCON system is used for increased departure-resistance in the event of thrust vectoring controller (TVC) failure at a post-stall attitude. It can also be used for trimming the aircraft, and optimizing the lift to drag ratio during cruise.

The idea of Large Eddy BreakUp (LEBU) devices as a method to reduce skin friction in turbulent boundary layers and ultimately drag on bodies moving through fluids can be traced back to this time. It was believed that the near wall region where the turbulence production has it maximum is influenced by the large scales (of the order of the boundary layer thickness) and that the interaction between the outer and inner regions was important for turbulence production and hence skin friction. By interfering with the large scales it was suggested that the interaction could be disrupted (or at least limited) and would result in a lower turbulence production. The devices themselves would have some inherent penalty drag, but with a smart design it was believed that the integrated reduction of skin friction could be larger than the penalty drag.

The NACA airfoil series

The early NACA airfoil series, the 4-digit, 5-digit, and modified 4-/5-digit, were generated using analytical equations that describe the camber (curvature) of the mean-line (geometric centerline) of the airfoil section as well as the section's thickness distribution along the length of the airfoil. Later families, including the 6-Series, are more complicated shapes derived using theoretical rather than geometrical methods. Before the National Advisory Committee fo r Aeronautics (NACA) developed these series, airfoil design was rather arbitrary with nothing to guide the designer except past experience with known shapes and experimentation with modifications to those shapes.

This methodology began to change in the early 1930s with the publishing of a NACA report entitled *The Characteristics of 78 Related Airfoil Sections from Tests in the Variable Density Wind Tunnel*. In this landmark report, the authors noted that there were many similarities between the airfoils that were most successful, and the two primary variables that affect those shapes are the slope of the airfoil mean camber line and the thickness distribution above and below this line. They then presented a series of equations incorporating these two variables that could be used to generate an entire family of related airfoil shapes. As airfoil design became more sophisticated, this basic approach was modified to include additional variables, but these two basic geometrical values remained at the heart of all NACA airfoil series, as illustrated below.

NACA airfoil geometrical construction

NACAFour-Digit Series:

The first family of airfoils designed using this approach became known as the NACA Four-Digit Series. The first digit specifies the maximum camber (m) in percentage of the chord (airfoil length), the second indicates the position of the maximum camber (p) in tenths of chord, and the last two numbers provide the maximum thickness (t) of the airfoil in percentage of chord. For example, the NACA 2415 airfoil has a maximum thickness of 15% with a camber of 2% located 40% back from the airfoil leading edge (or 0.4c). Utilizing these m, p, and t values, we can compute the coordinates for an entire airfoil using the following relationships:

1. Pick values of x from 0 to the maximum chord c.
2. Compute the mean camber line coordinates by plugging the values of m and p into the following equations for each of the x coordinates.

$$y_c = \frac{m}{p^2}\left(2px - x^2\right) \qquad \text{from } x = 0 \text{ to } x = p$$

$$y_c = \frac{m}{(1-p)^2}\left[(1 - 2p) + 2px - x^2\right] \qquad \text{from } x = p \text{ to } x = c$$

where

x = coordinates along the length of the airfoil, from 0 to c (which stands for chord, or length) y = coordinates above and below the line extending along the length of the airfoil, these are either y_t for thickness coordinates or y_c for camber coordinates t = maximum airfoil thickness in tenths of chord (i.e. a 15% thick airfoil would be 0.15) m = maximum camber in tenths of the chord
p = position of the maximum camber along the chord in tenths of chord

3. Calculate the thickness distribution above (+) and below (-) the mean line by plugging the value of t into the following equation for each of the x coordinates.

$$\pm y_t = \frac{t}{0.2}\left(0.2969\sqrt{x} - 0.1260x - 0.3516x^2 + 0.2843x^3 - 0.1015x^4\right)$$

4. Determine the final coordinates for the airfoil upper surface (x_U, y_U) and lower surface (x_L, y_L) using the following relationships.

$$x_U = x - y_t \sin\theta$$
$$y_U = y_c + y_t \cos\theta$$
$$x_L = x + y_t \sin\theta$$
$$y_L = y_c - y_t \cos\theta$$
$$\text{where } \theta = \arctan\left(\frac{dy_c}{dx}\right)$$

NACA Five-Digit Series:

The NACA Five-Digit Series uses the same thickness forms as the Four-Digit Series but the mean camber line is defined differently and the naming convention is a bit more complex. The first digit, when multiplied by 3/2, yields the design lift coefficient (c_l) in tenths. The next two digits, when divided by 2, give the position of the maximum camber (p) in tenths of chord. The final two digits again indicate the maximum thickness (t) in percentage of chord. For example, the NACA 23012 has a maximum thickness of 12%, a design lift coefficient of 0.3, and a maximum camber located 15% back from the leading edge. The steps needed to

1. Pick values of x from 0 to the maximum chord c.
2. Compute the mean camber line coordinates for each x location using the following equations, and since we know p, determine the values of m and k_1 using the table shown below.

$$y_c = \frac{k_1}{6}\left[x^3 - 3mx^2 + m^2(3-m)\,x\right] \qquad \text{from } x = 0 \text{ to } x = p$$

$$y_c = \frac{k_1\,m^3}{6}(1-x) \qquad\qquad \text{from } x = p \text{ to } x = c$$

Mean-line designation	Position of max camber (p)	m	k1
210	0.05	0.0580	361.400
220	0.10	0.1260	51.640
230	0.15	0.2025	15.957
240	0.20	0.2900	6.643
250	0.25	0.3910	3.230

3. Calculate the thickness distribution using the same equation as the Four-Digit Series.
4. Determine the final coordinates using the same equations as the Four-Digit Series.

Modified NACA Four- and Five-Digit Series:

The airfoil sections you mention for the B-58 bomber are members of the Four-Digit Series, but the names are slightly different as these shapes have been modified. Let us consider the root section, the NACA 0003.46-64.069, as an example. The basic shape is the 0003, a 3% thick airfoil with 0% camber. This shape is a symmetrical airfoil that is identical above and below the mean camber line. The first modification we will consider is the 0003-64. The first digit following the dash refers to the roundedness of the nose. A value of 6 indicates that the nose radius is the same as the original airfoil while a value of 0 indicates a sharp leading edge. Increasing this value specifies an increasingly more rounded nose. The second digit determines the location of maximum thickness in tenths of chord. The default location for all four- and five-digit airfoils is 30% back from the leading edge. In this example, the location of maximum thickness has been moved back to 40% chord.

Finally, notice that the 0003.46-64.069 features two sets of digits preceeded by decimals. These merely indicate slight adjustments to the maximum thickness and location thereof. Instead of being 3% thick, this airfoil is 3.46% thick. Instead of the maximum thickness being located at 40% chord, the position on this airfoil is at 40.69% chord. To compute the coordinates for a

modified airfoil shape:

1. Pick values of x from 0 to the maximum chord c.
2. Compute the mean camber line coordinates using the same equations provided for the Four- or Five-Digit Series as appropriate.
3. Calculate the thickness distribution above (+) and below (-) the mean line using these equations. The values of the a_x and d_x coefficients are determined from the following table (these are derived for a 20% thick airfoil).

$$\pm y_t = a_0\sqrt{x} + a_1 x + a_2 x^2 + a_3 x^3 \qquad \text{ahead of } t_{max}$$

$$\pm y_t = d_0 + d_1(1-x) + d_2(1-x)^2 + d_3(1-x)^3 \qquad \text{aft of } t_{max}$$

Airfoil	a_0	a_1	a_2	a_3	d_0	d_1	d_2	d_3
0020-62	0.296900	0.213337	-2.931954	5.229170	0.002000	0.200000	-0.040625	-0.070312
0020-63	0.296900	-0.096082	-0.543310	0.559395	0.002000	0.234000	-0.068571	-0.093878
0020-64	0.296900	-0.246867	0.175384	-0.266917	0.002000	0.315000	-0.233333	-0.032407
0020-65	0.296900	-0.310275	0.341700	-0.321820	0.002000	0.465000	-0.684000	0.292000
0020-66	0.296900	-0.271180	0.140200	-0.082137	0.002000	0.700000	-1.662500	1.312500
0020-03	0.000000	0.920286	-2.801900	2.817990	0.002000	0.234000	-0.068571	-0.093878
0020-33	0.148450	0.412103	-1.672610	1.688690	0.002000	0.234000	-0.068571	-0.093878
0020-93	0.514246	-0.840115	1.110100	-1.094010	0.002000	0.234000	-0.068571	-0.093878
0020-05	0.000000	0.477000	-0.708000	0.308000	0.002000	0.465000	-0.684000	0.292000
0020-35	0.148450	0.083362	-0.183150	-0.006910	0.002000	0.465000	-0.684000	0.292000
0020-34	0.148450	0.193233	-0.558166	0.283208	0.002000	0.315000	-0.233333	-0.032407

4. Determine the "final" coordinates using the same equations as the Four-Digit Series.
5. As noted above, this procedure yields a 20% thick airfoil. To obtain the desired thickness, simply scale the airfoil by multiplying the "final" y coordinates by **[t / 0.2]**.

NACA 1-Series or 16-Series:

Unlike those airfoil families discussed so far, the 1-Series was developed based on airfoil theory rather than on geometrical relationships. By the time these airfoils were designed during the late 1930s, many advances had been made in inverse airfoil design methods. The basic concept behind this design approach is to specify the desired pressure distribution over the airfoil (this distribution dictates the lift characteristics of the shape) and then derive the geometrical shape that produces this pressure distribution. As a result, these airfoils were not generated using some set of analytical expressions like the Four- or Five-Digit Series. The 1-

Series airfoils are identified by five digits, as exemplified by the NACA 16-212. The first digit, 1, indicates the series (this series was designed for airfoils with regions of barely supersonic flow). The 6 specifies the location of minimum pressure in tenths of chord, i.e. 60% back from the leading edge in this case. Following a dash, the first digit indicates the design lift coefficient in tenths (0.2) and the final two digits specify the maximum thickness in tenths of chord (12%). Since the 16-XXX airfoils are the only ones that have ever seen much use, this family is often referred to as the 16-Series rather than as a subset of the 1-Series.

NACA 6-Series:

Although NACA experimented with approximate theoretical methods that produced the 2-Series through the 5-Series, none of these approaches was found to accurately produce the desired airfoil behavior. The 6-Series was derived using an improved theoretical method that, like the 1-Series, relied on specifying the desired pressure distribution and employed advanced mathematics to derive the required geometrical shape. The goal of this approach was to design airfoils that maximized the region over which the airflow remains laminar. In so doing, the drag over a small range of lift coefficients can be substantially reduced. The naming convention of the 6-Series is by far the most confusing of any of the families discussed thus far, especially since many different variations exist. One of the more common examples is the NACA 64_1-212, a=0.6.

In this example, 6 denotes the series and indicates that this family is designed for greater laminar flow than the Four- or Five-Digit Series. The second digit, 4, is the location of the minimum pressure in tenths of chord (0.4c). The subscript 1 indicates that low drag is maintained at lift coefficients 0.1 above and below the design lift coefficient (0.2) specified by the first digit after the dash in tenths.

The final two digits specify the thickness in percentage of chord, 12%. The fraction specified by a=____indicates the percentage of the airfoil chord over which the pressure distribution on the airfoil is uniform, 60% chord in this case. If not specified, the quantity is assumed to be 1, or the distribution is constant over the entire airfoil.

NACA 7-Series:

The 7-Series was a further attempt to maximize the regions of laminar flow over an airfoil differentiating the locations of the minimum pressure on the upper and lower surfaces. An example is the NACA 747A315. The 7 denotes the series, the 4 provides the location of the minimum pressure on the upper surface in tenths of chord (40%), and the 7 provides the location of the minimum pressure on the lower surface in tenths of chord (70%). The fourth character, a letter, indicates the thickness distribution and mean line forms used. A series of standaradized forms derived from earlier families are designated by different letters. Again, the

fifth digit incidates the design lift coefficient in tenths (0.3) and the final two integers are the airfoil thickness in perecentage of chord (15%).

NACA 8-Series:

A final variation on the 6- and 7-Series methodology was the NACA 8-Series designed for flight at supercritical speeds. Like the earlier airfoils, the goal was to maximize the extent of laminar flow on the upper and lower surfaces independently. The naming convention is very similar to the 7-Series, an example being the NACA 835A216. The 8 designates the series, 3 is the location of minimum pressure on the upper surface in tenths of chord (0.3c), 5 is the location of minimum pressure on the lower surface in tenths of chord (50%), the letter A distinguishes airfoils having different camber or thickness forms, 2 denotes the design lift coefficient in tenths (0.2), and 16 provides the airfoil thickness in percentage of chord (16%).

Summary:

Though we have introduced the primary airfoil families developed in the United States before the advent of supersonic flight, we haven't said anything about their uses. So let's briefly explore the advantages, disadvantages, and applications of each of these families.
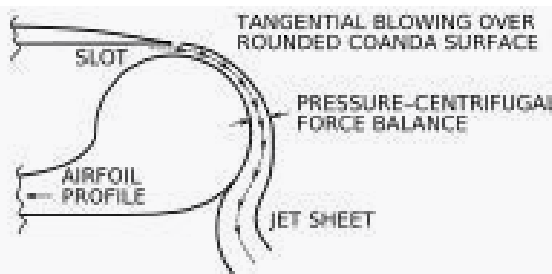
Family	Advantages	Disadvantages	Applications
4-Digit	1. Good stall characteristics 2. Small center of pressure movement across large speed range 3. Roughness has littleeffect	1. Lowmaximum lift coefficient 2. Relatively high drag 3. High pitching moment	1. General aviation 2. Horizontal tails *Symmetrical:* 3. Supersonic jets 4. Helicopter blades 5. Shrouds
5-Digit	1. Higher maximum lift coefficient 2. Lowpitching moment 3. Roughness has littleeffect	1. Poor stall behavior 2. Relatively high drag	1. General aviation 2. Piston-powered bombers, transports 3. Commuters 4. Business jets
16-Series	1. Avoids lowpressure peaks 2. Lowdrag at high speed	1. Relatively lowlift	1. Aircraft propellers 2. Ship propellers
6-Series	1. High maximum lift coefficient 2. Very low drag over a small range of operating conditions 3. Optimized for high speed	1. High drag outside of the optimum range of operating conditions 2. High pitching moment 3. Poor stall behavior	1. Piston-powered fighters 2. Business jets 3. Jet trainers 4. Supersonic jets

7-Series	1. Very low drag over a small range of operating conditions	1. Reduced maximum lift coefficient	Seldom used
	2. Lowpitching moment	2. High drag outside of the optimum range of operating conditions	
		3. Poor stall behavior	
8-Series	Unknown	Unknown	Very seldom used

Today, airfoil design has in many ways returned to an earlier time before the NACA fa milies were created. The computational resources available now allow the designer to quickly design and optimize an airfoil specifically tailored to a particular application rather than making a selection from an existing family.

A **circulation control wing** (CCW) is a form of high-lift device for use on the main wing of an aircraft to increase the maximum lift coefficient. CCW technology has been in the research and development phase for over sixty years. Blown flaps were an early example of CCW.

The CCW works by increasing the velocity of the airflow over the leading edge and trailing edge of a specially designed aircraft wing using a series of blowing slots that eject jets of high-pressure air. The wing has a rounded trailing edge to tangentially eject the air through the Coandă effect thus causing lift.[2] The increase in velocity of the airflow over the wing also adds to the lift force through conventional airfoil lift production.

The trailing edge of a CCW showing the blowing slot and tangential coanda airflow.

Purpose

The main purpose of the circulation control wing is to increase the lifting force of an aircraft at times when large lifting forces at low speeds are required, such as takeoff and landing. Wing flaps and slats are currently used during landing on almost all aircraft and on takeoff by larger jets. While flaps and slats are effective in increasing lift, they do so at a high cost of drag. The benefit of the circulation control wing is that no extra drag is created and the lift coefficient is greatly increased. It is being claimed that such a system could increase the landing coefficient of lift of a Boeing 737 by 150% to 250%, thus reducing approach speeds by 35% to 45% and landing distances by 55% to 75% and that such advances in wing design could allow for dramatic wing size

Other uses

Increased maneuverability

At low speeds, an aircraft has reduced airflow over the wing and vertical stabilizer. This causes the control surfaces (ailerons, elevators and rudder) to be less effective. The CCW system increases the airflow over these surfaces and consequently can allow much higher maneuverability at low speeds. However, if one of the CCW systems should fail at low speed, the affected wing is likely to stall which could result in an inescapable spin. Finally, the CCW system could be used on multi-engine aircraft in the result of an engine failure to cancel the asymmetric forces from the loss of power on one wing.

Noise reduction

The use of a CCW system eliminates the need for large complex components in the free stream such as flaps and slats, greatly reducing the noise pollution of modern aircraft. Additionally, a much shorter ground roll coupled with steeper climb outs and approaches reduces the ground noise footprint. The blowing slots themselves will contribute very little to the noise of the aircraft as each slot is just a fraction of an inch wide.
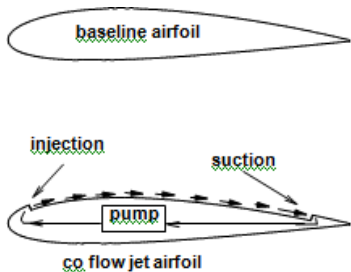
Powering the wing

The main problem with the circulation control wing is the need for high energy air to be blown over the wing's surface. Such air is often bled from the engine; however, this drastically reduces engine power production and consequently counteracts the purpose of the wing. Other options are taking the exhaust gases (which must first be cooled) or using multiple, lightweight gas generators, which are separate from the main aircraft engines.

In the CFJ airfoil concept, an injection slot near leading edge and a suction slot near trailing edge on the airfoil suction surface are created as sketched in Fig. A small amount of mass flow is withdrawn into the airfoil near the trailing edge(TE), pressurized and energized by a pumping system inside the airfoil, and then injected near the leading edge(LE) in the direction tangent to the main flo w. The whole process does not add any mass flow to the system and hence is a Zero net mass flow (ZNMF) flo w control.

The CFJ airfoil flow process provides a unique low energy expenditure ZNMF flow control, which has the injection near the suction peak of the airfoil where the lowest main flow pressure is located, and jet suction at the near trailing edge where the highest main flo w pressure is located. In other words, the required pumping work of CFJ airfoil would be lower than those of the flow control methods injecting near trailing edge such as a CC airfoil. Furthermore, a flow control method using injection only will have to do more work to overcome the ram and captured area drag, which do not exist for CFJ airfoil

they both enhance boundary layer momentum and airfoil circulation. Most of other flow control methods will suffer greater penalties at suction process either due to ram drag, captured area drag or larger flow ducting loss.

The fundamental mechanism of CFJ airfoil is that the turbulent mixing between the jet and main flow makes a lateral transport of energy between the jet, boundary layer, and main flow to energize the wall boundary layer. The large vortex structures and adverse pressure gradient are all beneficial to enhance mixing. The mixing allows the flow to overcome a large adverse pressure gradient and remain attached at a very high angle of attack. Hence, the stall margin is significantly increased. At the same time, the energized boundary layer drastically increases the circulation, augments lift, and reduces the total drag or generates thrust (net negative drag). The portion of CFJ energy used to overcome the increased local drag due to higher jet speed is small since the mixing occurs immediately when the jet penetrates into the boundary layer under an adverse pressure gradient. Unlike a jet in cross flow (JICF) which enhances mixing between the jet and main flow but retards the main fl w due to the cross fl w blockage created by the jet, the co-flow jet mixing only enhances the stream- wise fl w momentum since the jet is tangential to the main flow. The momentum retardation due to JICF will result in a significant entropy and drag increase.

a **spoiler** (sometimes called a **lift spoiler** or **lift dumper**) is a device intended to intentionally reduce the lift component of an airfoil in a controlled way. Most often, spoilers are plates on the top surface of a wing that can be extended upward into the airflow to *spoil* it. By so doing, the spoiler creates a controlled stall over the portion of the wing behind it, greatly reducing the lift of that wing section. Spoilers differ from airbrakes in that airbrakes are designed to increase drag without affecting lift, while spoilers reduce lift as well as increasing drag.

Spoilers fall into two categories: those that are deployed at controlled angles during flight to increase descent rate or control roll, and those that are fully deployed immediately on landing to greatly reduce lift ("lift dumpers") and increase drag. In modern fly-by-wire aircraft, the same set of control surfaces serve both functions.

Spoilers are used by nearly every glider (sailplane) to control their rate of descent and thus achieve a controlled landing. An increased rate of descent can also be achieved by lowering the nose of an aircraft, but this would result in increased speed. Spoilers enable the approach to be made at a safe speed for landing.

Spoiler controls

Spoiler controls can be used for roll control (outboard or mid-span spoilers) or descent control (inboard spoilers).

Some aircraft use spoilers in combination with or in lieu of ailerons for roll control, primarily to reduce adverse yaw when rudder input is limited by higher speeds. For such spoilers the term spoileron has been coined. In the case of a spoileron, in order for it to be used as a control surface, it is raised on one wing only, thus decreasing lift and increasing drag, causing roll and yaw. Spoilerons also avoid the problem of control reversal that affects ailerons.

Almost all modern jet airliners are fitted with inboard lift spoilers which are used together during descent to increase the rate of descent and control speed. Some aircraft use lift spoilers on landing approach to control descent without changing the aircraft's attitude.

One jet airliner not fitted with lift spoilers was the Douglas DC-8 which used reverse thrust in flight on the two inboard engines to control descent speed (however the aircraft was fitted with **lift dumpers**). The Lockheed Tristar was fitted with a system called **Direct Lift Control** using the spoilers on landing approach to control descent.

Airbus aircraft with fly-by-wire control utilise wide-span spoilers for descent control, spoilerons, gust alleviation, and lift dumpers. Especially on landing approach, the full width of spoilers can be seen controlling the aircraft's descent rate and bank.

Lift dumpers

Lift dumpers are a special type of spoiler extending along much of the wing's length and designed to dump as much lift as possible on landing. Lift dumpers have only two positions, deployed and retracted. Lift dumpers have three main functions: putting most of the weight of the aircraft on the wheels for maximum braking effect, increasing form drag, and preventing aircraft ' bounce' on landing.

Lift dumpers are almost always deployed automatically on touch down. The flight deck control has three positions: off, automatic ('armed'), and manual (rarely used). On landing approach 'automatic' is selected and, at the moment of touchdown, lift dumpers are deployed in a fraction of a second, with flight control spoilers also being raised automatically as additional lift dumpers.

Virtually all modern jet aircraft are fitted with lift dumpers. The British Aerospace 146 is fitted with particularly wide span spoilers to generate additional drag and make reverse thrust unnecessary.

An air brake is a panel conforming the shape of an aircraft that can be opened with hydraulic pressure in order to create drag, similar to spoilers which are on the edges of the aircraft wings and open in an upward position forcing the plane towards the ground.[3] Air brakes are used when the aircraft needs to reduce its airspeed, while spoilers are only able to be opened when the airplane is approaching the runway and about to touch down. Lift dumpers, a type of air brake, are mounted on the top of a fuselage. When the panel is opened, it acts as a small spoiler, gently pushing the aircraft down. Flaps also increase drag and decrease airspeed, but are primarily for reducing the stall speed, allowing the aircraft to land at a slower speed.

UNIT – V
Experimental Aerodynamics

Wind tunnel is a large tube with air moving inside which is used to copy the actions of an object in flight. In wind tunnel air moves around an object, so the object seems like really flying. Although the form of a wind tunnel can vary, all wind tunnels have a high pressure system, heater, settling chamber and a test section. Air is compressed and stored in the high pressure system. It is released through a pressure regulating valve to create the desired pressure in the settling chamber. In high speed wind tunnels, heater is used to heat the air while passing through the heater bed to avoid liquefaction when it is expanded through the nozzle to get high Mach numbers. Scaled models of aircraft or space craft are placed in the test section for testing as shown in Figure 1.1. Some wind tunnels are big enough to hold full- scale versions of vehicles.

Air is blown or sucked through a duct equipped with a viewing port and instrumentation where models or geometrical shapes are mounted for study. The movement of air through the tunnel is done by using a series of fans, which are usually powered by stationary turbo rather than electric motors. Vertical and horizontal air vanes make the turbulent air flow smooth, before reaching the test section. The cross section of the tunnel is circular to provide a smoother air flow. The smooth inner surface reduces the surface drag. The circular walls of the tunnel are usually embedded with light, which shines through the windows. Pressure taps are included in the model for measuring pressure. Lift, drag, yaw, roll, lateral forces and pitching moments over a range of angle of attack can be measured by a force balance mounted on the model. The movement of air around the model is difficult to observe directly, since air is transparent. Different flow visualization methods have been developed for testing in a wind tunnel. Tufts attached to the model during testing can be used to gauge air flow. Another method is by using evaporating suspensions, where the liquid evaporates leaving behind the clay in the pattern characteristic of the air flow. Applying oil to the surface of the model can show the transition from laminar to turbulent flow as well as flow separation. Smoke or bubbles of liquid can be introduced into the airflow upstream of the test model, so that their path around the model can be photographed.

1 TYPES OF WIND TUNNEL Wind tunnels can be classified based on air flow speed in test section and based on shape. Flow speed in wind tunnel is generally referred in terms of Mach number. Mach number is a dimensionless quantity representing the ratio of speed of an object moving through a medium and the local speed of sound. Based on flow speed, wind tunnels are classified as Subsonic, Transonic, Supersonic and Hypersonic.

In Subsonic or low speed wind tunnels flow speed in terms of Mach number comes out to be around 0.4. These types of wind tunnels are most cost effective due to the simplicity of the design and low wind speed. Generally low speed wind tunnels are used in schools and universities because of low budget. Maximum velocity in test section of transonic wind tunnels can reach up to speed of sound i.e. 340m/s or Mach number of 1. They are very common in aircraft industry as most aircrafts operate around this speed. Velocity of air in test section of Supersonic wind tunnels wind tunnels can be up to Mach 5. This is accomplished using convergent or divergent nozzles and the power requirements for such wind tunnels are very high.
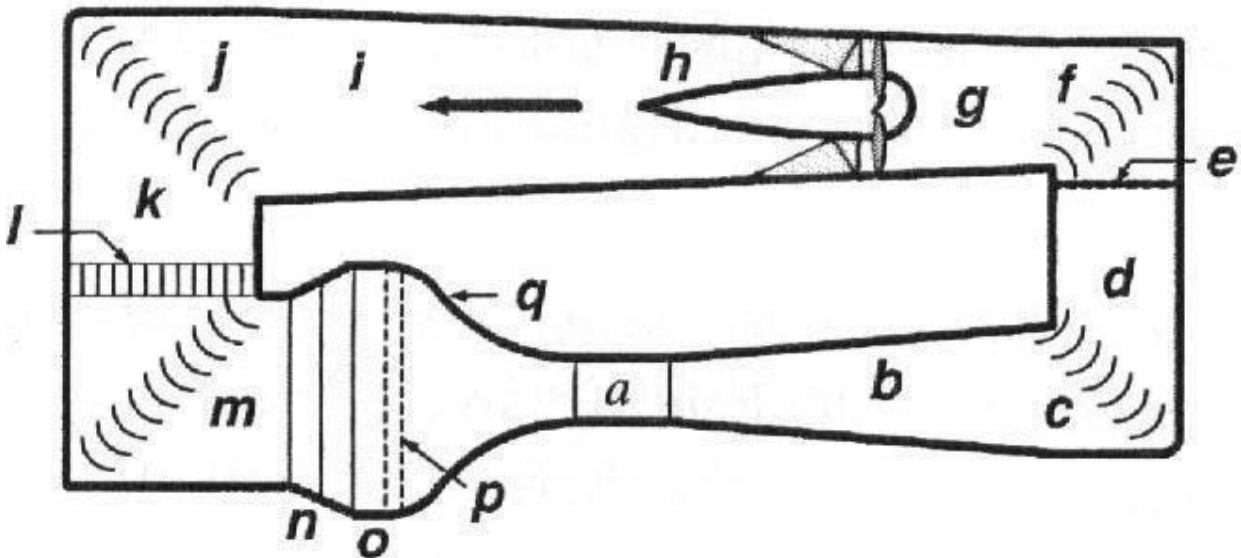
Hypersonic wind tunnels can have wind velocity in test section between Mach 5 and Mach 15. This is also achieved using convergent - divergent nozzles. They are used to test ultra fast air craft and space vehicles. The technological problems in designing and constructing a hyper-velocity wind tunnel are supply of high temperatures and pressures for times long enough to perform a measurement, reproduction of equilibrium conditions, structural damage produced by overheating, fast instrumentation and power requirements to run the tunnel.

Based on shape, wind tunnels are classified as Open circuit wind tunnel and Closed circuit wind tunnel. Open circuit wind tunnel is open at both ends. The chances of dirt particles entering with air are more and so more honeycombs (mesh to clean incoming air) are required for cleaning the air. Open type wind tunnels can further be divided into two categories: Suckdown tunnel and Blower tunnel. In Suckdown tunnel, the inlet open to atmosphere and the axial fan or centrifugal blower is connected after the test 4

section. These types of wind tunnels are not preferred because incoming air enters with significant swirl. In blower tunnel a blower is installed at the inlet of wind tunnel which throws the air into wind tunnel.

For supersonic and hypersonic type wind tunnel, the desired speed cannot be attained with the help of a blower. Hence a tank with high air pressure is maintained and the flow is obtained by releasing the air from this high pressure system. Outlet of closed circuit wind tunnel is connected to inlet and so the same air circulates in the system in a regulated way. The chances of dirt entering the system are very low. Closed wind tunnels have more uniform flow compared to open type. Closed tunnel is usually a choice for large wind tunnels as these are more costly than open type wind tunnels.

Parts of Wind Tunnel

(a) *The test section, which may be closed, open, partially open or convertible.*
The **test-section-length-to-hydraulic-diameter**ragt io may typically be chosen to be 2 or more, in contrast to the shorter test sections of earlier era tunnels.
(b) *A difiser of at least three or four test-section lengths.* The typical equivalent cone angle is in the range of 2-33" with the smaller angles being more desirable. The area ratio is typically 2-3, again with the smaller values being more desirable.
(c) *"First comer" inco?porating fuming vanes.*
(d) *Second leg that may continue the diffuser or may be constant area.*
(e) *Safety screen to prevent parts of failed models or other unintended flying objectsfrom reaching the fan.* This screen is usually just ahead of the secondcomer turning vanes.
(f) *"Second comer" incorporating tuming vanes that may be essentially copies*

of the first comer vanes solely to gain a small engineering and construction cost reduction.

(g) *Transitionhm rectangular to circular cmss section to takeflow into the fan.*

(h) *Fan and straightener section.* Other drive devices such as ejectors have also been used.

(i) *Return or second diffuse]:* This will commonly incorporate a transition back to rectangular from the circular cross section at the fan. The transition will likely have begun in the straightener section. The second diffuser should follow similar design guides as the first diffuser.

(j) "Third corner" incorporating tuming vanes.

*(k) Third leg that may be constant area.*

(1) *Heat exhangel:*
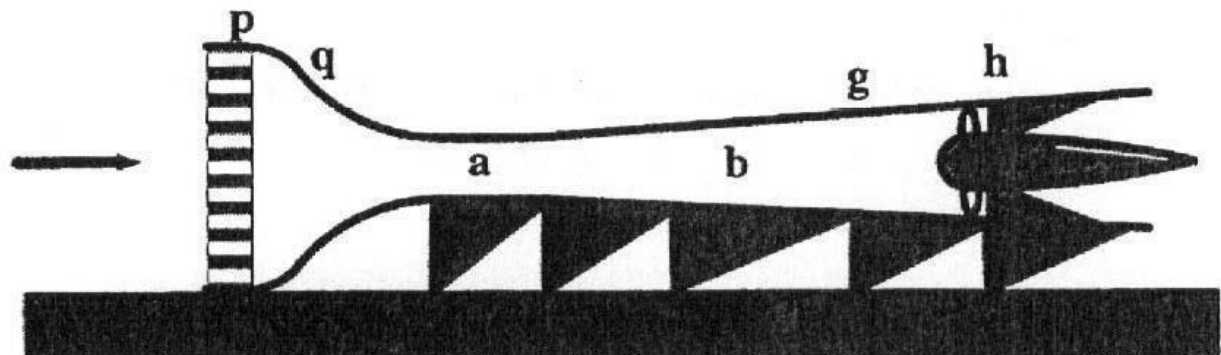
(m) *"Fourth comer" incorporating turning vanes that may be copies of the third-corner vanes.*
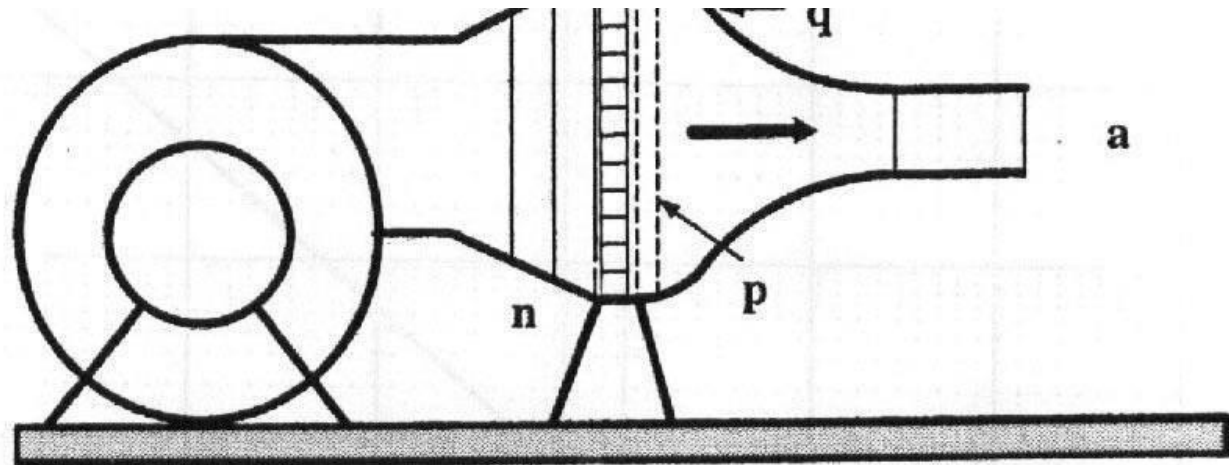
(n) Wide-angle diffuser with separation control screens. Typical properties are angles of about **45"** and area ratios of 24.

(0) *Settling area.*

(p) *Flow conditioners typically including jlow straighteners and turbulence control screens.*
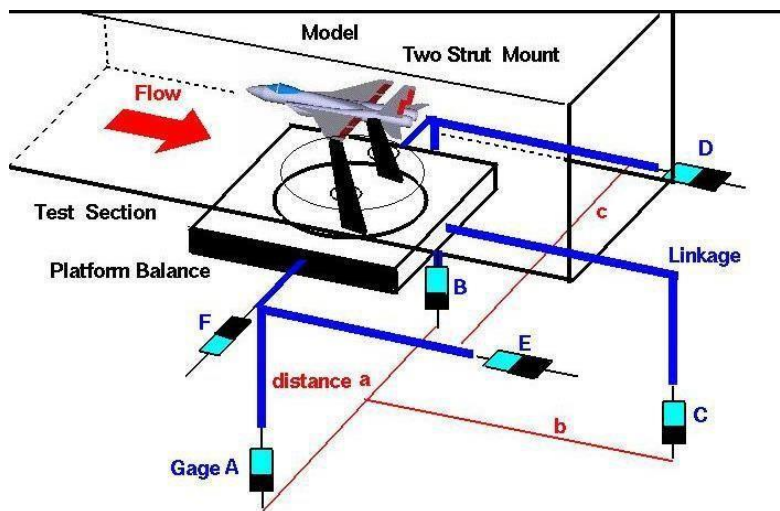
(q) *Contraction or node.* Typical area ratins are in the range of 7-12, although lower and higher values are not uncommon.

Wind tunnel Balances

Aerodynamicists use wind tunnels to test models of proposed aircraft and engine components. During a test, the model is placed in the test section of the tunnel and air is made to flow past the model. Various types of tests can be run in a wind tunnel. Some tests are performed to directly measure the aerodynamic forces and moments on the model. The most basic type of instrument used in this type of testing is the force balance. We must measure six components, three forces (lift, drag, and side) and three moments (pitch, roll, and yaw), to completely describe the conditions on the model. For some tests, only three components (lift, drag, and pitch) are measured.

In some wind tunnels, the measuring devices are located **external** to the model and the test section. In other tunnels, the measuring devices are placed inside the model. The location of the device affects the choice of mounting system for the model and the data reduction necessary to determine the aerodynamic forces. On this web page we will examine the **external balance**.

As shown in the figure, an idealized fighter plane model is attached to a platform located beneath the test section by a two strut mount. There are six strain gages, labeled A through F, that are connected to the platform. Each gage measures a force by the stretching of an electrical element in the gage. The stretching changes the resistance of the e lement which changes the measured current through the element according to Ohm's law. The model can be rotated in pitch and roll by its connections to the struts, and rotated in yaw by the circular section in the floor of the test section.

A test is conducted in the following manner. With the tunnel turned off and no air passing through the test section, the weight (W) of the model and mounting system is determined as the sum of the forces from gages A, B, and C. The tunnel is then turned on and air flows over the model. The model generates aerodynamic forces and moments that changes the readings on the strain gages.

The lift (L) is given by:

$$L = A + B + C - W$$

The drag (Dr) is given by:

$$Dr = E + D$$

The side force Y is:

$$Y = F$$

If there is no rolling moment, the values of A and B are equal. If there is a rolling moment (RM), the value is equal to:

$$RM = (A - B) * a / 2$$

Similarly, the yawing moment, (YM) is equal to

$$YM = (D - E) * c / 2$$

and the pitching moment, (PM) is equal to

$$PM = C * b$$

Notice that the gages are aligned with or perpendicular to the walls of the wind tunnel. The reduction of the data from the gages gives forces and moments that are aligned with the wind tunnel walls. An assumption is made that the flow in the tunnel is perfectly aligned with the walls.

Because air is transparent it is difficult to directly observe the air movement itself. Instead, multiple methods of both quantitative and qualitative flow visualization methods have been developed for testing in a wind tunnel.

Qualitative methods

- Smoke
- Carbon Dioxide Injection
- Tufts, mini-tufts, or flow cones can be applied to a model and remain attached during testing. Tufts can be used to gauge air flow patterns and flow separation. Tufts are sometimes made of fluorescent material and are illuminated under black light to aid in visualization.
- Evaporating suspensions are simply a mixture of some sort or fine powder, talc, or clay mixed into a liquid with a low latent heat of evaporation. When the wind is turned on the liquid quickly evaporates, leaving behind the clay in a pattern characteristic of the air flow.
- Oil: When oil is applied to the model surface it can clearly show the transition from laminar to turbulent flow as well as flow separation.
- Tempera Paint: Similar to oil, tempera paint can be applied to the surface of the model by initially applying the paint in spaced out dots. After running the wind tunnel, the flow direction and separation can be ide ntified. An additional strategy in the use of tempera paint is to use blacklights to create a luminous flow pattern with the tempera paint.
- Fog (usually from water particles) is created with an ultrasonic piezoelectric nebulizer. The fog is transported inside the wind tunnel (preferably of the closed circuit and closed test section type). An electrically heated grid is inserted before the test section, which evaporates the water particles at its vicinity, thus forming fog sheets. The fog sheets function as streamlines over the test model when illuminated by a light sheet.
- Sublimation: If the air movement in the tunnel is sufficiently non-turbulent, a particle stream released into the airflow will not break up as the air moves along, but stay together as a sharp thin line. Multiple particle streams released from a grid of many nozzles can provide a dynamic three-dimensional shape of the airflow around a body. As with the force balance, these injection pipes and nozzles need to be shaped in a manner that minimizes the introduction of turbulent airflow into the airstream.
- Sublimation (alternate definition): A flow visualization technique is to coat the model in a sublimatable material where once the wind is turned on in regions where the airflow is laminar, the material will remain attached to the model, while conversely in turbulent areas the material will evaporate off of the model. This technique is primarily employed to verify that trip dots placed at the leading edge in order to force a transition are successfully achieving the intended goal.

High-speed turbulence and vortices can be difficult to see directly, but strobe lights and film cameras or high-speed digital cameras can help to capture events that are a blur to the naked eye.

High-speed cameras are also required when the subject of the test is itself moving at high speed, such as an airplane propeller. The camera can capture stop- motion images of how the blade cuts through the particulate streams and how vortices are generated along the trailing edges of the moving blade.

Quantitative methods

- Pressure Sensitive Paint (PSP): PSP is a technique whereby a model is spray coated with a paint that reacts to variations in pressure by changing color. In conjunction with this technique, cameras are usually positioned at strategic viewing angles through the walls, ceiling, and floor of the wind tunnel to photograph the model while the wind is on. The photographic results can be digitized to create a full distr ibution of the external pressures acting on the model, and subsequently mapped onto a computational geometric mesh for direct comparison with CFD results. PSP measurements can be effective at capturing pressure variations across the model however often require supplemental pressure taps on the surface of the model to verify the absolute magnitude of the pressure coefficients. An important property of well behaved PSP paints is they also should be insensitive to temperature effects since the temperature inside the wind tunnel could vary considerably after continuously running. Common difficulties encountered when using PSP include the inability to accurately measure the leading and trailing edge effects in areas where there is high curvature due to limitations in the cameras ability to gain an advantageous viewing angle. Additionally application of PSP on the leading edge is sometimes avoided because it introduces a finite thickness that could cause early flow separation thus corrupting results. Since the pressure variations at the leading edge is typically of primary interest, the lack of accurate results in that region is very problematic. Once a model is painted with pressure sensitive paint, certain paints have been known to adhere and continue to perform for a matter of months after initially applied. Finally PSP paints have been known to have certain frequency characteristics where some require a few moments to stabilize before achieving accurate results while others converge rapidly. In the latter instance paints that have ability to reflect rapid changes in pressure can be used for Dynamic PSP applications where the intent is to measure unsteady flow characteristics.
- Particle Image Velocimetry (PIV): PIV is a technique in which a laser sheet is emitted through a slit in the wall of the tunnel where an imaging device is able to track the local velocity direction of particles in the plane of the laser sheet. Sometimes this technique involves seeding the airflow with observable material. This technique allows for the quantitative measurement of the velocity and direction of the flow across the areas captured in the plane of the laser.
- Model Deformation Measurement (MDM): MDM works by placing markers at known geometric locations on the wind tunnel model and tak ing photographs of the change in the marker's location as the wind in the tunnel is applied. By analyzing the change in marker positions from different camera viewing angles, the translational change in location of the marker can be calculated. By collecting results from a few markers, the degree to which the model is flexibly yielding due to the air load can be calculated.

Schlieren Technique

The Schlieren method is one more technique prevalently used for visualizing the compressible flow due to presence of large density gradients. Schematic diagram of a typical Schlieren arrangement used for supersonic flow visualization is shown in Fig. 2.
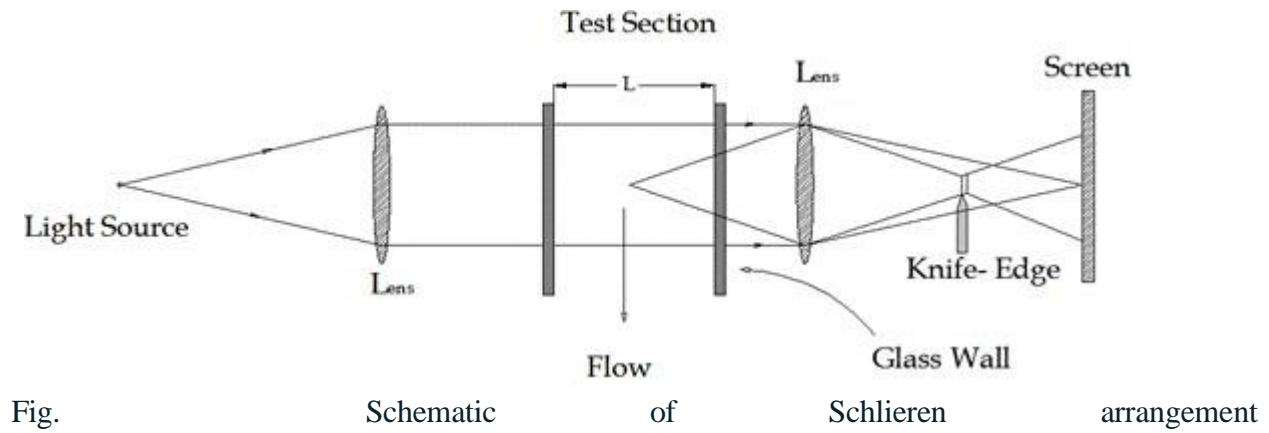

Fig.   Schematic   of   Schlieren   arrangement

This techniques also uses a light source and lens where Light emitted from the source is collimated by the lens before passing through the test section. These light beams are then passed through one more lens before getting on the screen. A knife edge is placed at the focal point of the second lens where the image of the source is formed. Kinfe edge can be any opaque object which can be placed at the same location. This object or knife object is obstructing the light beam. If the beams of light escape the knife edge the screen gets uniformly illumination. This situation is seen for no flow case through the test section since both the beams pass through the medium of same density. However during the flow taking place in the test section with test model mounted in it, both the light beams encounter different densities therefore make different deflections one of the beams pass through uniform or freestream density region while other beam passes through the portion of shock placed ahead the test model. in this way one beam passes through a region of uniform density while other passes through differential density regions or sees the density gradient. It is similar to the light beam passing through a prism when that ray of light bends. This is the reason for orientation of the knife edge for the known density gradient since the ray of light which encounters the density gradient creates differential illumination on the screen presence of knife edge. In this way Schlieren technique makes it possible to visualize density gradient by differential illuminations on the screen. A photographic plate or cameras are generally   used   for   viewing   instead   of   screen.

The major requirement for the Schlieren imaging is to have high optical quality lenses and with large diameter and long focal length. The need for large diameter is necessitate that the coverage of entire flow field. The demand for larger focal length is to acquire proper images on the screen. The quality of the lenses should also be higher in order to avoid chromatic and spherical aberrations and lessen the astigmatism.

It has been observed that is difficult to visualize images using this technique for very large cross section wind tunnels due to unavailability of high optical quality and diameter of lenses. The cost of such lenses is the major concern is such cases. Use of concave mirro rs is the immediate remedy on such situations. This is due to the fact that these lenses are easy to fabricate and also

to correct during the experimental setting. The minimum optical quality is implicit in these lenses. The Schlieren arrangement with such low cost lenses is as shown in Fig **.**
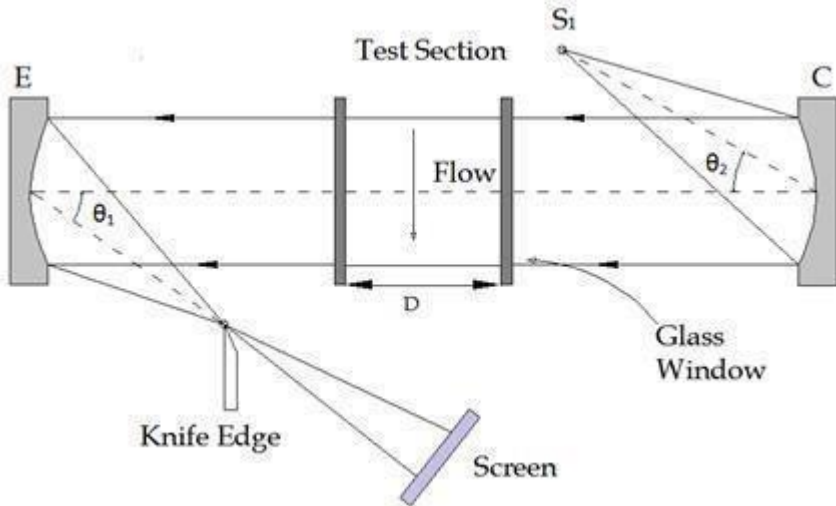

Fig.. Schematic of twin Schlieren arrangement

The shadowgraph arrangement depends on the change in the light intensity arising from beam displacement from its original path. When passing through the test field under investigation, the individual light rays are refracted and bent out of their original path. The rays traversing the region that has no gradient are not deflected, whereas the rays traversing the region that has non zero gradients are bent up. Figure illustrates the shadowgraph effect using simple geometric ray tracing. Here a plane wave traverses a medium that has a nonuniform index of refraction distribution and is allowed to illuminate a screen. The resulting image on the screen consists of regions where the rays converege and diverge; these appear as light and dark regions respectively. It is this effect that gives the technique its name because gradients leave a shadow, or dark region, on the viewing screen. A particular deflected light ray that arrives at a point different from the original point of the recording plane should be traced. It leads to a distribution of light intensity in that plane altered with respect to the undistributed case.

When subjected to linear approximations that include small displacement of the light ray, a second order partial differential equation can be derived for the refractive index field with respect to intensity contrast in the shadowgraph image. Let D be the distance of the screen from the optical window on the beaker. The governing equation for a shadowgraph process can be expressed as (22)

$$\frac{\Delta I}{I_0} = D \int \left(\frac{\partial^2}{\partial x^2} + \frac{\partial^2}{\partial y^2} \right) (\ln n)\, dz \qquad\qquad (22)$$
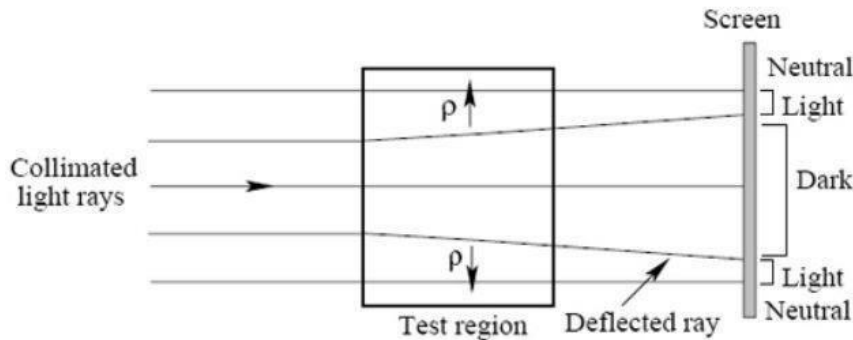

Figure 5.7: Illustration of the shadowgraph arrangement

Here is the change in illumination on the screen due to the beam displacement from its original path and is the original intensity distribution. Equation 22 implies that the shadowgraph is sensitive to changes in the second derivative of the refractive index along the line of sight of the light beam in the fluid medium. Integration of the Poisson equation (22) can be performed by a numerical technique, say the method of finite differences. From Equation 22 it is evident that the shadowgraph is not a suitable method for quantitative measurement of the fluid density, since such an evaluation requires one to perform a double integration of the data. However, owing to its simplicity the shadowgraph is a convenient method for obtaining a quick survey of flow fields with varying fluid density. When the approximations involved in Equation 22 do not apply, shadowgraph can be used for flow visualization alone.